



UNIVERSITÀ DI PARMA

UNIVERSITA' DEGLI STUDI DI PARMA

DOTTORATO DI RICERCA IN

“SCIENZE DEL FARMACO”

CICLO XXXV

THE ROLE OF MICROSCALE THERMOPHORESIS (MST) IN DRUG DISCOVERY OF PROTEIN KINASE INHIBITORS

Coordinatore:

Chiar.mo Prof. Marco Mor

Tutori:

Chiar.mo Prof. Marco Mor

Dott.ssa Barbara Pioselli

Dottorando: Elena Picchi

Anni Accademici 2019/2020 – 2021/2022

TABLE OF CONTENTS

	ABSTRACT.....	5
1.	INTRODUCTION	7
1.1	PROTEIN INTERACTIONS.....	7
1.1.1	PROTEIN INTERACTIONS KEY ROLE AND CHARACTERIZATION	7
1.1.2	BINDING THEORY: THE LAW OF MASS ACTION	8
1.1.3	CORRELATION BETWEEN K_D , K_i and IC_{50} : THE CHENG-PRUSOFF EQUATION	10
1.1.4	FITTING MODELS	11
1.1.5	KEY CRITERIA TO MEASURE BINDING REACTIONS.....	14
1.1.6	MODES OF INHIBITOR INTERACTIONS.....	15
	TIGHT BINDING	16
	SLOW BINDING	19
	COVALENT BINDING	20
1.2	THE MICROSCALE THERMOPHORESIS (MST).....	21
1.2.1	GENERAL DESCRIPTION	21
1.2.2	MST APPROACHES	25
1.3	PROTEIN KINASES AS DRUG TARGETS.....	27
1.3.1	EPIDERMAL GROWTH FACTOR RECEPTOR (EGFR).....	29
1.3.2	RHO-ASSOCIATED PROTEIN KINASE (ROCK)	31
2.	AIM OF THE WORK	33
3.	MATERIALS AND METHODS	35
3.1	EGFR	35
3.1.1	MATERIALS	35
3.1.2	MATERIAL HANDLING AND STORAGE	36
3.1.3	GENERAL PROTOCOL FOR EGFR INTERACTION ASSAYS	36
3.1.4	STOICHIOMETRY ASSAYS	38
3.1.5	REVERSIBLE LIGAND RETENTION ASSAY	40
3.2	ROCK.....	42
3.2.1	MATERIALS	42
3.2.2	MATERIAL HANDLING AND STORAGE	42
3.2.3	GENERAL PROTOCOL FOR ROCK COMPETITION ASSAYS.....	43
3.2.4	LABELING PROTOCOL	45
3.2.5	GENERAL PROTOCOL FOR ROCK BINDING ASSAYS.....	45
3.3	MST-ON TIME CHOICE	47

3.4	DATA ELABORATION AND FITTING MODELS.....	57
4.	RESULTS AND DISCUSSION	59
4.1	EGFR (Epidermal Growth Factor Receptor)	59
4.1.1	INTERACTION WITH KINASE TRACER 199	60
4.1.2	COMPETITION ASSAYS	72
	GEFITINIB - TIGHT BINDING CONDITIONS	72
	LAPATINIB - SLOW BINDING TYPE II INHIBITOR.....	80
	OSIMERITINIB - IRREVERSIBLE BINDING	87
4.2	ROCK (Rho-associated protein kinase).....	95
4.2.1	COMPETITION ASSAYS	96
	INTERACTION WITH KINASE TRACER 236	96
	OPTIMIZATION OF THE INTERACTION WITH COMPOUND A.....	97
	COMPETITION WITH ALLOSTERIC COMPOUNDS.....	99
4.2.2	DIRECT BINDING ASSAYS	102
	ROCK-1 COVALENT LABELING AND BINDING COMPETENCE TEST	102
	INTERACTION WITH ALLOSTERIC COMPOUNDS.....	107
5.	CONCLUSIONS.....	111
6.	BIBLIOGRAPHY	113

ABSTRACT

MicroScale Thermophoresis (MST) is one of the biophysical techniques commonly used for the characterization of ligand/protein interactions. The phenomenon of "thermophoresis" is the directed movement of molecules along a temperature gradient generated by an IR laser and MST can detect changes in charge, size, and hydration shell or conformation of a biomolecular complex caused by the interaction between a target protein and the cognate ligand. This phenomenon can be quantified by titrating the ligand to obtain a binding curve from which the dissociation constant (K_D) can be derived. Even though the main application of MST is to determine binding parameters, the technique can also be employed to gain insights into other aspects of protein interactions such as stoichiometry, conformational states, time dependency, selectivity over mutations, and thermodynamics.

In this project different types of interactions were investigated by using two model protein kinases of pharmaceutical interest, EGFR (Epidermal Growth Factor Receptor) and ROCK (Rho-associated protein kinase) in the presence of their well-known inhibitors. The main purpose was to investigate MST ability to characterize various binding modes with a particular emphasis on potent inhibitors, slow binders, covalent binders, and allosteric binders.

First, EGFR system enabled the characterization of potent inhibitors while facing their intrinsic limitation of resulting in tight binding experimental conditions. Second, a time dependence analysis revealed the MST potential for describing conformational changes in protein kinases, whereas a targeted stoichiometry experiments facilitated the identification of various protein states as well as a difference in the propensity of Type I and Type II inhibitors to bind them. Finally, an alternative method to *Jump Dilution* for differentiating reversible and irreversible inhibitors was developed using MST.

ROCK system, on the other hand, has been used to differentiate between orthosteric and allosteric binders by combining orthogonal approaches of competition and direct binding assays. Furthermore, an analysis of the best labeling conditions revealed differences between the two examined allosteric compounds, indicating a possible distinct interaction mechanism due to their different sensitivity to the dye position on the protein.

These results enabled the development of a wide range of knowledge in the field of protein kinase interactions, providing a suitable background for future and unknown interaction systems.

1. INTRODUCTION

1.1 PROTEIN INTERACTIONS

1.1.1 PROTEIN INTERACTIONS KEY ROLE AND CHARACTERIZATION

Proteins are macromolecules performing essential roles in the cell, including biochemical (enzymes), structural (cytoskeleton), mechanical (muscle), and cell signaling (hormones) functions^[1].

Protein interactions are the basis of every biological function, from the simplest biochemical signal to the more complex cellular rearrangement. They are usually very specific and can either involve small molecules and cofactor or other proteins and macromolecules^[2].

The intricate system of pathways and specific interactions typically contribute to the maintenance of the correct homeostasis of a whole organism but in certain cases can be the cause of undesired altered states, leading to disease mechanisms^[3]. Indeed, almost every drug works by binding proteins (specific *target*) and interfere with their biological function.

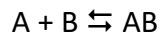
Therefore, a deep understanding of protein interactions mechanism and its characterization play a crucial role in biochemistry studies and Drug Discovery pipeline. To do this, orthogonal biophysical measures could be applied, allowing for a comprehensive description of the interactions in terms of affinity, kinetics, and thermodynamics. A complete characterization also includes data on conformational changes, stoichiometry, and the identification of specific binding regions^[4].

The most appropriate biophysical technique for a specific goal must take into account a variety of factors, including the availability of protein and ligand in terms of quantity, purity, and concentration, all prior knowledge about the interaction system, and, most importantly, which output would best answer a specific question^[2].

Once these aspects are clarified, it is possible to optimize an adequate experimental design and proceed with the assays. A leading approach is often chosen as the primary investigative method, while a few other techniques are applied for cross-validation and to gain complementary information^[5].

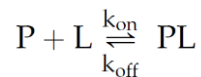
1.1.2 BINDING THEORY: THE LAW OF MASS ACTION

Most of the binding interactions occur between proteins and smaller molecules generically called ligands. These interactions are typically reversible and can be quantified using the law of mass action, a simple physical-mathematical model in which a molecule A binds a molecule B to form the complex AB^[6]:



The binding process is described by the binding kinetics and depends on the rate of association and dissociation of the two binding partners.

When a protein molecule (P) and its specific ligand molecule (L) find each other in solution the interaction system can be described as follow:



where PL is the protein-ligand complex, k_{on} is the association rate constant and k_{off} is the dissociation rate constant. The units of measurement of these two parameters are respectively $M^{-1}s^{-1}$ and s^{-1} .

When the reaction reaches the equilibrium state the association rate is equal to the dissociation rate:

$$k_{\text{on}}[P][L] = k_{\text{off}}[PL]$$

Here the square brackets indicate the concentration of the molecule in solution.

The rate of association k_{on} depends on the concentration of both free protein and free ligand in solution (or the “active masses” of the reactants), because the higher the number of molecules, the higher the probability of their collision. Moreover, because larger proteins have a larger surface area of interaction, the association rate will be higher. Although not every encounter result in a beneficial interaction, once the two binding partners are in proximity, electrostatic forces can draw them towards one other and direct the charged ligand onto the binding site. Furthermore, the organization of the surface chemical groups on the protein can force a ligand that collides anywhere on the protein's surface towards the binding site. On the contrary, if only a fraction of the protein and ligand are in a binding-competent state, the rate of association may be reduced^[2].

The rate of dissociation is a stochastic event and describes the probability of a complex to dissociate the next second and it is only proportional to the concentration of the complex.

Therefore, at equilibrium it is possible to rearrange the equation:

$$K_D = \frac{k_{off}}{k_{on}} \quad K_D = \frac{[P][L]}{[PL]}$$

where K_D is the dissociation constant, a parameter directly related to the affinity of the ligand for the protein. When a ligand concentration is equal to the K_D , the amount of the ligand present in the solution would be statistically enough to bind half of the total number of the binding sites.

Knowing that the total protein concentration is the sum of the free protein in solution and the protein in complex with the ligand as described below:

$$[P] = [P]_{tot} - [PL]$$

the equation can rearrange as follow:

$$[PL] = \frac{[L][P]_{tot}}{[L] + K_D}$$

Considering $[PL]$ as a function of $[L]$, this equation is that of a hyperbola called "Binding Isotherm", becoming a sigmoidal curve using a semi-logarithmic scale, the mostly used model to describe biophysical, biochemical and pharmacological interaction data (**Figure 1**).

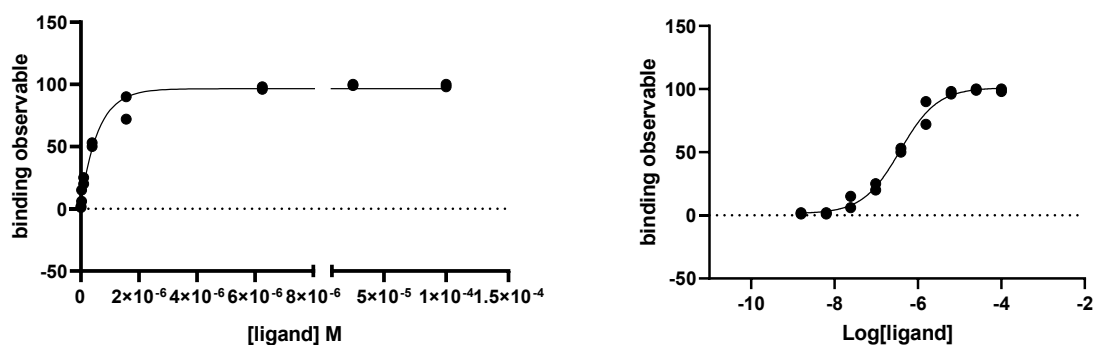


Figure 1 Binding isotherm represented as a rectangular hyperbola (on the left) and as a sigmoidal curve (on the right).

It is important to emphasize that the law of mass action is based on some prerequisites:

1. The reaction must be reversible, so an equilibrium state can be reached.
2. Every protein molecule needs to be equally accessible to the ligand.
3. The protein and the ligand must exist only in the bound or in the unbound state.
4. The interaction must not alter the protein or the ligand.

Some of these assumptions are violated when the mass action equation is applied to complex biological systems, and it is important to recognize these violations in order to comprehend the meaning of the parameters obtained by an interaction assay^[7].

1.1.3 CORRELATION BETWEEN K_D , K_i and IC_{50} : THE CHENG-PRUSOFF EQUATION

When the general concept of the equilibrium dissociation constant (K_D) is applied to enzyme-inhibitor systems it becomes defined as inhibitor constant, K_i . However, the experimental value obtained from an enzyme-inhibitor interaction assay is often the phenomenological term of IC_{50} (half maximal inhibitory concentration)^[8] also defined as the molar concentration of the inhibitor at which the response or binding is reduced by half. In every case the potency term (K_D , K_i or IC_{50} in molar concentration units) is better expressed in the negative logarithm to base 10 (pK_D , pK_i and pIC_{50}), this to reduce the orders of magnitude and to have a symmetrical normal distribution of the standard deviations^[9].

The main difference between the K_i and the IC_{50} is that the first one is an absolute value, only dependent on the real affinity of the enzyme and the inhibitor; instead, the IC_{50} is a relative value that depends on the experimental conditions, such as the enzyme concentration; therefore the IC_{50} term is assay specific and it is always higher or equal to the K_i ^[10].

There are essentially two types of binding assays:

- Saturation experiments
- Competition experiments

In the saturation experiments it is possible to describe the direct interaction of the protein and the ligand by using a labeled form of one of the binding partners. In this case the K_D value can be directly determined^[9] as the equilibrium concentration of the ligand that results in the half of the specific binding signal observed at the maximum binding (B_{max})^[11]. Theoretically this value indicates the ligand concentration that is able to occupy the half of the available binding sites of the protein.

The competition assays are usually performed by fixing a single concentration of the protein and a labeled ligand while increasing the concentration of a non-labeled compound to compete with the labeled reference^[12]. In this type of analysis, the obtained interaction parameter is called IC_{50} (also referred as apparent K_i), and it refers to the concentration of the competitive ligand that inhibits 50% of the binding of the labeled ligand to the protein^[11].

The IC₅₀ value depends on:

- The real affinity of the protein for the non-labeled inhibitor (K_i)
- The affinity of the protein for the labeled ligand (K_D)
- The concentration of the labeled ligand ([L*])^[13]

These terms are in correlation through the Cheng-Prusoff equation:

$$K_i = \frac{IC_{50}}{1 + \frac{[L^*]}{K_D}}$$

The equation is based on some assumptions:

1. The system has reached the equilibrium state;
2. The binding is reversible and follows the law of mass action;
3. The affinity between the protein and the labeled ligand (K_D) is known;
4. There is no cooperativity;
5. The ligand can be considered free at every considered concentration due to the small bound fraction bound to the protein;
6. All protein molecules have the same affinity for the ligand.

It follows that in some experimental conditions that violates the assumptions, the simple derivation of K_i from IC₅₀ becomes unachievable, necessitating the use of more complex models to quantify inhibitor potency.

1.1.4 FITTING MODELS

An experimental x-y data set should be described by using an appropriate fitting model. As mentioned before [paragraph 1.1.2], the nonlinear models are the mostly used to describe biological data and the method that allows to find the best parameters to closely fit the model to the experimental data is the nonlinear regression^[14].

A fitting model is a description of the experimental system. It could be more or less complex, and as it increases in complexity, the model will always better accommodate the data set. However, by increasing the complexity it is possible the model will have too many parameters to be considered really useful, falling into the problem of the *overfitting*.

Therefore, the main goal is to find the simplest model to best-fit the experimental data, while having sufficient complexity to understand the biology system through a reasonable number of parameters^[15].

A general nonlinear model can be expressed as:

$$y_i = f(x_i, \beta) + \varepsilon_i$$

where y_i is the continuous dependent variable (the biological observable); this is function of the x_i , the explanatory variable, and of β , the unknown parameters of the model. The ε_i is the residual error term.

The nonlinear model makes some assumptions:

- The error terms follow a normal distribution
- The variances of the error term are homogenous (homoscedasticity)
- The observations are independent.

The nonlinear regression is an iterative process that, through the *nonlinear least-square* (NLS) method, systematically changes the parameters of the chosen fitting model until it minimizes the squared differences between the observed and estimated y values^[15].

It is important to notice that, unlike linear regression, an iterative method implies a choice of starting values. The analysis software usually chooses the values automatically, but the experimenter needs to be aware of the possible presence of a false minimum in the system (**Figure 2**). This intrinsic problem can be overcome by choosing an appropriate x values range and by attempting a different set of initial values to ensure obtaining similar parameter values^[15].

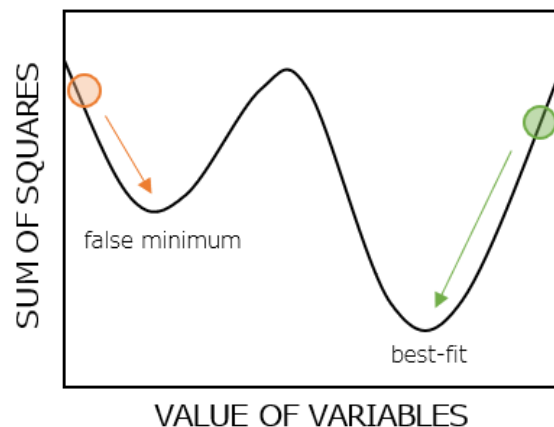


Figure 2 By choosing the orange point as the initial value for a given parameter, the system will converge into a false minimum. Instead, by trying a second different starting value of the parameter (the green one), the system will find the best-fit value.

There are two main decisions to make when first approaching an interaction data set:

- 1) The model to choose
- 2) The parameters that need to be held constant

The most commonly used sigmoidal model to fit biological data is the "Hill equation," also known as the "**four parameters logistic equation**":

$$Response = Bottom + \frac{Top - Bottom}{1 + 10^{(Log IC50-x)HillSlope}}$$

where Bottom is the Y baseline value, Top is the Y value at the top plateau and the Hill Slope is the steepness of the curve. This latter parameter could give important information about the biological system; however, in ideal experimental conditions of single site interaction and when the data follow all the assumptions of the law of mass action, the Hill Slope should be equal to 1. In these cases, it is possible to simplify the fitting model by constraining the slope to the expected value of 1 by using the "**three parameters equation**".

$$Response = Bottom + \frac{Top - Bottom}{1 + 10^{(Log IC50-x)}}$$

With a given data set, it is possible to perform a statistical analysis in order to evaluate which model better fits the data and if the Hill Slope value in the unconstrained model is significantly different from 1. In analysis software such as GraphPad Prism two approaches can be used: the extra sum-of-squares F test (based on ANOVA and the test of statistical hypothesis) and the AIC (Akaike's Information Criterion) method^[15]. The F test can be performed only when the two models being compared are *nested* (one model is a simplified case of the other), which is the situation for the comparison of the three and four parameter equations. When the models are not *nested*, the AIC method should be used to compare them^[15].

A statistical test can determine whether the slope is significantly different from the ideal value of 1. If this is the case, the slope value may provide information about the experimental system. A high Hill Slope value, for example, could reflect an experimental condition of ligand depletion due to a high protein concentration: the protein concentration can normally be neglected but in this case needs to be included into the fitting model as independent parameter and the best fitting model could become the "**quadratic Morrison equation**"^[8]:

$$Response = Bottom + \frac{(Top - Bottom)([L] + [P] + K_D) - \sqrt{([L] + [P] + K_D)^2 - 4[L][P]}}{2[P]}$$

where [P] is the protein concentration and [L] is the ligand concentration.

In other circumstances, the interaction system is just too complex for quadratic equation resolution, and the parameters become ambiguous or nonsensical due to the constraints that won't accommodate the experimental data and the too low number of fitted parameters. In such cases, a more complex model, such as a cubic equation, may provide more robust parameters, although it would be more difficult to resolve and interpret in terms of its biological meaning^[15].

1.1.5 KEY CRITERIA TO MEASURE BINDING REACTIONS

During the design of an interaction assay, two crucial experimental aspects must be considered:

- The concentration of the interacting components
- The time of equilibration

A lack of equilibration time or an improper concentration regime may result in unreliable binding measurements^[16].

CONCENTRATION OF THE BINDING PARTNERS

Usually a binding assay is performed by fixing the total concentration of one of the two binding partners and by titrating the other. The assay reading can be any arbitrary observable as long as the registered signal is directly proportional to the amount of the formed complex^[2].

Ideally, the concentration of the variable component should be well above the K_D value to be sure of reaching the saturation plateau. This is important to not compromise the value of the affinity results by using an incomplete binding curve.

On the contrary, the concentration of the fixed reactant should be at least ten times lower than the K_D , this simplifies data interpretation because the other reactant can be considered free under all conditions. Indeed, at high concentration of the titrating compound, its difference with the fixed compound is significant, and the second one can be neglected. When the titrating compound concentration goes below the K_D most of the latter is free since minimal binding occurs due to the

low concentrations of both reactants^[6]. If this is the case, the experimental points should be plotted with the hyperbola function described above, and the half-saturating value of the titrating component is equal to the K_D .

However, in some cases for experimental or practical reasons it is not possible to use a concentration lower than the K_D ; if this happens, the concentration of the constant component should be taken into account in order to not underestimate the real affinities and avoid artifacts. As mentioned above, in this case the best fitting model will become the quadratic Morrison equation^[16] and it is likely the system has encountered a tight binding condition.

TIME OF EQUILIBRATION

The dissociation constant, as previously noted, is an equilibrium parameter. As a result, the system should reach equilibrium before making any assumptions about the affinity of the interaction partners and the needed time depend on vary experimental conditions such as ligand and protein concentrations and temperature. The equilibration time increases at lower concentrations; therefore, equilibration time should be evaluated at low concentration of the ligand (around the 10-20% of the K_D)^[15].

1.1.6 MODES OF INHIBITOR INTERACTIONS

Protein inhibitors can act in different modes, either in a reversible or irreversible way. However, the most commonly observed interaction behavior is reversible binding, and by proceeding along the Drug Discovery pipeline, the number of potent inhibitors that can potentially become approved drugs increases as well. Therefore, it becomes significant to implement biophysical methods able to reliably describe potent interactions. On the other hand, since the number of irreversible and time-dependent inhibitors has expanded in the last few decades, the best biophysical description of non-equilibrium interaction systems, such as slow binding and covalent binding, can also be a critical aspect to investigate.

TIGHT BINDING^{[14][16][17][18][19]}

The tight binding experimental conditions occur when the analyzed inhibitor has an inhibition constant, K_i , lower than the specific protein concentration selected for the assay. As a result, tight binding is not an absolute characteristic inherent to the potent compound, but rather a relative condition strictly dependent to the experimental chosen concentrations.

When tight binding occurs, at inhibitor concentrations lower than the protein concentration every ligand molecule added to the system is sequestered by the protein itself. Therefore, the protein-inhibitor interaction will be governed by the amount of protein in the system rather than the actual affinity of the small molecule.

When an interaction experiment is performed, the derived phenomenological IC_{50} value becomes strongly dependent on the protein concentration and, since the IC_{50} is the inhibitor concentration required to achieve 50% binding, it will never be less than half the protein concentration.

In classical binding conditions, when $K_i > [P]$, it is possible to assume that $IC_{50} \sim K_i$.

Instead in tight binding conditions the protein concentration becomes a relevant parameter. If $K_i/[P]$ is between 0.01 and 10, the IC_{50} depends on both the protein concentration, $[P]$, and the K_i , according to the following equation:

$$IC_{50} = \frac{[P]}{2} + K_i$$

When $K_i/[P]$ is lower than 0.01 the IC_{50} becomes independent from the K_i value and the equation is rearranged:

$$IC_{50} = \frac{1}{2} [P]$$

In these conditions the system has entered the *titration regime*, the “ IC_{50} wall” has been hit and the IC_{50} will not fall below the half the protein concentration (if it does, the latter has been probably overestimated in terms of active fraction).

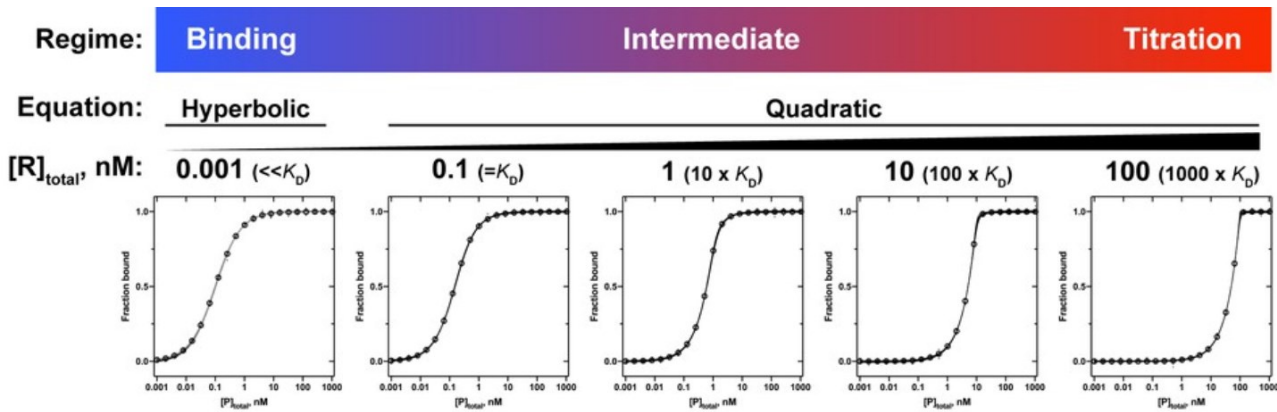
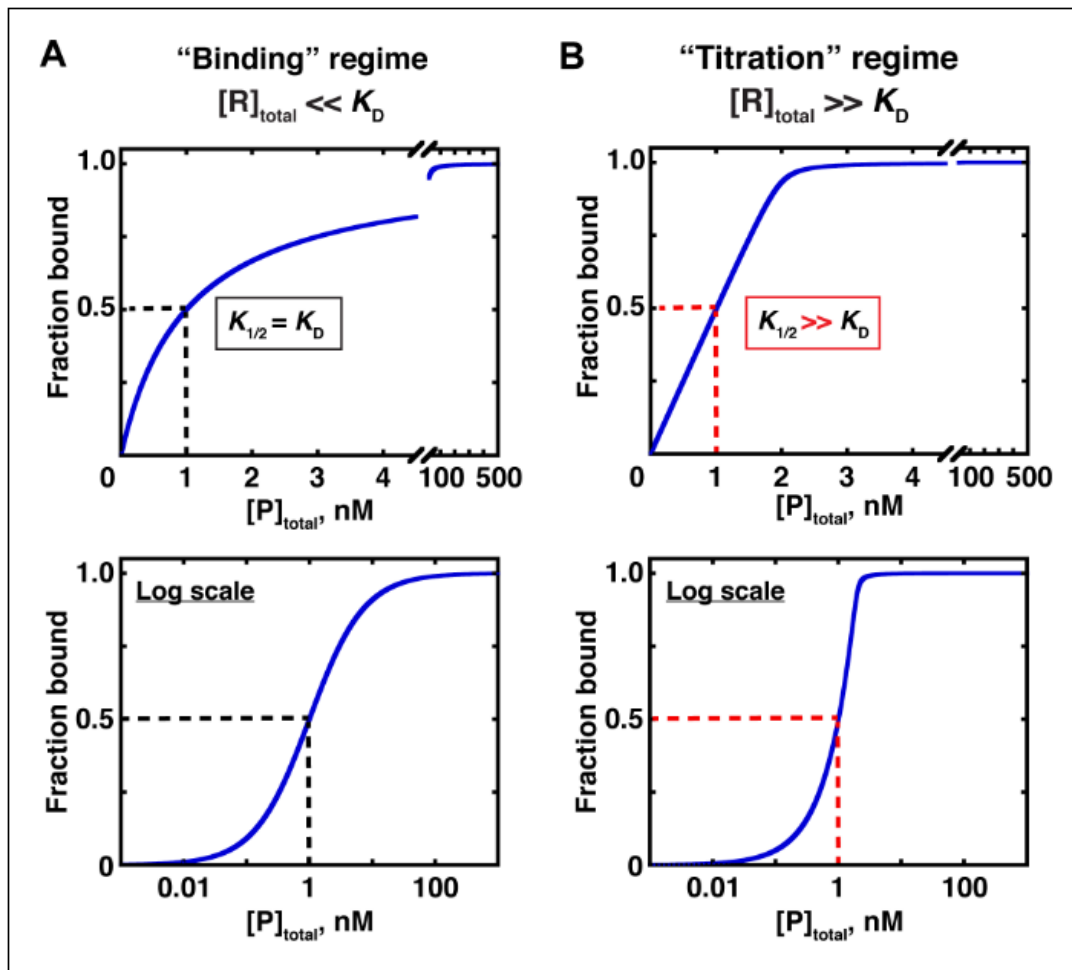


Figure 3 Different aspect of interaction curves: in the “A” section is reported the classical binding curve (when $K_D > [P]$), while in the “B” section is indicated the titration regime when $K_D \ll [P]$. The steepness of the curve becomes higher and the best fitting model becomes the quadratic.

Adapted from: Jarmoskaite, I. et al. (2020) ‘How to measure and evaluate binding affinities’, eLife, 9, pp. 1–34. doi: 10.7554/ELIFE.57264.

When the system is in tight binding conditions, the data can be elaborated using the quadratic Morrison equation, which includes the protein concentration as a parameter into the fitting model.

One issue of debate is whether to leave the $[P]$ float and so consider it as a variable parameter, or to keep it constant when applying the Morrison model. Kuzmic (2000) and Murphy (2004) reported distinct simulation studies in which they concluded that as the ratio of K_i to $[P]$ drops, the inaccuracy in calculating K_i increases by fixing the protein concentration. The proposed solution involves working in two steps: first, fixing the protein concentration to its nominal value and observing the resulting inhibition constant: if the K_i value is greater than the fixed $[P]$ value, the final result can be accepted. Alternatively, the fitting analysis must be repeated while allowing the model to fit the protein concentration as a variable parameter.

Otherwise, according to Copeland (2005 and 2013), allowing the protein concentration to fluctuate may result in physically incoherent estimations of $[P]$ as well as errors in estimating K_i .

However, both points of view agree on the importance of accurately estimating the protein active fraction. The protein population is assumed to exist in at least two states, one of which is binding competent and the other unfolded or denatured. The competent state may be in turn populated by different conformational states.

The active fraction can be determined by exploiting the tight binding situation itself. One of the two binding partners has to be fixed at a concentration greater than K_i (the optimum would be a factor 200) to achieve tight binding conditions. The concentration of the other binding partner must be titrated over a narrow range, which includes the first one. As a result, there will be two distributions of points that can be fit by two different linear regressions. The distribution at high titrant concentrations indicates the totally bound condition, whereas the distribution at lower titrant concentrations indicates the titrating regime. Assuming a stoichiometry of 1:1 the amount of the active fraction is determined by the breaking point between the two distributions. By increasing the tight binding condition, the breaking point becomes sharper, and the active fraction is more precisely defined (**Figure 4**).

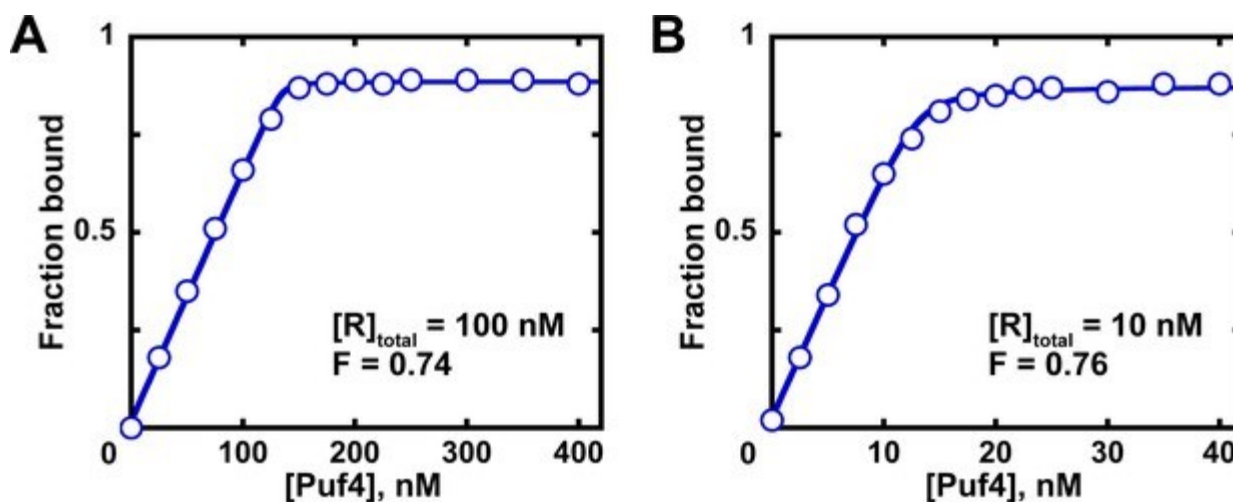


Figure 4 The figure is referred to a case study reported by Jarmoskaite (2020) in which RNA is used as biological target and tested at the fixed concentration of 100 nM (on the left) and 10 nM (on the right). The measure of the protein active fraction was conducted by titrating the protein Puf4 while in tight binding conditions. By using a higher RNA concentration (on the left), the two distributions of points are better described, and the breaking point is sharper.

Jarmoskaite, I. et al. (2020) 'How to measure and evaluate binding affinities', eLife, 9, pp. 1–34. doi: 10.7554/ELIFE.57264.

Once the amount of active protein has been identified, the binding data can be fitted by using the Morrison equation, by including the actual amount of protein capable of binding into the model.

SLOW BINDING^[17]

Slow binders are compounds that either associate or dissociate slowly from the protein. Therefore, due to their time dependence, affinity and potence need to be established only after the reaching of equilibrium.

Slow binding can occur with different mechanisms:

- Simple reversible slow binding: mechanism in which the association, the dissociation or both are slow;
- Induced-fit: two-step reaction with a first rapid interaction and a following slow interconversion of the protein to a form that better accommodates the ligand;
- Conformation selection: two-step reaction with a first slow conformational interconversion of the protein and then a rapid interaction with the inhibitor.

Usually a complete characterization of slow binders yields the inhibition mechanisms, the true affinity based on enzymatic assays and the indication of the residence time, the period of time that the ligand spends bound to its target.

COVALENT BINDING^{[17][20][21][22]}

Covalent inhibitors are molecule with a reactive warhead aimed to form covalent bond with specific residues of target proteins. They often involve a two-step reaction, the first of which is a reversible interaction between the inhibitor and its binding pocket while the covalent bond itself is formed as a result of the second following reaction. The possible difficulty in selectivity is balanced by a longer duration of action, improved ligand efficiency, and the capacity to avoid drug resistance.

Therefore, the covalent interaction consists of two components: the binding affinity between the inhibitor and the protein (K_i) and the chemical reactivity described by the rate of enzyme inactivation (k_{inact}), the required time to covalently modify half of the protein^[23]. Usually covalent inhibition is described with the covalent efficiency constant (k_{inact}/K_i) a preferred parameter describing the inhibitory potency without the time dependence interference. However, in some cases the inhibitory concentration at a specific time, $IC_{50}(t)$, can be carefully used as surrogate of the parameter k_{inact}/K_i , to can more easily correlate data with other activity assays^[24].

Finally, the verification that the irreversible reaction has occurred is a critical element to take into account. The methods usually employed for this purpose are mass spectrometry analyses to identify the covalent adduct and the enzymatic test of activity recovery after a massive dilution (Jump Dilution).

1.2 THE MICROSCALE THERMOPHORESIS (MST)^{[25][26][27][28]}

Among the different biophysical approaches aimed at the characterization of protein-ligand interactions (e.g. ITC, SPR, fluorescence spectroscopy, etc.), the MicroScale Thermophoresis emerges as a versatile technique for the detection of binding between a large variety of molecular species. The approach main advantages are its minimal sample consumption, quickness of analysis, ability to utilize almost any type of buffer, and ability to discover binding of any nature (orthosteric, allosteric, etc.) as long as a sufficient ligand-dependent change in thermophoretic mobility occurs.

1.2.1 GENERAL DESCRIPTION

The MicroScale Thermophoresis (NanoTemper) is an immobilization-free biophysical technique for the characterization of bimolecular interactions. The method is based on a physical phenomenon called *thermophoresis*, according to which every molecule in a fluid and subjected to a temperature gradient will start to migrate along the gradient, with a rate directly related to its physical characteristics; in particular it has been demonstrated the three aspects that mainly impact on the thermophoretic migration are:

- Size
- Charge
- Hydration shell

These characteristics are strongly influenced by external perturbation of the system; indeed, by considering the single molecule of a protein, its size, charge and conformation may significantly change in the presence of a specific interactor like an inhibitor. Therefore, it is by titrating the protein with a ligand molecule that is possible to monitor the change in thermophoresis migration of the resulting complex and to use that information as observable to obtain a binding curve and specific interaction parameters.

In the MicroScale Thermophoresis (MST), the molecule movement start with the activation of an infrared laser (wavelength 1480 nm) and its energy absorption by the water molecule in solution. This rapidly results in the generation of a temperature gradient along the capillary tube inside of which the sample is loaded; the molecules start to migrate from the hotter to the colder zone as a consequence of the so-called *Soret's effect*. The movement continues until it would be contrasted by the back-diffusion of the molecules.

The *Soret's effect* is described by the following equation:

$$S_T = \frac{A}{k_B T} (-\Delta S_{\text{hyd}}(T) + \frac{\beta \sigma_{\text{eff}}^2}{4\epsilon\epsilon_0 T} \lambda_{\text{DH}})$$

where S_T is the Soret coefficient, A is the molecule surface, λ_{DH} is the Debye length, k_B is the Boltzmann constant, ΔS_{hyd} is the particle-area-specific hydration entropy, σ_{eff} is the effective surface charge density, ϵ is the dielectric constant, β is the coefficient that describe the correlation between the dielectric constant and the Debye length, T is the temperature (expressed in Kelvin)^[29].

Once the IR ray has activated and generated the temperature gradient, the movement of the molecules is detected by their intrinsic fluorescence or through the use of fluorophores covalently attached to the protein. Indeed, a fluorescence detector is placed in the same spot of the IR activator and collects the information of decrease in the observed fluorescence in the center of the temperature gradient.

The IR laser intensity is determined by the MST power, which may be regulated in three modes: low, medium, and high. The irradiation sample volume is approximately 2 nL, with a heated zone diameter of 100 μm , and the temperature gradient amplitude increases with intensity. In **Figure 5** is reported a representation of every step of an MST experiment.

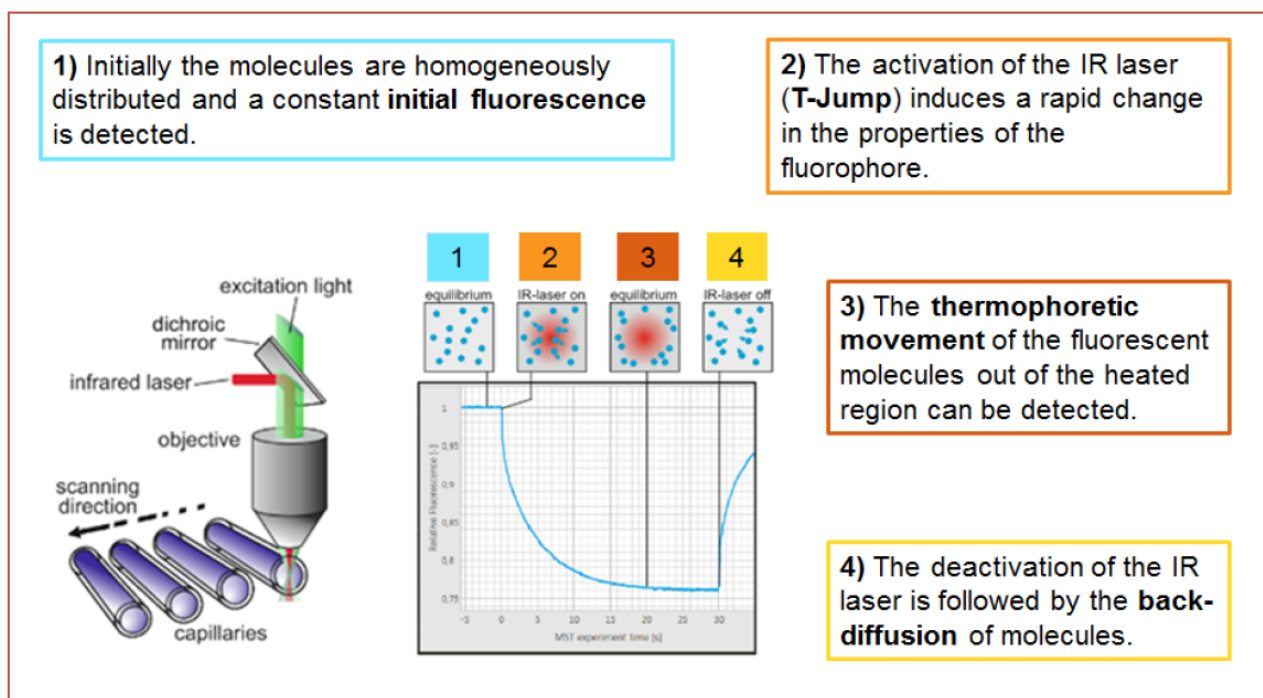


Figure 5 Representation of an MST experiment and its phases.

Adapted from M. Jerabek-Willemsen et al., "MicroScale Thermophoresis: Interaction analysis and beyond," *J. Mol. Struct.*, vol. 1077, pp. 101–113, Dec. 2014, doi: 10.1016/j.molstruc.2014.03.009.

The time along which the IR laser remains active is named MST-ON time and usually the experimenter can arbitrarily choose among six different MST-ON time, (1.5, 2.5, 5, 10, 15 and 20 seconds). Immediately after the IR activation the system detects a consistent drop in relative fluorescence called T-Jump. The initial change in fluorescence is most likely caused by the greater fluorophore collisional quenching at elevated temperatures (TRIC, Temperature Dependent Intensity Change) rather than the actual *thermophoresis* of the molecules^[28]. The later migration times, instead, are most likely to be governed by the global properties of the molecule or complex in terms of size, charge and hydration shell.

The fluorescence decrease at every MST-ON time (F_{hot}) is compared to the initial fluorescence (F_{cold}) and plotted as normalized fluorescence ($FNorm$), on a fractional or *per mille* scale:

$$FNorm = \frac{F_{hot}}{F_{cold}} \text{ ‰}$$

As already mentioned, the thermophoretic mobility of a protein should change in the presence of a ligand that modifies the migration characteristics of the protein alone. Therefore, by titrating the interactor from an appropriate starting concentration, around 50-100-fold the estimated K_D , it is possible to obtain a symmetrical distribution around the ligand concentration corresponding to the K_D value. Then, by choosing an arbitrary MST-ON time, the relative experimental points set can be fitted to obtain an interaction curve and the relative parameters (**Figure 6**).

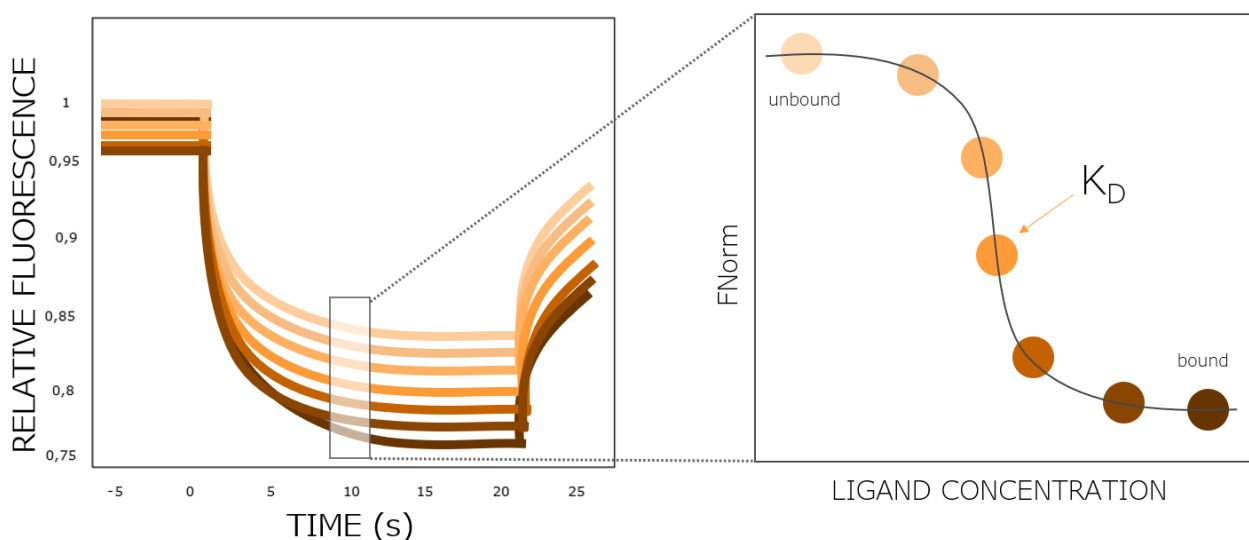


Figure 6 Representation of how a binding curve is derived from thermophoresis traces.

The difference between the MST signal of the unbound and bound states is called Response Amplitude and depends on both the MST-ON time (later times are always characterized by a higher Response Amplitude) and on the MST power.

An indication of the quality of the binding curve is the signal-to-noise ratio (S/N) defined as follow:

$$\frac{S}{N} = \frac{\text{Response Amplitude}}{\text{Noise}}$$

where the Noise is the standard deviation of the measurement and it is defined as the MST signal variation do not caused by the interactor:

$$\text{Noise} = \sqrt{\frac{\sum_i (r_i - \bar{r})^2}{n - 1}}$$

with r_i indicating the residual of the fit, \bar{r} the average of all residuals and n the number of data points^[30].

Another method to indicate the Noise is the standard deviation of the residuals (Sy.x), reported by software like GraphPad Prism:

$$Sy.x = \sqrt{\frac{\sum_i (\text{residual}^2)}{n - K}}$$

where the residual is the vertical distance (Y units) of the experimental points from the curve and n-K is the number of degrees of freedom of the regression.

1.2.2 MST APPROACHES

The MicroScale Thermophoresis can be used for two different approaches: the competition assay and the direct binding assay.

The competition assay relies on the use of a fluorescent molecule to bind the protein target; then, a second non-fluorescent molecule is titrated to displace the first one, and an indirect indication of the affinity of the titrating molecule is collected.

The direct binding assay relies on the use of a fluorescent molecule as one of the binding partners to obtain affinity information on the interaction system with a non-fluorescent molecule which is titrated. To employ the direct binding strategy, one of the interactors must be fluorescent, either intrinsically or extrinsically, and fall within the emission-excitation range in order to be detected correctly throughout the experiments. In **Figure 7** are reported different types of fluorescent dyes and their excitation and emission ranges.




























Fluorophore	Excitation [nm]		NT.115 Blue/Green	NT.115 Blue/Red	NT.115 Green/Red	NT.115 pico	Emission [nm]
BCECF	480						525
GFP	488						507
NT-495 (BLUE)	493						521
Fluorescein (FITC)	495						519
Alexa488	495						519
YFP	514						527
Alexa532	530						555
TAMRA	546						579
Cy3	550						570
RFP	555						584
NT-547 (GREEN)	557						574
Alexa546	560						572
Cy5	649						670
NT-647 (RED)	650						670
Alexa647	652						668

Figure 7 Different types of dyes and their excitation and emission ranges. The instrument used for the analysis of this work and the potentially applicable fluorophores for measurements on the device are indicated in the red box.

Adapted from NanoPedia - Monolith NT.115, NanoTemper Technologies GmbH.

The binding approach frequently requires covalent labeling of the protein, which can be a difficult step due to the likelihood of dye interference with the structure and functionality of the protein, and thus with its binding competence^[31]. Furthermore, the degree of labeling must be optimized because a low amount of dye covalently attached to the protein may result in a low fluorescence

signal, necessitating the use of a high protein concentration to compensate; this exposes another issue with the characterization of potent inhibitors, which instead require a low protein concentration to avoid the tight binding condition. Finally, an efficient purification system must be applied to reduce the free dye in solution, source of noise in the interaction system and of an overestimated DOL.

Therefore, the labeling conditions must be carefully investigated by testing different labeling times and dyes, as well as protein and dye ratios. Where possible, the use of an active site protector can be a reasonable choice to avoid the reaction of any residue essential for binding and protein activity.

Typically the most commonly covalent dyes used in MST are the **N-hydroxysuccinimide esters (NHS)**, which binds the aminic terminal group of lysines by following the reported reaction scheme:

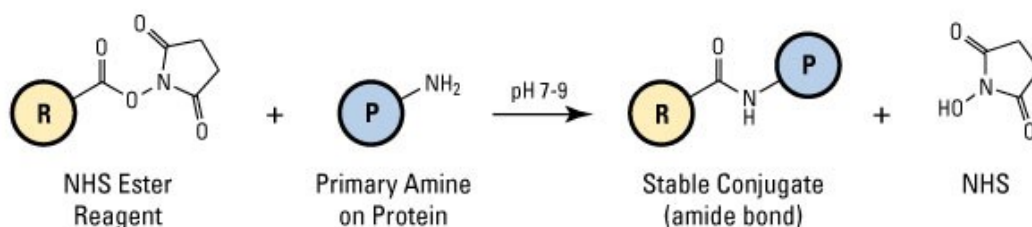


Figure 8 Scheme of a labeling reaction on the lysines by using NHS esters.

<https://www.thermofisher.com>

In general, the fluorescence signal is proportional to the target concentration and the Excitation Power, which is the intensity of the LED lamp used for fluorophore excitation. The Excitation Power can be modulated up to 100 % to obtain a fluorescence intensity in the optimal range of 200 and 2000 counts. The fluorescence signal will be stronger when the Excitation Power is set to 100%, but the noise in the measurements may increase due to photobleaching, a decay of fluorescence intensity caused by excitation light that is typically caused by reactive oxygen species that react with the excited states of fluorophores. Due to these effect the experimenter should always ponder the use of high Excitation Power to avoid an undesired reduction in signal-to-noise ratio^[32].

1.3 PROTEIN KINASES AS DRUG TARGETS

Protein kinases are more than 500, constitute around 2% of all human genome and their enzymatic activity occurs by the transfer of a phosphate group from ATP to specific substrates^[33]. This has an impact on cellular signaling cascades, which have a wide range of effects on the overall homeostasis of the organism. Because their dysregulation frequently leads to a variety of disorders, this protein class has emerged as an important therapeutic target.

Despite the fact that protein kinases have a highly conserved ATP binding region, drug development for protein kinase inhibitors has yielded a large number of molecules with good selectivity and a diverse variety of binding modes^[34] that can be classified in different groups:

- Type I: inhibitors that target and bind the active form of the kinase;
- Type II: inhibitors that interact with the kinase inactive conformation;
- Type III: inhibitors which target an allosteric pocket;
- Type IV: inhibitors targeting a pocket placed in a distal portion of the protein compared to the ATP binding pocket.

Kinase inhibitors can also be either covalent or reversible and usually the covalent drugs target a non-conserved residue such as cysteine or lysine placed in proximity of the ATP pocket^[35].

A common characteristic of protein kinases is their wide number of microstates in which they interconvert through conformational changes to effectively perform the catalytic activity. Their catalytic domain consists of two lobes (N-terminal and C-terminal) and the ATP binding pocket is located between them. In the N-lobe it has been found different motifs important for the regulation of the kinase activity and its conformational state. Of particular significance are the α C-Helix, the P-Loop (rich in glycine), and the DFG motif (Asp-Phe-Gly) found at the end of the Activation Loop (A-Loop). Conformational changes in protein kinases are associated with several rearrangements of these and other motifs^[36] and, in particular, the DFG motif can take a movement (DFG-flip) that interconverts the protein from the active (DFG-in) to the inactive (DFG-out) state. The latter is the conformation bonded by the Type II inhibitors^[37].

In **Figure 9** an EGFR crystal shows the kinase motifs important for the conformational change of the protein.

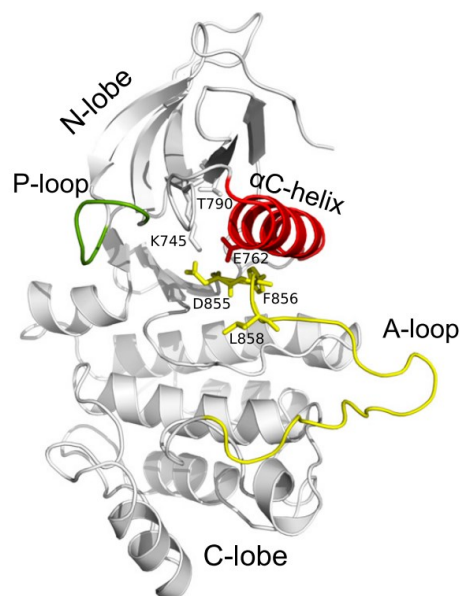


Figure 9 Crystal representation of EGFR active state and its motifs P-loop, α C-Helix and A-loop that contribute to protein conformational changes. PDB: 2GS2.

Sutto, L. and Gervasio, F. L. (2013) 'Effects of oncogenic mutations on the conformational free-energy landscape of EGFR kinase', PNAS, 110, pp. 10616–10621. doi: 10.1073/pnas.1221953110.

The conformational states in the protein molecules yield to the formation of a variety of binding pockets and, as a consequence, drugs and ligands can have different propensities to interact with the target when in a specific conformation. Other than that, the binding of a specific ligand to its binding pocket may stabilize a particular conformational state and shift the natural equilibrium of interconversion towards that microstate, representing an opportunity for the diversification of Drug Design efforts^[17].

As a result, having reliable methods for identifying and characterizing binding mechanisms of as many binding modalities as possible becomes important for both gaining a deeper understanding of drugs already known in the drug science landscape and characterization of new small molecules potential drugs.

1.3.1 EPIDERMAL GROWTH FACTOR RECEPTOR (EGFR)

EGFR is a protein kinase belonging to the family of transmembrane epidermal growth factor receptor (EGF/ErbB), it is normally activated by the Epidermal Growth Factor EGF and in physiologic conditions is involved in regulation of epithelial tissue development. Its anomalous activation and overexpression due to mutated forms is an oncogenic driver of several types of cancer, making the study of this target and investment in EGFR inhibitor Drug Discovery an important field of research^{[36],[38],[39]}. One of the most common mutations involves the L858R residue, changing from a leucine to an arginine (L858R); this mutation, which is unfortunately very common in cancer, results in hyperactivation of the protein, that assumes a catalytic efficiency 20-50-fold higher than the wild type^[40]. Normally EGFR activation is preceded by protein dimerization: it has been observed that the higher activity of the L858R mutated form can be attributed to its tendency to dimerization even in the absence of its extracellular growth factor, EGF^[41].

Gefitinib (Iressa[®]) is a 4-anilinoquinazoline EGFR L858R-selective inhibitor in clinical use that binds the active conformation of the protein (Type I inhibitor). Gefitinib has been demonstrated to not stabilize the inactive conformations of EGFR^[42] and to selectively bind the active form of both EGFR wild type and L858R^[43]; thus, its selectivity toward the mutated form can be attributed to the more highly populated active conformational state in the EGFR L858R^[40] (**Figure 10**).

Targeting the inactive conformation can improve selectivity and safety^[43]; thus, inhibitory strategies for EGFR proteins can include the development of different classes of inhibitors that target both the active and inactive conformations, and various binding modes have been investigated in an effort to overcome cancer resistance in treated patients^[39].

For example, Lapatinib (another 4-anilinoquinazoline) has been shown to have the ability to stabilize EGFR inactive conformation^[42], making it a Type II inhibitor. This feature results in a slow off-rate of the inhibitor from the active site, which can have a positive effect on increasing its inhibitory activity duration *in vivo*^{[34][44]}.

It has been seen that EGFR exhibits different conformational states and the interconversion is ruled by the displacement of α C-Helix and flipping of DFG motif^[39].

In particular, three EGFR conformations have been reported: the active (DFG-in), the inactive (DFG-out) and the Src-like inactive (similar to the conformation observed in the Src tyrosine kinase) that is intermediate between them. The EGFR wild type mainly populates the inactive form, while the active mutants change the conformational free energy landscape leading to a more populated active

state^[40]. It has been suggested that Lapatinib slow kinetics is probably due to the rate-limiting transition of EGFR to the inactive conformation starting from the intermediate Src-like inactive conformation^[41].

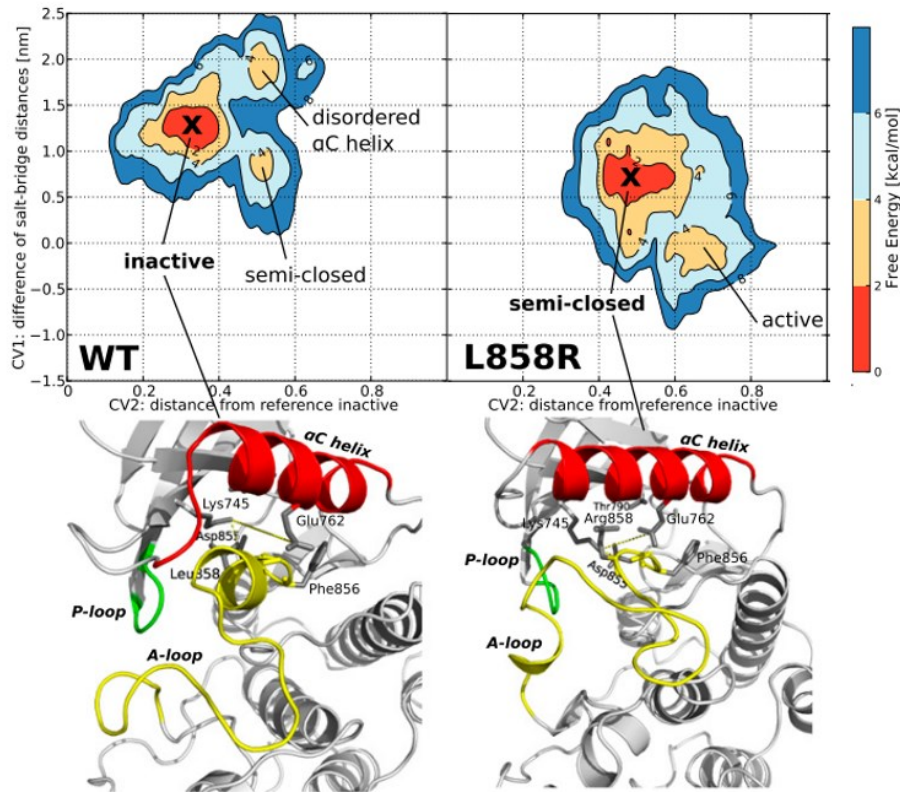


Figure 10 Free energy surface of EGFR (wild type and L858R) that shows how EGFR wild type populates the inactive state while the L858R mutant most stable state corresponds to a structure in between the active and inactive conformations. The active state is however populated even if with a thermodynamic penalty.

Adapted from: Sutto, L. and Gervasio, F. L. (2013) 'Effects of oncogenic mutations on the conformational free-energy landscape of EGFR kinase', PNAS, 110, pp. 10616–10621. doi: 10.1073/pnas.1221953110.

Finally, another strategy, this time to overcome the emergence of drug resistance (mainly due to secondary mutations of the protein into the EGFR L858R/T790M and T790M activated forms), resulted in the development of third-generation inhibitors, which are aimed at irreversibly blocking the protein activity via a covalent interaction with the C797^[45]. A representative drug of this class is Osimertinib, which has been demonstrated to covalently modify the catalytic domain of EGFR^[46].

1.3.2 RHO-ASSOCIATED PROTEIN KINASE (ROCK)

ROCKs are cytoplasmatic proteins that belong to the serine/threonine kinase family. Two isoforms have been identified: ROCK-1 and ROCK-2^[47]. Rho-GTPase proteins bind ROCK, its downstream effector, activating a variety of pathways primarily involved in cytoskeletal structure and vascular smooth muscle contraction^[48] proliferation and apoptosis^[49].

Because abnormal ROCK activation contributes to a variety of clinical diseases, these proteins have emerged as interesting pharmacological targets for several inhibitors currently being tested in various disease models. ROCK inhibitors can find therapeutic applications in cardiovascular pathologies, kidney disease, pulmonary hypertension, neurodegenerative diseases, atherosclerosis, and cancer^{[49],[50]} with the majority of compounds being Type I inhibitors competing for ATP^[49]. An example is Fasudil, a clinically approved ROCK inhibitor targeting the ATP kinase domain, that has been widely used for the treatment of cerebral consequences of subarachnoid hemorrhage^[50].

2. AIM OF THE WORK

This work aims to validate the MicroScale Thermophoresis (MST) as a biophysical technique to obtain valuable information on different binding modes in the field of protein kinase inhibitors.

The relevance and the therapeutic potential that kinase inhibitors assumed in pharmaceutical research are due to the essential role these proteins play in life processes and in several pathologic conditions. Therefore, in the last decades medicinal chemistry directed its efforts to the characterization of kinase-inhibitor interaction in order to optimize drug design. Most of the information addressing SARs (Structure-Activity Relationship) choices result from in vitro studies^[3].

Protein kinase inhibitors have a wide range of inhibition mechanisms, thus having a biophysical platform from which obtaining reliable information on these mode of action varieties is important for both a deeper understanding of already known mechanisms and a more trustable investigation of new potential drugs.

MicroScale Thermophoresis is in most cases only applied to gain the affinity information of K_D or IC_{50} , but this perspective might be limiting considering the potential of the technique and its low sample consumption and rapidity of analysis.

In this study, the MST has been employed to characterize, from different perspectives, the interaction modalities of two model protein kinases of pharmaceutical interest (EGFR and ROCK) and their well-known inhibitors to create a wide range knowledge to be used in future and unknown interaction systems.

3. MATERIALS AND METHODS

The following methods are referred to the interaction experiments performed with the instrument Monolith NT.115 (NanoTemper).

3.1 EGFR

3.1.1 MATERIALS

The EGFR (Epidermal Growth Factor Receptor) interaction system has been investigated through the competition assay and the isoforms considered were the catalytic domains of EGFR wild type and the mutate form EGFR L858R. The tested inhibitors were the three orthosteric compounds Gefitinib, Lapatinib and Osimertinib. For the competition assay the selected fluorescent species was the Kinase Tracer 199.

In the table below are reported the characteristic of the starting material purchased for the experiments.

Item	Supplier	Product Number	Lot	Tag	Sequence (start-end)	MW Da	Concentration	Purity	Storage buffer
EGFR (ErbB1) Wild Type	Thermo Fisher	PR7295B	2281133H	GST	668-1210	90500	4.86 μ M (0.44 g/L)	70 %	50 mM Tris (pH 7.5), 150 mM NaCl, 0.5 mM EDTA, 0.02% Triton [®] X-100, 2 mM DTT and 50% Glycerol
EGFR (ErbB1) L858R	Thermo Fisher	PR7447A	2468986C	GST	668-1210	90500	3.09 μ M (0.28 g/L)	70 %	50 mM Tris (pH 7.5), 150 mM NaCl, 0.5 mM EDTA, 0.02% Triton [®] X-100, 2 mM DTT and 50% Glycerol
Kinase Tracer 199	Thermo Fisher	PV5830	-	-	-	-	25 μ M	-	DMSO
Gefitinib (Iressa [®])	UniPR	-	-	-	-	446.90	-	-	Powder
Lapatinib (GW572016)	Med Chem Express	HY-50898	-	-	-	581.06	10 mM	-	DMSO
Osimertinib (AZD9291)	Med Chem Express	HY-15772	-	-	-	499.61	10 mM	-	DMSO

The employed proteins are recombinant and fused to glutathione S-transferase (GST-tag), a commonly used method to improve purified protein solubility^[51]. The constructs are the same employed in two cited works^{[52][53]} and this allowed a direct comparison between the reported results and the different interaction systems to further validate MST as a valuable technique orthogonal to other biophysical approaches.

3.1.2 MATERIAL HANDLING AND STORAGE

Both proteins and small molecules in DMSO are stored at -80°C upon their arrival.

The Kinase Tracer 199 is stored at -20°C.

Proteins

For the first use (and for every thawing cycles) the proteins were thawed in ice, gently pipetted, and then centrifuged at 5000 rpm, 0°C, 5 minutes.

Then, the proteins were aliquoted in PCR tubes 10 µL each and used only with a single further freeze-thaw cycle, besides the first one.

Small molecules

A 10 mM stock solution in DMSO was prepared also for the Gefitinib, provided in powder.

The stock solutions of the three inhibitors were stored at -80°C in 100 µL aliquots and thawed and vortexed prior the use for every experimental session.

The stock solution 10 mM in DMSO is the starting solution for the assays.

Kinase Tracer 199

An intermediate solution of Tracer 199 is prepared at 250 nM by diluting 2 µL of stock solution (25 µM) in 198 µL of buffer 50 mM HEPES (pH 7.5), 150 mM NaCl. The solution is then stored in vial at -20°C and thawed and vortexed prior the use for every experimental session. This intermediate solution is the starting solution for the assays.

3.1.3 GENERAL PROTOCOL FOR EGFR INTERACTION ASSAYS

The interaction assays for the EGFR system are performed as follow:

- 1) Thawing of the protein, the Kinase Tracer 199 and the inhibitor of interest; centrifugation of the protein at 5000 rpm, 0°C, 5 minutes and vortex of the Tracer and the small molecules.
- 2) Preparation of the interaction buffer: **50 mM HEPES (pH 7.5), 150 mM NaCl, 1 mM TCEP, 0.005% Tween 20**, by adding fresh TCEP and Tween every experimental session to the base buffer 50 mM HEPES (pH 7.5), 150 mM NaCl (stored at +4°C).
- 3) Preparation of three solutions for the titration:
 - (T) or (PT)** → Fluorescent molecule: Tracer alone or in complex with the protein.
 - (P) or (L)** → Titrating molecule: the protein alone or the inhibitor of interest.

(C) → Control solution at the same composition of the titrating molecule solution.

NOTE: Every solution has to be prepared at twice the final desired concentration.

- BINDING ASSAY BETWEEN EGFR AND THE KINASE TRACER 199 (25 nM or 5 nM)

SOLUTION	FUNCTION	COMPOSITION	INITIAL CONCENTRATION (2X)	FINAL CONCENTRATION (IN THE ASSAY)
(T)	FLUORESCENT	TRACER 199	50 nM or 10 nM	25 nM or 5 nM
(P)	TITRANT	EGFR	3.76 μ M	1.88 μ M – 0.45 nM
(C)	CONTROL	GLYCEROL	50 % glycerol	25 % glycerol

- COMPETITION ASSAY WITH THE ORTHOSTERIC INHIBITORS

SOLUTION	FUNCTION	COMPOSITION	INITIAL CONCENTRATION (2X)	FINAL CONCENTRATION (IN THE ASSAY)
(PT)	FLUORESCENT	EGFR + TRACER 199	40 nM + 10 nM	20 nM + 5 nM
(L)	TITRANT	GEFITINIB or LAPATINIB or OSIMERTINIB	200 nM	100 nM – 0.02 nM
(C)	CONTROL	DMSO	0.002 %	0.001 %

4) Preparation of the titration on 8 points, with a dilution factor of 4; the last point is lacking in titrating molecule and is taken as control of the fluorescent molecule/complex thermophoretic mobility.

- Number 8 PCR tubes from 1 to 8.
- Add an appropriate volume (at least 10 or 15 μ L) of (C) to the 2 - 8 tubes and the same volume of (L) or (P) to the tube number 1.
- Titrate (L) or (P) from the tube 2 to the tube 7, by using a volume 3-times lower than the (C) volume. Then discard the last volume without adding it to 8.
- Add (T) or (PT) to every tube, from 1 to 8, in the same volume used for (C).
- Centrifuge the tubes at 15000 g, 22°C, 5 minutes.

5) Loading of the solutions into the capillaries (two capillaries for every concentration point) and set 10 minutes incubation inside the instrument at the desired temperature.

6) The assay is performed applying the following instrument setup.

Capillaries type	Premium coated
Excitation Power	100 %*
MST-Power	Medium
Temperature	25°C

*as mentioned in the Introduction paragraph 1.2.2, the choice of using 100 % of the Excitation Power was pondered for every experiment of this work, in order to maximize the yield at low fluorophore concentration, once the maintenance of a good signal-to-noise ratio had been verified.

3.1.4 STOICHIOMETRY ASSAYS

The stoichiometry assays are performed in a narrow range of titrant concentration and at high non-titrant concentration, in order to exploit ligand depletion and to obtain stoichiometry information.

This type of assay is performed as follow:

- 1) Thawing of the protein, the Kinase Tracer 199 and the inhibitor of interest; centrifugation of the protein at 5000 rpm, 0°C, 5 minutes and vortex of the Tracer and the small molecules.
- 2) Preparation of the interaction buffer: **50 mM HEPES (pH 7.5), 150 mM NaCl, 1 mM TCEP, 0.005% Tween 20**, by adding fresh TCEP and Tween every experimental session to the base buffer 50 mM HEPES (pH 7.5), 150 mM NaCl (stored at +4°C).
- 3) Preparation of three solutions for the titration:
 - (T) or (PT)** → Fluorescent molecule: Tracer alone or in complex with the protein.
 - (P) or (L)** → Titrating molecule: the protein alone or the inhibitor of interest.
 - (C)** → Control solution at the same composition of the titrating molecule solution.

NOTE: Every solution has to be prepared at twice the final desired concentration.

- STOICHIOMETRY TITRATING THE PROTEIN OVER THE TRACER 199

SOLUTION	FUNCTION	COMPOSITION	INITIAL CONCENTRATION (2X)	FINAL CONCENTRATION (IN THE ASSAY)
(T)	FLUORESCENT	TRACER 199	100 nM	50 nM
(P)	TITRANT	EGFR	2 μM	1 μM – 35.18 nM
(C)	CONTROL	GLYCEROL	50 % glycerol	25 % glycerol

- STOICHIOMETRY TITRATING THE INHIBITOR OVER THE TRACER 199/EGFR COMPLEX

SOLUTION	FUNCTION	COMPOSITION	INITIAL CONCENTRATION (2X)	FINAL CONCENTRATION (IN THE ASSAY)
(PT)	FLUORESCENT	EGFR + TRACER 199	280 nM + 10 nM	140 nM + 5 nM
(L)	TITRANT	GEFITINIB or LAPATINIB	200 nM	100 nM – 0.02 nM
(C)	CONTROL	DMSO	0.002 %	0.001 %

- 4) Preparation of the titration on 16 points, with a dilution factor of 1.25:
- Number 16 PCR tubes from 1 to 16.
 - Add an appropriate volume (at least 5 μL) of (C) to the 2 - 16 tubes and the same volume of (L) or (P) to the tube number 1.
 - Titrate (L) or (P) from the tube 2 to the tube 16, by using a volume 4-times higher than the (C) volume. Then discard the last volume.
 - Add (T) or (PT) to every tube, from 1 to 16, in the same volume used for (C).
 - Centrifuge the tubes at 15000 g, 22°C, 5 minutes.
- 5) Loading of the solutions into the capillaries (one capillary for every concentration point) and set 5 minutes incubation inside the instrument at the desired temperature.
- 6) The assay is performed applying the following instrument setup.

Capillaries type	Premium coated
Excitation Power	100 %
MST-Power	Medium
Temperature	25°C

NOTE: In these experiments the time dependence (10 minutes and 3 hours) has been explored in two ways:

- 7) Preparation of the solutions (bullet points from 1 to 4) and setting of two timers, 10 minutes and 3 hours. Once past the 10 minutes loading of the first set of capillaries and incubation of further 5 minutes inside the instrument before the analysis. After 3 hours loading of the second set of capillaries from the same solutions, incubation of further 5 minutes inside the instrument before the analysis.
- 8) Preparation of the (PT) starting solution and setting of two timers, 10 minutes and 3 hours. Proceed with the bullet points from 4 to 6 two times, after 10 minutes and then after 3 hours.

3.1.5 REVERSIBLE LIGAND RETENTION ASSAY

This assay has been developed as an alternative to the Jump Dilution for the differentiation of reversible and irreversible ligands. The approach is based on the size exclusion retention of small reversible molecules, while the large molecules and every small molecule covalently attached to it will not be retained and will be mechanically separated from the others without strong change in their concentration.

The experiments have been performed as follow:

- 1) Thawing of the protein, the Kinase Tracer 199 and the inhibitor of interest; centrifugation of the protein at 5000 rpm, 0°C, 5 minutes and vortex of the Tracer and the small molecules.
- 2) Preparation of the interaction buffer: **50 mM HEPES (pH 7.5), 150 mM NaCl, 1 mM TCEP, 0.005% Tween 20**, by adding fresh TCEP and Tween every experimental session to the base buffer 50 mM HEPES (pH 7.5), 150 mM NaCl (stored at +4°C).
- 3) Preparation of three solutions (at least 320 µL each):
(P) → Protein alone with the same concentration of DMSO than the other two solutions.
(PG) → Protein in complex with the Gefitinib.
(PO) → Protein in complex with the Osimertinib.

SOLUTION	FUNCTION	COMPOSITION	CONCENTRATION
(P)	CONTROL	EGFR	20 nM
(PG)	REVERSIBLE LIGAND	EGFR + GEFITINIB	20 nM + 10 nM
(PO)	IRREVERSIBLE LIGAND	EGFR + OSIMERTINIB	20 nM + 10 nM

- 4) Incubation of the solutions for 60 minutes and 150 minutes.
- 5) **Preliminary Binding Check** after every time point and before the Spin Column passages: addition of 0.6 µL Tracer 199 (stock solution 250 nM) to 29.4 µL of every solution in order to obtain 30 µL at Tracer concentration of 5 nM. Centrifugation at 15000 g, 22°C, 5 minutes. Every solution is used to load three capillaries and the capillaries are then incubated for 5 minutes inside the instrument before the analysis.
- 6) **Size exclusion:** for each time point 9 size exclusion Zeba™ Spin Desalting Columns, 7K MWCO, 0.5 mL, Thermo are used. Every Zeba™ Spin Desalting Column needs three steps of conditioning with the dilution buffer (50 mM HEPES pH 7.5, 150 mM NaCl, 1 mM TCEP, 0.005% Tween 20). After the conditioning, 130 µL of each solution (P), (PG), and (PO),

endures a passage in a Zeba Column each and then the eluted solutions undergo two further sequential passages in as many Zeba Columns (three Zeba column are used for every solution).

7) **Final Binding Check** in the same conditions of point number 5 after every incubation time and passage steps through the Zeba Spin Columns.

8) The assay is performed applying the following instrument setup.

Capillaries type	Premium coated
Excitation Power	100 %
MST-Power	Medium
Temperature	25°C

3.2 ROCK

3.2.1 MATERIALS

The ROCK (Rho-associated protein kinase) interaction system has been investigated through both the competition and the binding assay and the isoforms considered was the catalytic domains of ROCK-1. The tested inhibitors were the orthosteric Compound A and two allosteric compounds (Compound B and C). For the competition assay the selected fluorescent species was the Kinase Tracer 236 while for the binding assay the ROCK-1 was labeled both in the presence and in the absence of an orthosteric low potent compound (Compound X).

In the table below are reported the characteristic of the starting material used for the experiments.

Item	Supplier	Product Number	Lot	Tag	Sequence (start-end)	MW Da	Concentration	Purity	Storage buffer
ROCK-1	-	-	-	-	6-415	47428	30 μ M (1.4 g/L)	> 95 %	50 mM HEPES (pH 7.5), 150 mM NaCl, 2 mM DTT
Kinase Tracer 236	Thermo Fisher	PV5592	-	-	-	-	50 μ M	-	DMSO

All the tested compounds are stock solution of 10 mM in DMSO.

3.2.2 MATERIAL HANDLING AND STORAGE

ROCK-1 is stored at -80°C while the Kinase Tracer 236 and the inhibitors are stored at -20°C .

Proteins

For the first use (and for every thawing cycles) the protein was thawed in ice, gently mixed and then centrifuged at 10000 rpm, 0°C , 5 minutes.

Then, the protein was aliquoted in PCR tubes 10 μ L each and used only with a single further freeze-thaw cycle, besides the first one.

Small molecules

The stock solutions of the inhibitors were stored at -20°C in 100 μ L aliquots and thawed and vortexed prior the use for every experimental session.

The stock solution 10 mM in DMSO is the starting solution for the assays.

Kinase Tracer 236

An intermediate solution of Tracer 236 is prepared at 250 nM by diluting 1 μ L of stock solution (50 μ M) in 199 μ L of buffer 50 mM HEPES (pH 7.5), 150 mM NaCl. The solution is then stored in vial at -20°C and thawed and vortexed prior the use for every experimental session. This intermediate solution is the starting solution for the assays.

3.2.3 GENERAL PROTOCOL FOR ROCK COMPETITION ASSAYS

The competition assays for the ROCK system are performed as follow:

- 1) Thawing of the protein, the Kinase Tracer 236 and the inhibitor of interest; centrifugation of the protein at 10000 rpm, 0°C, 5 minutes and vortex of the Tracer and the small molecules.
- 2) Preparation of the interaction buffer: **50 mM HEPES (pH 7.5), 150 mM NaCl, 2 mM DTT, 0.01% Tween 20**, by adding fresh DTT and Tween every experimental session to the base buffer 50 mM HEPES (pH 7.5), 150 mM NaCl (stored at +4°C).

3) Preparation of three solutions for the titration:

(T) or (PT) → Fluorescent molecule: Tracer alone or in complex with the protein.

(P) or (L) → Titrating molecule: the protein alone or the inhibitor of interest.

(C) → Control solution at the same composition of the titrating molecule solution.

NOTE: Every solution has to be prepared at twice the final desired concentration.

BINDING ASSAY BETWEEN ROCK AND THE KINASE TRACER 236 (25 nM or 5 nM)

SOLUTION	FUNCTION	COMPOSITION	INITIAL CONCENTRATION (2X)	FINAL CONCENTRATION (IN THE ASSAY)
(T)	FLUORESCENT	TRACER 236	50 nM or 10 nM	25 nM or 5 nM
(P)	TITRANT	ROCK-1	30 μ M	15 μ M – 3.6 nM
(C)	CONTROL	ROCK storage buffer	-	-

COMPETITION ASSAY WITH THE INHIBITORS

SOLUTION	FUNCTION	COMPOSITION	INITIAL CONCENTRATION (2X)	FINAL CONCENTRATION (IN THE ASSAY)
(PT)	FLUORESCENT	ROCK-1 + TRACER 236	100 nM + 30 nM	50 nM + 15 nM
(L)	TITRANT	COMPOUND A	2 μ M	1 μ M – 0.24 nM
(L)	TITRANT	COMPOUND B COMPOUND C	2 μ M or 20 μ M	1 μ M – 0.24 nM or 10 μ M – 2.4 nM
(C)	CONTROL	DMSO	0.02 % or 0.2 %	0.01 % or 0.1 %

4) Preparation of the titration on 8 points, with a dilution factor of 4; the last point is lacking in titrating molecule and is taken as control of the fluorescent molecule/complex thermophoretic mobility.

- Number 8 PCR tubes from 1 to 8.

- Add an appropriate volume (at least 10 or 15 μ L) of (C) to the 2 - 8 tubes and the same volume of (L) or (P) to the tube number 1.

- Titrate (L) or (P) from the tube 2 to the tube 7, by using a volume 3-times lower than the (C) volume. Then discard the last volume without adding it to 8.

- Add (T) or (PT) to every tube, from 1 to 8, in the same volume used for (C).

- Centrifuge the tubes at 15000 g, 22°C, 5 minutes.

5) Loading of the solutions into the capillaries (two capillaries for every concentration point) and set 10 minutes incubation inside the instrument at the desired temperature.

6) The assay is performed applying the following instrument setup.

Capillaries type	Premium coated
Excitation Power	100 %
MST-Power	Medium
Temperature	22°C

3.2.4 LABELING PROTOCOL

ROCK-1 has been covalently labeled on lysines by using the Monolith Protein Labeling Kit RED-NHS 2nd Generation (NanoTemper), both in the presence or the absence of a low potent orthosteric inhibitor (Compound X, $pIC_{50} < 7$).

The labeling reaction was performed as follow:

- 1) Dilution of ROCK-1 in Labeling Buffer NHS (NanoTemper) 130 mM NaHCO₃, 50 mM NaCl, pH 8.2-8.3 at the final concentration of 10 μ M and addition of Compound X ($pIC_{50} < 7$) 100 μ M or DMSO 1%. Final volume 25 μ L incubated at room temperature for 20 minutes.
- 2) Addition of RED-NHS 2nd Generation (NanoTemper) at the final concentration of 30 μ M and incubation for 30' in the dark at 25°C.
- 3) Dilution at 150 μ L with the purification buffer 50 mM HEPES (pH 7.4), 150 mM NaCl, 2 mM DTT.
- 4) Purification with PD SpinTrap G-25 (Cytiva), washed with the final buffer 50 mM HEPES (pH 7.4), 150 mM NaCl, 2 mM DTT.
- 5) Collection of the UV-spectra 260 nm – 700 nm for the quantification of labeled protein concentration and the determination of the degree of labeling (DOL).
- 6) Aliquotation of the labeled protein in PCR tubes 10 μ L each and storage at -80°C.

3.2.5 GENERAL PROTOCOL FOR ROCK BINDING ASSAYS

The binding assays for the ROCK system are performed as follow:

- 1) Thawing of the labeled protein and the inhibitor of interest; centrifugation of the protein at 10000 rpm, 0°C, 5 minutes and vortex of the small molecules.
- 2) Preparation of the interaction buffer: **50 mM HEPES (pH 7.5), 150 mM NaCl, 2 mM DTT, 0.01% Tween 20**, by adding fresh DTT and Tween every experimental session to the base buffer 50 mM HEPES (pH 7.5), 150 mM NaCl (stored at +4°C).
- 3) Preparation of three solutions for the titration:
 - (P) → Fluorescent protein
 - (L) → Titrating molecule: the inhibitor of interest.
 - (C) → Control solution at the same composition of the titrating molecule solution.

NOTE: Every solution has to be prepared at twice the final desired concentration.

BINDING ASSAY WITH COMPOUND A

SOLUTION	FUNCTION	COMPOSITION	INITIAL CONCENTRATION (2X)	FINAL CONCENTRATION (IN THE ASSAY)
(P)	FLUORESCENT	ROCK-1 LABELED	40 nM	20 nM
(L)	TITRANT	COMPOUND A	200 nM	100 nM – 0.02 nM
(C)	CONTROL	DMSO	0.002 %	0.001 %

BINDING ASSAY WITH COMPOUND B AND C

SOLUTION	FUNCTION	COMPOSITION	INITIAL CONCENTRATION (2X)	FINAL CONCENTRATION (IN THE ASSAY)
(P)	FLUORESCENT	ROCK-1 LABELED	40 nM	20 nM
(L)	TITRANT	COMPOUND B COMPOUND C	20 µM	10 µM – 2.4 nM
(C)	CONTROL	DMSO	0.2 %	0.1 %

4) Preparation of the titration on 8 points, with a dilution factor of 4; the last point is lacking in titrating molecule and is taken as control of the fluorescent molecule/complex thermophoretic mobility.

- Number 8 PCR tubes from 1 to 8.
- Add an appropriate volume (at least 10 or 15 µL) of (C) to the 2 - 8 tubes and the same volume of (L) or (P) to the tube number 1.
- Titrate (L) or (P) from the tube 2 to the tube 7, by using a volume 3-times lower than the (C) volume. Then discard the last volume without adding it to 8.
- Add (T) or (PT) to every tube, from 1 to 8, in the same volume used for (C).
- Centrifuge the tubes at 15000 g, 22°C, 5 minutes.

5) Loading of the solutions into the capillaries (two capillaries for every concentration point) and set 10 minutes incubation inside the instrument at the desired temperature.

6) The assay is performed applying the following instrument setup.

Capillaries type	Premium coated
Excitation Power	100 %
MST-Power	Medium
Temperature	22°C

3.3 MST-ON TIME CHOICE

MST data relies on the registration of the fluorescent decay over time due to the physical movement of the fluorescent molecules from the center of the temperature gradient to the marginal area of the fluorescence detection (**Figure 11**).

It follows that every time-point of the migration (MST-ON time) yields a different set of experimental points and, even if the interaction information should be the same at every time point, some differences can emerge by selecting different MST-ON times. Indeed, it has been observed that the early time points (T-Jump region) are mainly affected by the sensitivity to the temperature of the fluorescent molecule, while the late times (Thermophoresis region) are mainly affected by the comprehensive migration properties of the complex^{[31][54][55]}.

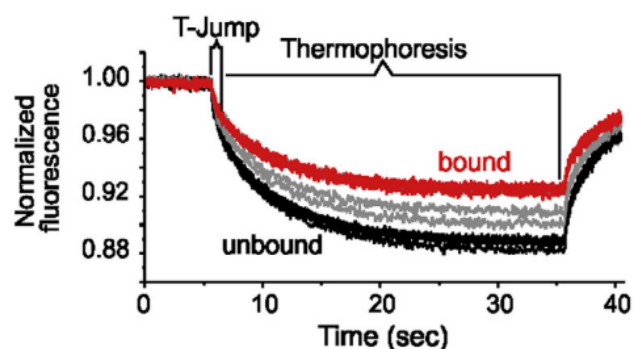


Figure 11 Representation of the two main thermophoretic zones of migration: the early times that correspond to the T-Jump region and the late times which correspond to the Thermophoresis region.

Adapted from Jerabek-Willemsen, M. et al. (2014) 'MicroScale Thermophoresis: Interaction analysis and beyond', Journal of Molecular Structure, 1077, pp. 101–113. doi: 10.1016/j.molstruc.2014.03.009.

As a result, selecting a specific MST-ON time may reveal different interaction information and highlight a molecular mechanism hidden by another MST-ON time. Again, it is possible to erroneously rely fine experimental consideration on a data set referred to not reproducible timepoints: this problem arises mostly under challenging experimental settings, such as low fluorescent complex concentration, and can result in unreliable information regarding potency and Hill slope, leading to inaccurate knowledge about possible tight binding or cooperativity conditions. Therefore, an important aspect to take into account is what time is better to choose to gain reliable and reproducible interaction parameters.

In this work the adopted method to select the MST-ON time was based on performing a triplicate with a reference compound, fitting the data set with the nonlinear regression four parameters logistic model and then to evaluate the 95% confidence interval (CI 95%) yielded by the GraphPad

Prism software for the fitted parameters pIC_{50} , Hill Slope, Top and Bottom, other than the S/N (obtained by dividing the Response Amplitude for the $Sy.x$) and the R^2 . The MST-ON time were then ranked on the basis of the narrowest interval confidence and goodness of fit to choose the most reproducible time point for that system. The same experimental set has been repeated for every different system of detection such as the covalent labeling of the protein.

EGFR COMPETITION

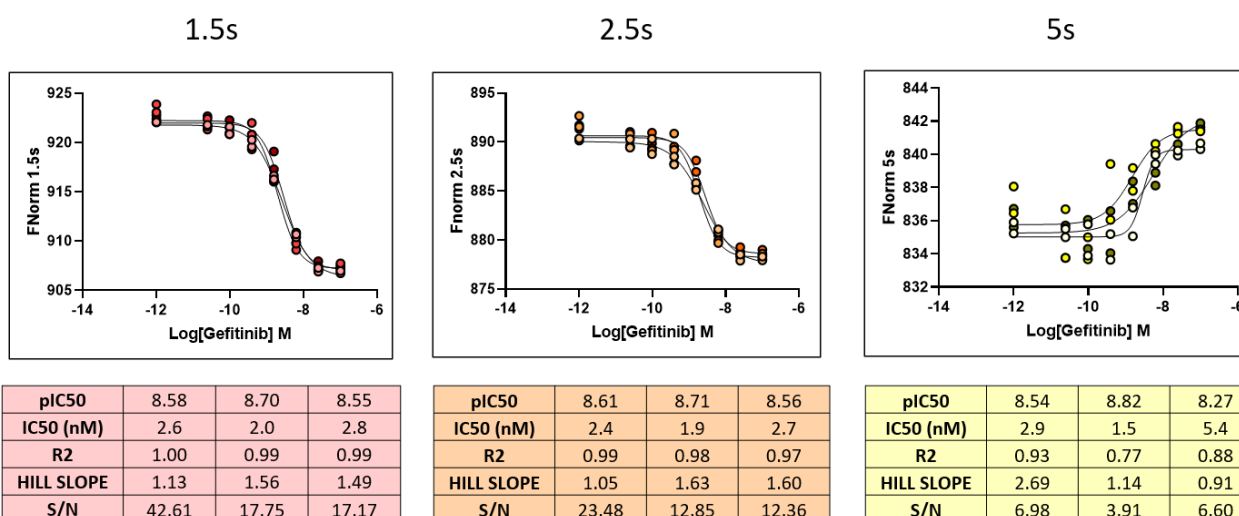
For the EGFR system (both wild type and L858R) three protein concentrations (70 nM, 20 nM, 5 nM) have been tested in order to consolidate the robustness of the method. The chosen reference is the Gefitinib, titrated starting from 100 nM.

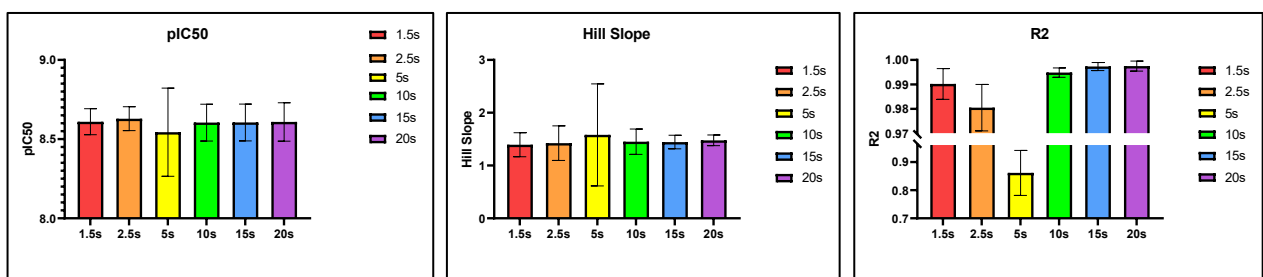
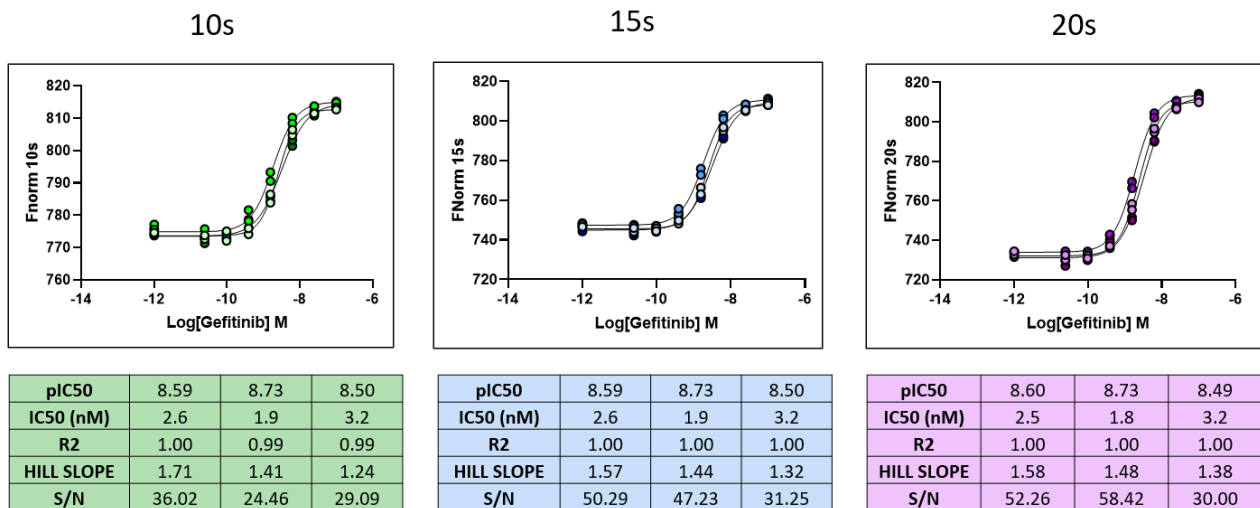
[EGFR]	70 nM, 20 nM, 5 nM
[INHIBITOR]	100 nM – 0.02 nM + CONTROL POINTS
[TRACER 199]	5 nM
TITRATION	1:3, 8 POINTS IN DUPLICATE
DILUTION BUFFER	50 mM HEPES (pH 7.5), 150 mM NaCl, 1 mM TCEP, 0.005 % Tween 20
TEMPERATURE	25°C

The binding curves were first analyzed as separated replicates in order to evaluate the macroscopic differences in fitting and parameters.

EGFR WILD TYPE

- EGFR WT, 70 nM + GEFITINIB





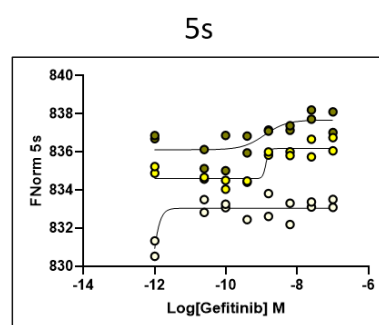
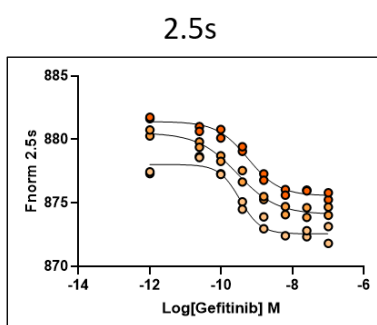
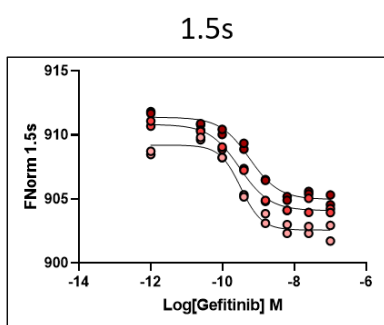
From the data collected at 70 nM it can be noticed that, except for the 5 s (coinciding with the cross-over of the MST traces), all the MST-ON time yield a comparable pIC₅₀ and Hill Slope information. The late MST-ON times however give a more robust fitting with a higher R² value. At this high protein concentration, the fraction of the tracer that is bound to the protein is nearly equal to the total amount of the tracer leading to a high signal/noise. In these situations, every MST-on time gives a solid fit.

The three replicates of each MST-ON time data set are then individually normalized from 0 to 100 and the obtained values are treated in GraphPad Prism as replicates values in side-by-side sub columns to get reliable confidence intervals (CI, 95%). Every MST-ON time is now ranked from 1 to 6, giving 1 to the time with the narrowest CI 95% for every fitting parameter (pIC₅₀, Hill Slope, Top, Bottom) and the highest S/N and R² value, and so on up to the worst MST-ON time in terms of confidence intervals and fitting at which is assigned the sixth value. The lowest sum of the ranked positions for every considered parameter gives the MST-ON time that yields the most reproducible information on three identical replicates.

MST-ON TIME (s)	pIC50		Hill Slope		Bottom		Top		S/N		R2		SUM Ranking position
	CI	Ranking	CI	Ranking	CI	Ranking	CI	Ranking	Value	Ranking	Value	Ranking	
1.5	0.13	4	0.52	4	8.10	4	5.48	2	17.81	4	0.98	4	22
2.5	0.18	5	0.73	5	10.56	5	7.31	5	13.56	5	0.97	5	30
5	0.55	6	1.73	6	14.28	6	26.14	6	5.01	6	0.82	6	36
10	0.11	3	0.45	3	4.39	3	6.6	4	20.82	3	0.99	3	19
15	0.09	2	0.37	1	3.64	1	5.5	3	25.87	1	0.99	2	10
20	0.09	1	0.38	2	3.65	2	5.4	1	25.64	2	0.99	1	9

In this case the best MST-ON time in terms of reproducibility is the 20 s.

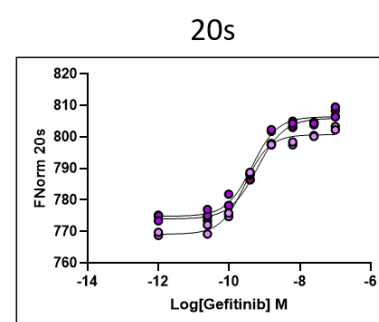
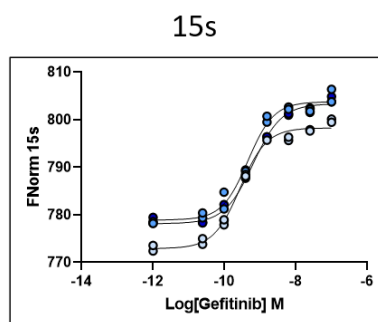
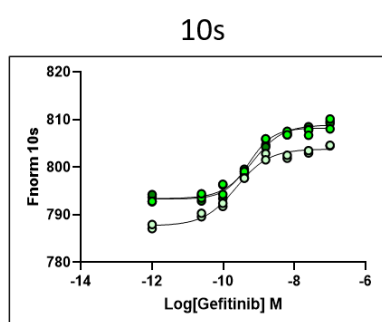
- EGFR WT, 20 nM + GEFITINIB



pIC50	9.49	9.53	9.25
IC50 (nM)	0.3	0.3	0.6
R2	0.97	0.99	0.98
HILL SLOPE	1.48	1.03	1.06
S/N	12.39	18.39	15.42

pIC50	9.48	9.55	9.25
IC50 (nM)	0.3	0.3	0.6
R2	0.96	0.98	0.98
HILL SLOPE	1.50	0.79	0.99
S/N	9.62	16.84	16.27

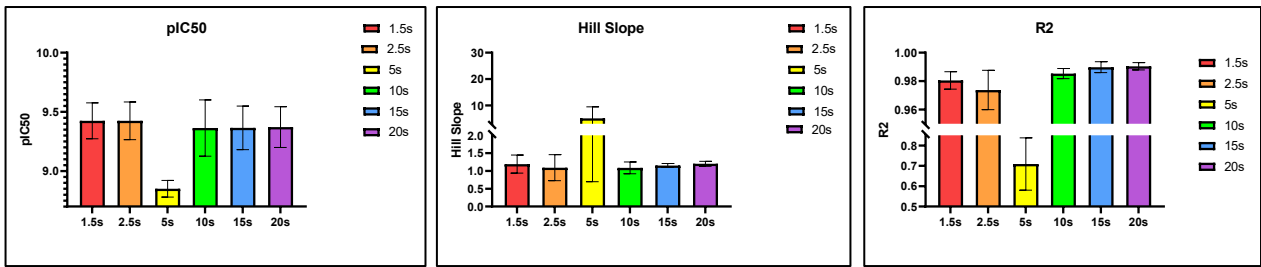
pIC50	-	-	-
IC50 (nM)	-	-	-
R2	-	-	-
HILL SLOPE	-	-	-
S/N	-	-	-



pIC50	9.63	9.28	9.18
IC50 (nM)	0.2	0.5	0.7
R2	0.99	0.98	0.99
HILL SLOPE	0.95	1.27	1.03
S/N	20.49	14.88	18.32

pIC50	9.56	9.34	9.19
IC50 (nM)	0.3	0.5	0.6
R2	0.99	0.99	0.99
HILL SLOPE	1.17	1.20	1.09
S/N	23.90	17.10	23.39

pIC50	9.55	9.35	9.21
IC50 (nM)	0.3	0.4	0.6
R2	0.99	0.99	0.99
HILL SLOPE	1.26	1.21	1.13
S/N	21.74	18.58	24.59

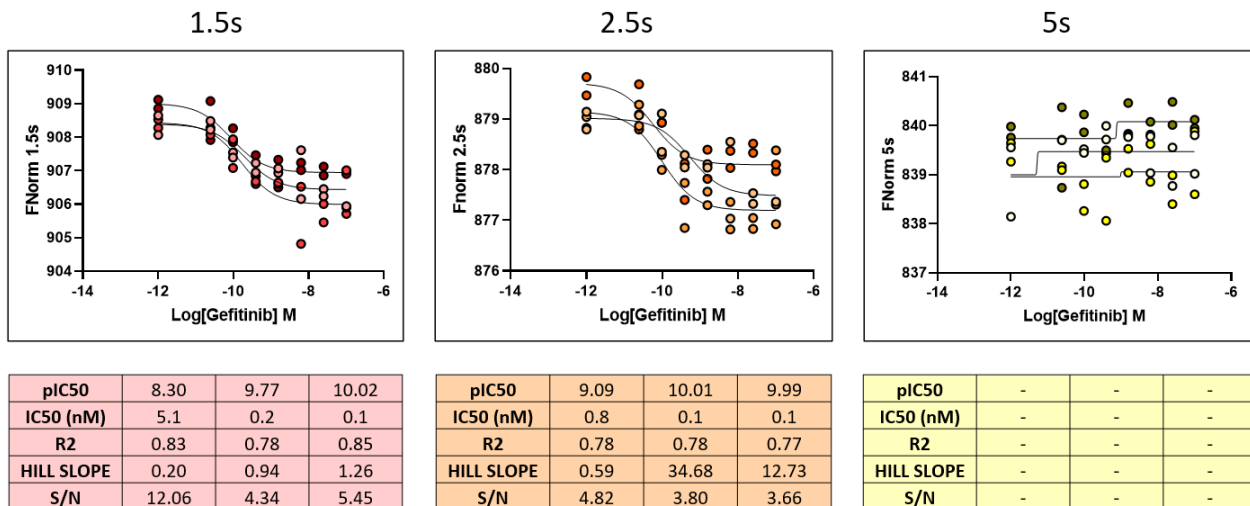


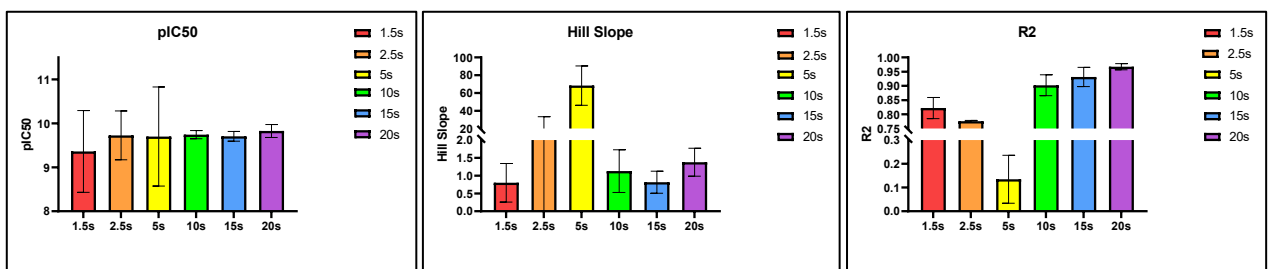
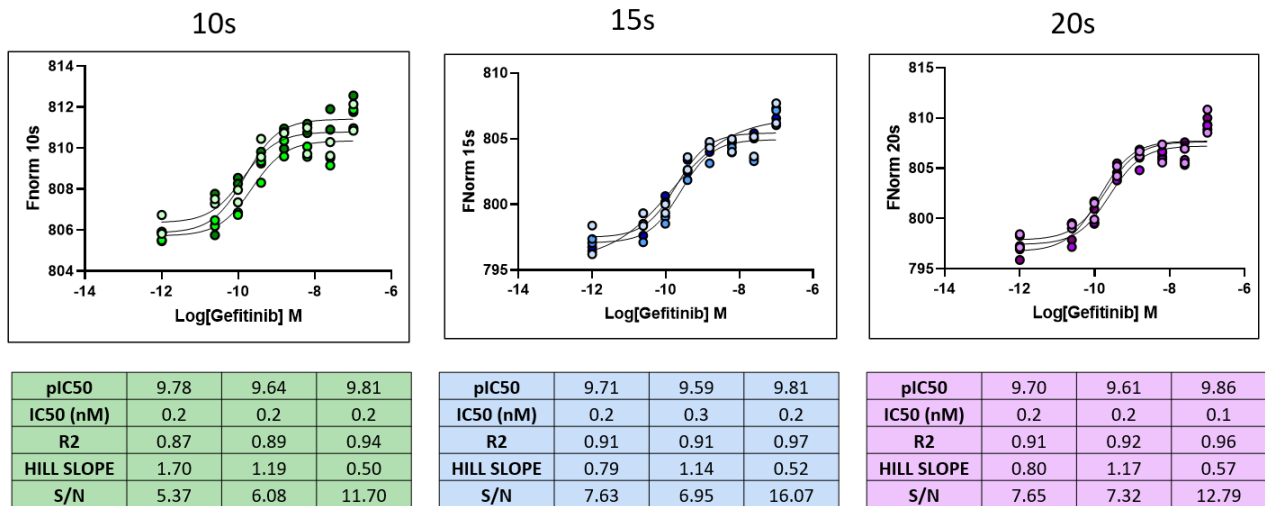
MST-ON TIME (s)	pIC50		Hill Slope		Bottom		Top		S/N		R2		SUM Ranking position
	CI	Ranking	CI	Ranking	CI	Ranking	CI	Ranking	Value	Ranking	Value	Ranking	
1.5	0.20	3	0.53	4	3.47	4	0.53	4	13.29	3	0.97	3	21
2.5	0.24	4	0.52	3	2.48	3	0.52	3	12.05	4	0.96	4	21
5	-	6	-	6	-	6	-	6	1.85	6	0.46	6	36
10	0.24	5	0.62	5	4.38	5	0.62	5	11.93	5	0.96	5	30
15	0.18	2	0.50	2	1.50	2	0.50	2	15.03	2	0.98	2	12
20	0.16	1	0.48	1	0.52	1	0.48	1	16.24	1	0.98	1	6

Also by using 20 nM of protein the best MST-ON time results being the 20 s.

The loss of fitting at 5 s is due to the cross-over of the thermophoretic traces.

- EGFR WT, 5 nM + GEFITINIB





By using a low protein concentration it is more evident that choosing the T-Jump region instead of the Thermophoresis region may lead to different conclusions in terms of potency and Hill Slope, especially when the number of replicates for a single conditions are not high. In this case a significant amount of Tracer is free in solution, therefore the noise is high and identifying the more robust MST-ON time become relevant to rely the interaction interpretation on trustworthy fitting parameters.

MST-ON TIME (s)	pIC50		Hill Slope		Bottom		Top		S/N		R2		SUM Ranking position
	CI	Ranking	CI	Ranking	CI	Ranking	CI	Ranking	Value	Ranking	Value	Ranking	
1.5	0.84	5	1.78	4	24.90	4	36.16	5	4.76	4	0.77	4	26
2.5	0.53	3	-	6	15.78	1	25.66	4	3.41	5	0.70	5	23
5	-	6	-	6	-	6	-	6	-	6	-	6	36
10	0.55	4	1.09	3	26.18	5	18.99	1	7.10	3	0.88	3	19
15	0.52	2	0.84	1	23.76	3	21.34	3	8.57	2	0.91	2	13
20	0.47	1	0.90	2	21.21	2	19.16	2	8.64	1	0.91	1	9

By applying the ranking method, the 20 s resulted once again as the best MST-ON time in terms of reproducibility.

Therefore, it seems that the protein concentration had a little impact on which MST-ON time yield the most robust fitting parameters, even if at high concentrations, and consequently high signal-to-noise ratio, every time point seems to be able of yielding comparable information. The choice has

more impact at low protein concentrations, condition that is the one more relevant for the investigation of potent inhibitors.

- EGFR WT, 20 nM + LAPATINIB

To confirm that the MST-ON time reproducibility was not dependent on the inhibitor, a triplicate with Lapatinib and EGFR WT 20 nM has been performed as well. Only the ranking table is reported below.

MST-ON TIME (s)	pIC50		Hill Slope		Bottom		Top		S/N		R2		SUM Ranking position
	CI	Ranking	CI	Ranking	CI	Ranking	CI	Ranking	Value	Ranking	Value	Ranking	
1.5	0.15	3	1.02	4	9.04	4	6.19	1	12.47	4	0.97	4	20
2.5	0.19	5	1.58	5	10.30	5	7.15	2	9.77	5	0.95	5	27
5	1.19	6	-	6	18.80	6	58.22	6	2.77	6	0.62	6	36
10	0.16	4	0.84	3	5.87	3	9.43	5	13.06	3	0.97	3	21
15	0.14	2	0.77	2	5.30	2	8.51	4	14.36	2	0.98	2	14
20	0.13	1	0.71	1	4.93	1	7.85	3	15.56	1	0.98	1	8

The 20 s is confirmed to be also in this case the most reproducible MST-ON time for the EGFR wild type interaction system in competition with the Tracer 199.

EGFR L858R

The mutant form of EGFR was also tested in triplicates with Gefitinib to identify the best MST-ON time in terms of reproducibility. Only the ranking tables are reported below.

- EGFR L8583 70 nM + GEFITINIB

MST-ON TIME (s)	pIC50		Hill Slope		Bottom		Top		S/N		R2		SUM Ranking position
	CI	Ranking	CI	Ranking	CI	Ranking	CI	Ranking	Value	Ranking	Value	Ranking	
1.5	0.14	3	1.28	1	12.38	5	5.76	1	14.35	5	0.97	5	20
2.5	-	6	-	6	-	6	-	6	4.28	6	0.74	6	36
5	0.14	2	2.28	3	4.09	4	9.44	5	16.75	4	0.98	4	22
10	-	6	-	6	3.74	3	8.54	4	18.60	3	0.98	3	25
15	-	6	-	6	3.56	2	8.07	3	19.81	2	0.99	2	21
20	0.11	1	2.14	2	3.40	1	7.68	2	20.97	1	0.99	1	8

- EGFR L8583 20 nM + GEFITINIB

MST-ON TIME (s)	pIC50		Hill Slope		Bottom		Top		S/N		R2		SUM Ranking position
	CI	Ranking	CI	Ranking	CI	Ranking	CI	Ranking	Value	Ranking	Value	Ranking	
1.5	0.16	5	0.39	1	8.26	5	6.2	5	18.49	5	0.98	5	26
2.5	-	6	-	6	-	6	-	6	3.29	6	0.69	6	36
5	0.08	4	0.40	2	3.55	4	5.25	4	25.69	4	0.99	4	22
10	0.08	2	0.41	3	3.49	2	4.98	2	26.39	2	0.99	2	13
15	0.08	3	0.44	5	3.52	3	5.01	3	25.74	3	0.99	3	20
20	0.08	1	0.42	4	3.42	1	4.84	1	26.68	1	0.99	1	9

- EGFR L8583 5 nM + GEFITINIB

MST-ON TIME (s)	pIC50		Hill Slope		Bottom		Top		S/N		R2		SUM Ranking position
	CI	Ranking	CI	Ranking	CI	Ranking	CI	Ranking	Value	Ranking	Value	Ranking	
1.5	5.07	5	-	6	265.00	6	332.81	5	1.74	5	0.39	5	32
2.5	-	6	-	6	106.75	5	-	6	0.14	6	-	6	35
5	1.01	4	-	6	47.93	4	38.7	4	2.91	4	0.60	4	26
10	0.44	3	1.70	3	21.76	3	15.36	3	5.89	3	0.86	3	18
15	0.32	2	1.18	2	15.67	2	11.34	2	7.76	2	0.92	2	12
20	0.27	1	0.98	1	13.61	1	9.52	1	9.06	1	0.94	1	6

From the collected data it is possible to conclude that also for the mutated form of EGFR the best MST-ON time for the competition assays with Tracer 199 is the 20 s.

ROCK-1 COMPETITION

For the ROCK-1 competition system the triplicate has been performed with the following experimental conditions and the inhibitor used for this purpose is the orthosteric Compound A.

[ROCK-1]	50 nM
[INHIBITOR]	1 μ M – 0.24 nM + CONTROL POINTS
[TRACER 236]	15 nM
TITRATION	1:3, 8 POINTS IN DUPLICATE
DILUTION BUFFER	50 mM HEPES (pH 7.5), 150 mM NaCl, 2 mM DTT, 0.01 % Tween 20
TEMPERATURE	22°C

The ranking table is reported below.

MST-ON TIME (s)	pIC50		Hill Slope		Bottom		Top		S/N		R2		SUM Ranking position
	CI	Ranking	CI	Ranking	CI	Ranking	CI	Ranking	Value	Ranking	Value	Ranking	
1.5	1.81	5	1.10	4	92.7	5	17.21	4	6.57	4	0.85	4	26
2.5	1.66	4	0.70	2	91.05	4	14.52	1	8.25	3	0.88	2	16
5	2.49	6	0.64	1	165.66	6	15.98	2	8.70	1	0.88	3	19
10	0.75	1	0.76	3	37.86	2	16.66	3	8.27	2	0.90	1	12
15	0.87	2	1.25	5	37.04	1	23.24	5	5.82	5	0.83	5	23
20	1.16	3	1.28	6	38.36	3	28.79	6	4.65	6	0.75	6	30

On the basis of the reported results, the 10 s was the selected MST-ON time for the ROCK-1 competition experiments.

ROCK-1 LABELED

The ROCK-1 covalently labeled system has been investigated with the ranking method for both labeling reaction in the presence of the active site protector: #1 and #3.

- ROCK-1 LB #1 (w/ active site protection)

MST-ON TIME (s)	pIC50		Hill Slope		Bottom		Top		S/N		R2		SUM Ranking position
	CI	Ranking	CI	Ranking	CI	Ranking	CI	Ranking	Value	Ranking	Value	Ranking	
1.5	0.35	4	1.79	3	10.18	3	15.97	3	6.26	3	0.88	3	19
2.5	0.27	2	1.30	2	8.71	2	13.65	2	8.11	2	0.92	2	12
5	0.21	1	1.26	1	7.58	1	11.83	1	9.48	1	0.95	1	6
10	0.34	3	-	6	10.81	4	19.08	4	5.71	4	0.86	4	25
15	0.52	5	-	6	13.12	5	28.03	5	4.60	5	0.78	5	31
20	0.58	6	-	6	14.03	6	30.48	6	4.19	6	0.74	6	36

- **ROCK-1 LB #3 (w/ active site protection)**

MST-ON TIME (s)	pIC50		Hill Slope		Bottom		Top		S/N		R2		SUM Ranking position
	CI	Ranking	CI	Ranking	CI	Ranking	CI	Ranking	Value	Ranking	Value	Ranking	
1.5	0.47	3	3.05	3	21.25	4	16.87	3	6.36	3	0.88	3	19
2.5	0.25	1	-	6	13.15	1	10.81	2	7.65	1	0.93	1	12
5	0.25	2	-	6	13.21	2	10.78	1	7.38	2	0.92	2	15
10	0.85	4	-	6	19.02	3	27.40	4	4.89	4	0.81	4	25
15	1.43	5	1.40	2	22.59	5	45.63	5	3.97	5	0.69	5	27
20	6.32	6	1.13	1	30.61	6	354.27	6	3.71	6	0.61	6	31

It is interesting to note that two different labeling reactions, as far as resulting in two equally competent labeled proteins that yield comparable potency information, still could rely their most robust fitting parameters on distinct MST-ON times. Indeed, in the case of ROCK-1 LB #1 the interaction with the Compound A is better described by the 5 s timing, while for the ROCK-1 LB #3 the 2.5 s resulted the best MST-ON time to choose. Therefore, to graphically compare two binding curves originating in the two different labeled systems, it has been employed a normalization from 0 to 100 and the y-axis became indicated as "Fraction Bound".

The ranking test was not performed for the protein labeled in the absence of an active site protector (ROCK-1 LB #2) since the information acquired from the experiment with that labeled protein was used as qualitative indication of the influence of the protector during the labeling phase. As a result, the MST-ON time of 5 s was arbitrarily chosen for the analysis of the binding curves in those conditions.

3.4 DATA ELABORATION AND FITTING MODELS

The main data elaboration has been performed by using GraphPad Prism 8.1.0 and the binding or competition data set have been fitted by using the **Nonlinear regression (curve fit), log(inhibitor) vs response - Variable slope (four parameters)** model.

Quadratic fitting was performed through Excel Solver Add-In or with the MST analysis software (MO.Affinity Analysis).

The Akaike's Information Criterion (AIC)^[15], a method developed for comparing models and assisting in determining which model is more likely to be correct, has been used to help decide whether to treat the protein concentration in the quadratic equation as a constant or as an adjustable parameter.

The method relies on three parameters:

- **N**: the number of data points
- **K**: the number of parameters fit by nonlinear regression plus 1 (constrained parameters are not counted)
- **SS**: sum-of-square of the nonlinear regression

The three values are then combined into the AIC equation:

$$AIC = N \ln \left(\frac{SS}{N} \right) + 2K + \frac{2K(K + 1)}{N - K - 1}$$

Once the value has been calculated for all the model to compare, the AIC deriving from the different models is observed: the model having the lower AIC score is more likely to be correct. By considering the difference between two AIC scores (ΔAIC), it is possible to calculate the Evidence Ratio, a parameter indicating how many times one model is likely to be correct in comparison with the other:

$$\text{Evidence Ratio} = \frac{1}{e^{-0.5 \Delta AIC}}$$

It is important to note that this method is not a statistical approach, it is an indication of which model is more likely to be correct and how much more likely. Therefore, in this work it has been considered as side support to better investigate the dependence of potency from the fixed parameter of protein concentration.

4. RESULTS AND DISCUSSION

In the context of the present work, two known kinase systems have been selected to investigate different types of kinase inhibitors binding mode by using MicroScale Thermophoresis as main biophysical tool:

- EGFR (Epidermal Growth Factor Receptor)
- ROCK (Rho-associated protein kinase)

In particular two different approaches have been applied: the **competition assay**, which requires a fluorescent ATP analog to compete with orthosteric inhibitors, and the **binding assay**, which uses a fluorescent label attached to the protein to observe the direct interaction between the target and the inhibitor. The two methods were used alone or in combination to obtain single and orthogonal information on different inhibitor binding modes such as allosteric inhibition, covalent binding and slow interaction.

4.1 EGFR (Epidermal Growth Factor Receptor)

The EGFR system has been explored using the competition approach, since the inhibitors evaluated for this study are known to be orthosteric and to compete with the ATP. As a result, this section is focused on describing different orthosteric binding modes and determining methods to differentiate them in order to obtain suitable information for future studies of similar but unknown kinase interaction systems.

In particular the three inhibitors chosen for the study are Gefitinib, Lapatinib and Osimertinib and their structures and binding poses are reported in **Figure 12**, **Figure 13** and **Figure 14**.

A. GEFITINIB

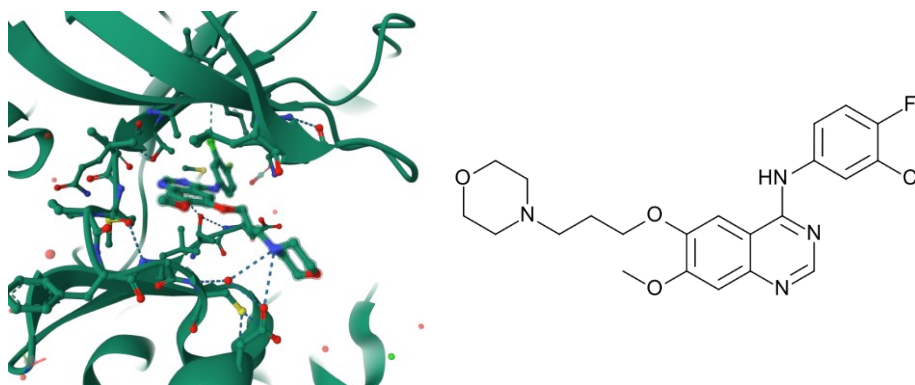


Figure 12 On the left crystal structure of EGFR kinase domain L858R mutation in complex with Gefitinib (PDB: 2ITZ). On the right Gefitinib structure.

B. LAPATINIB

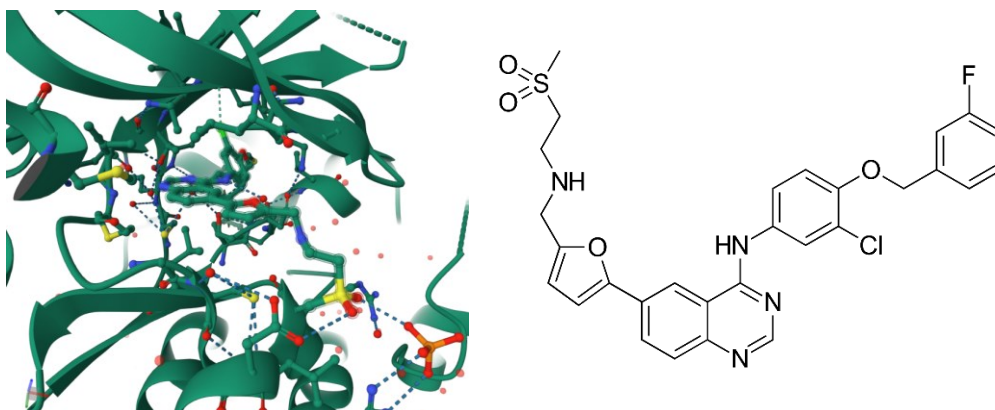


Figure 13 On the left crystal structure of EGFR kinase domain wild type in complex with Lapatinib (PDB: 1XKK). On the right Lapatinib structure.

C. OSIMERTINIB

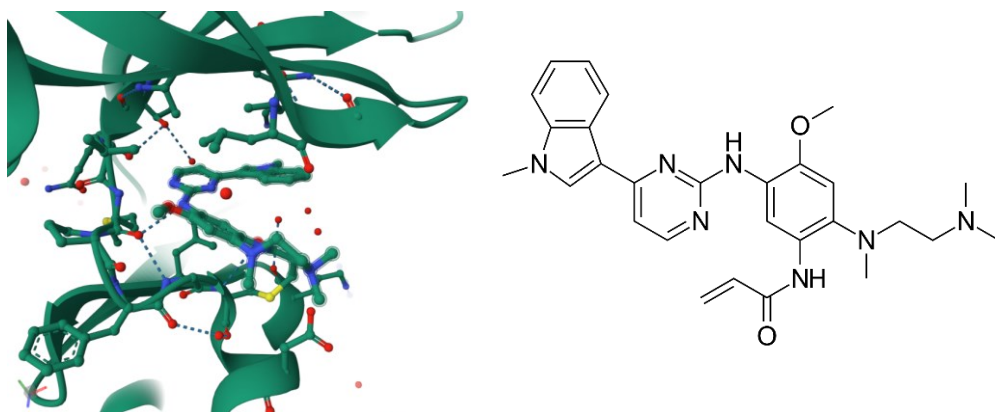


Figure 14 On the left crystal structure of EGFR kinase domain L858R mutation in complex with Osimertinib (PDB: 6JWL). On the right Osimertinib structure.

4.1.1 INTERACTION WITH KINASE TRACER 199

Before to perform a competition assay with an orthosteric inhibitor, the interaction system target protein-ATP fluorescent analog should be analyzed.

The ATP fluorescent analog indicated by Thermo for the Epidermal Growth Factor Receptor is the Kinase Tracer 199 (Thermo).

The first aspect to evaluate was the affinity of the proteins for the Tracer and, since the Tracer 199 is the fluorescent species, its concentration should remain constant in every sample; therefore, the titrating molecule needs to be the protein. In the table below, are indicated the experimental conditions for EGFR wild type (EGFR WT) and Tracer 199 interaction assay.

[EGFR WT]	1.88 μ M – 0.45 nM + CONTROL POINTS
[TRACER 199]	25 nM or 5 nM
TITRATION	1:3, 8 POINTS IN DUPLICATE
DILUTION BUFFER	50 mM HEPES (pH 7.5), 150 mM NaCl, 1 mM TCEP, 0.005% Tween 20
TEMPERATURE	25°C

Two Tracer 199 concentrations, 25 nM and 5 nM, were tested to determine whether there was an affinity dependence on Tracer concentration and both logistic and quadratic fitting (performed through Excel Solver Add-In) were considered (**Figure 15**). Unfortunately, due to the low starting concentration of the commercial protein, the selected concentrations range is not capable of yielding a complete saturation region, making the determination of that parameter less accurate than the baseline.

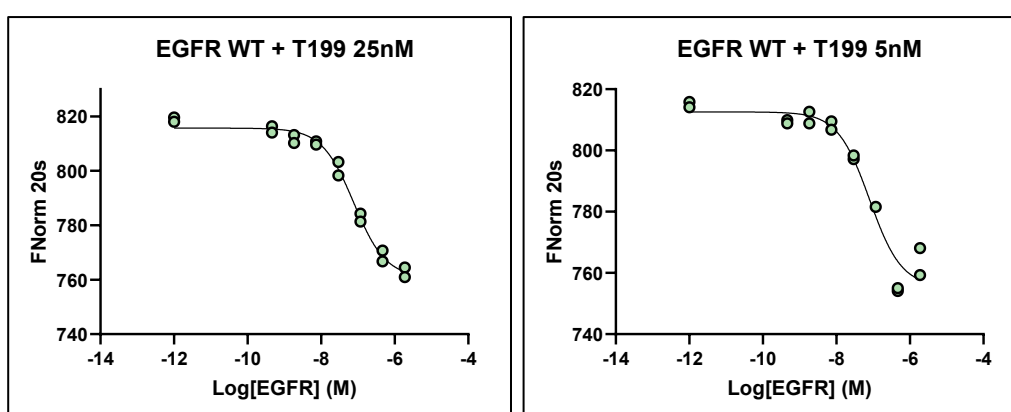


Figure 15 Binding assay between EGFR WT and T199 at 25 nM (on the left) and 5 nM (on the right).

EGFR WT	T199 25 nM		T199 5 nM	
	LOGISTIC FITTING (four parameters)	QUADRATIC FITTING	LOGISTIC FITTING (four parameters)	QUADRATIC FITTING
pK _D	7.08	7.19	7.10	7.12
K _D (nM)	83.5	64.0	79.5	76.7
R ²	0.99	0.99	0.96	0.96
HILL COEFF	0.85	/	1.34	/
RESPONSE AMPLITUDE	58.07	53.93	53.45	56.96
MST-on TIME	20 s	20 s	20 s	20 s

At Tracer 199 concentration of 25 nM and 5 nM both the logistic and the quadratic fitting yields quite the same parameter values and a pK_D near 7, with a slight increase in affinity registered by using the quadratic fitting.

By considering the quadratic fitting no tight binding evidence is detected and the affinity of the protein for the Tracer 199 seems to be independent from the Tracer concentration.

The same experimental workflow has been applied to the EGFR L858R system with conditions reported below.

[EGFR L858R]	1.88 μ M – 0.45 nM + CONTROL POINTS
[TRACER 199]	25 nM / 5 nM
TITRATION	1:3, 8 POINTS IN DUPLICATE
DILUTION BUFFER	50 mM HEPES (pH 7.5), 150 mM NaCl, 1 mM TCEP, 0.005% Tween 20
TEMPERATURE	25°C

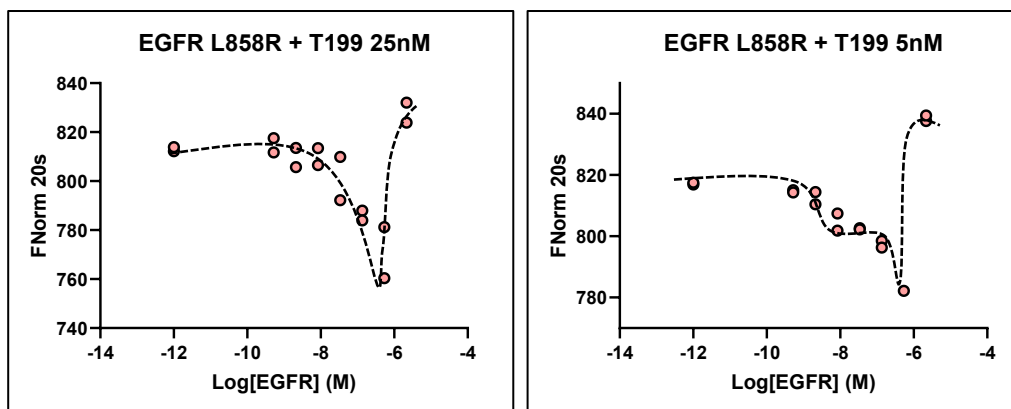


Figure 16 Binding assay between EGFR L858R and T199 at 25 nM (left) and 5 nM (right).

It is interesting to notice that the highest concentrations in this case exhibit unusual behavior (**Figure 16**). This could be attributed to a biphasic trend related to protein dimerization or to an abnormal migration of the tracer as a result of the chemical gradient induced by the thermophoretic flow of the unlabeled protein present at high concentration^[31].

For the purpose of this section, the evaluation of the affinity of the Tracer for the protein will be conducted without considering the titration highest concentrations (**Figure 17**).

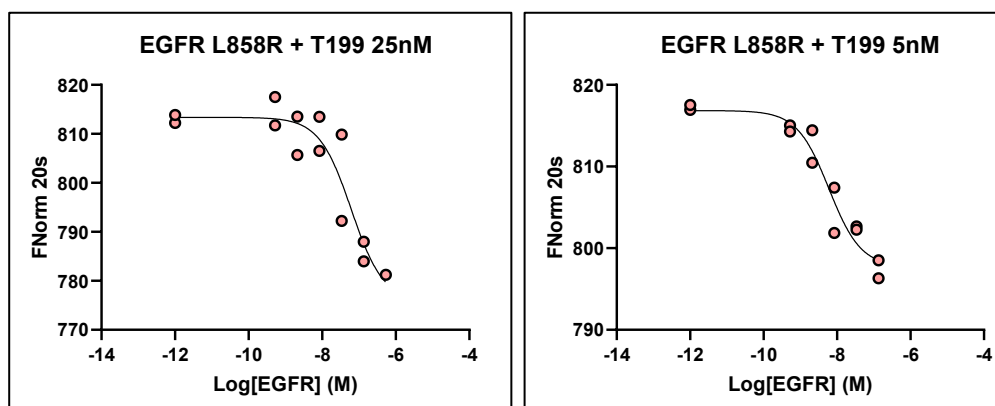


Figure 17 Binding assay between EGFR L858R and T199 at 25 nM and 5 nM without considering the highest concentrations.

EGFR L858R	T199 25 nM		T199 5 nM	
	LOGISTIC FITTING (four parameters)	QUADRATIC FITTING	LOGISTIC FITTING (four parameters)	QUADRATIC FITTING
pK _D	7.29	7.36	8.12	8.47
K _D (nM)	51.0	43.2	7.6	3.4
R ²	0.87	0.87	0.94	0.93
HILL COEFF	1.37	/	0.76	/
RESPONSE AMPLITUDE	33.15	35.80	21.51	18.04
MST-on TIME	20 s	20 s	20 s	20 s

In the case of EGFR L858R a dependence from the Tracer concentration is highlighted at 5 nM and it is made more evident by the quadratic fitting.

By considering these data it seems legit to conclude that the Tracer 199 has a higher affinity for the EGFR L858R isoform.

However, another hypothesis could involve the amount of active site in both the isoforms: if the two proteins have a different amount of active sites the nominal concentrations on the x-axis would be different from the real concentration of competent protein; therefore the affinity might be underestimated.

To test this theory a stoichiometry assay has been performed. In this type of experiment the fluorescent non-titrating species (Tracer 199) is fixed at a concentration near or above the K_D (ideally, 20-fold above the affinity), while the other molecule (EGFR) is titrated over a small range that usually encloses the Tracer concentration. The aim is to benefit from a condition of titration regime or at least a tight binding condition in order to have a consistent depletion of the titrating molecule. As a result at high protein concentration all the Tracer will be bound as only effect of the concentration due to the tight binding condition that makes the binding more efficient. By proceeding with the protein dilution, a specific concentration will be reached, specifically the concentration at which the protein active sites amount is equal to the Tracer concentration. Below this value the Tracer will not be completely bound anymore due to the lack of binding sites, and its signal will be a combination of its bound and unbound extent. The direct consequence is a visible change in the thermophoretic signal compared to the entirely bound condition. This point is called “kink” or “breaking point” and yields the exact information of how many protein molecules in the solution are able to bind the Tracer at the chosen concentration.

The experimental conditions for this assay are reported in the following table.

[EGFR]	1 μ M – 35.18 nM
[TRACER 199]	50 nM
TITRATION	4:1, 16 POINTS
DILUTION BUFFER	50 mM HEPES (pH 7.5), 150 mM NaCl, 1 mM TCEP, 0.005% Tween 20
TEMPERATURE	25°C

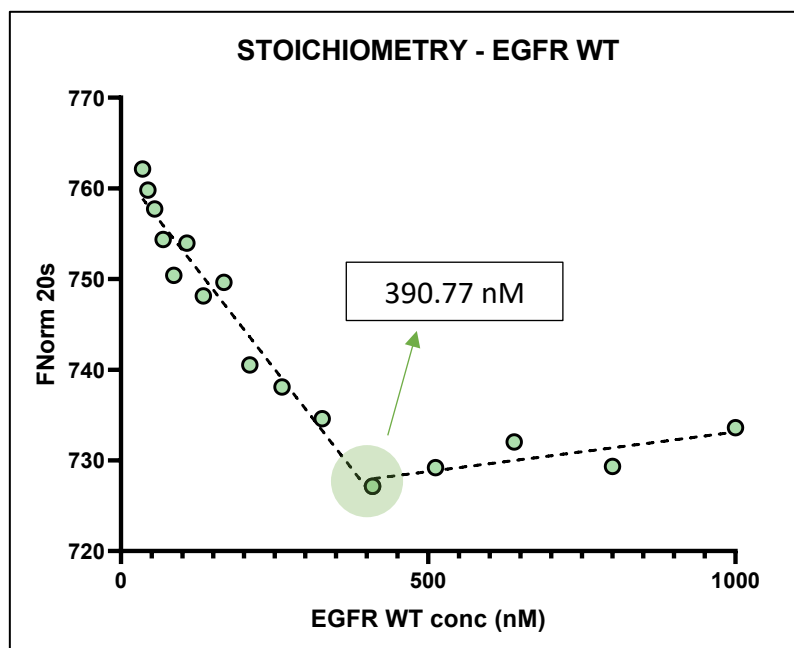


Figure 18 Stoichiometry assay in which EGFR WT is titrated from 1 μ M with a dilution factor of 1.25 over a fixed concentration of Tracer 199 (50 nM). The breaking point indicated by the arrow is the concentration of EGFR WT sites capable of binding 50 nM of Tracer.

The system clearly shows two different trends of points and the intersection of the two linear regression is the breaking point (**Figure 18**). The parameters of the linear regressions are indicated in the table below.

	LINEAR REGR. #1	LINEAR REGR. #2	Breaking Point (nM)
Slope	-0.087	0.0087	390.77
Y-intercept	762	724.4	
R ²	0.96	0.64	

The nominal concentration of tracer is fixed at 50 nM, therefore if the breaking point appears at 390.77 nM the percentage of the protein that is able to bind the Tracer is the **12.8%** of the total amount of the protein.

$$\% \text{ active sites (EGFR WT)} = \frac{50 \text{ nM}}{390.77 \text{ nM}} 100 = 12.8 \%$$

The same experimental set has been applied to the EGFR L858R:

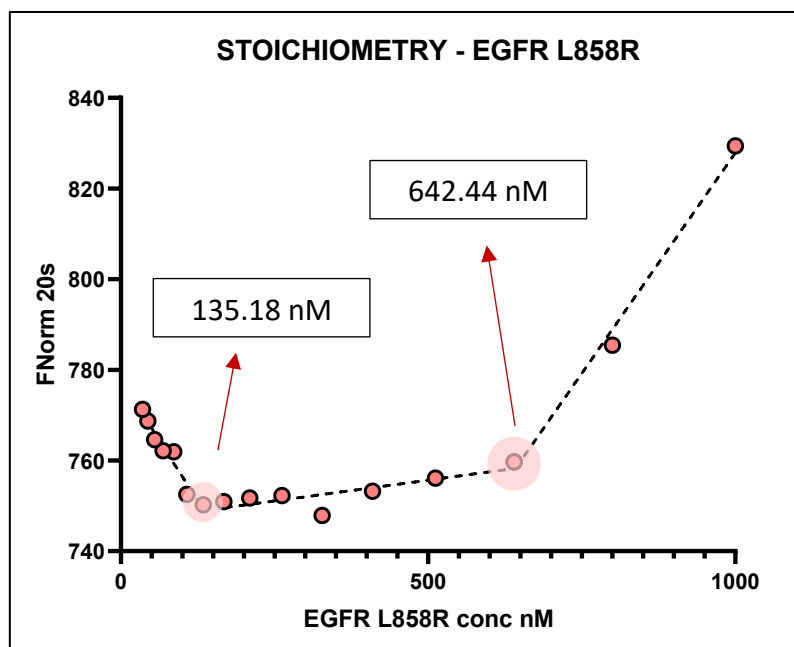


Figure 19 Stoichiometry assay in which EGFR L858R is titrated from 1 μM with a dilution factor of 1.25 over a fixed concentration of Tracer 199 (50 nM). The breaking point indicated by the arrow is the concentration of EGFR WT sites capable of binding 50 nM of Tracer.

	LINEAR REGR. #1	LINEAR REGR. #2	LINEAR REGR. #3	Breaking Point #1 (nM)	Breaking Point #2 (nM)
Slope	-0.21	0.018	0.19	135.18	642.44
Y-intercept	777.8	746.5	633.2		
R ²	0.95	0.67	0.99		

In this case two distinct breaking points are registered: one at 135.18 nM and the second at 642.44 nM (**Figure 19**). It is interesting to notice that the non-changing Tracer mobility values are in between the two breaking points; this suggests that the change in mobility at higher protein concentrations may be due to a massive variation in some of the protein physicochemical features. A possibility is that in these conditions MST registered protein oligomerization. Indeed, the Tracer mobility at protein concentrations above 642.44 nM could be a combination of the Tracer completely bound to the monomer and the Tracer bound to the dimer, a form that increases with protein concentration. As a result, the second breaking point might be the concentration at which the system begins to be populated by that new type of interaction form (**Figure 20**).

This hypothesis is consistent with the consolidated knowledge about the higher tendency of L858R to dimerization^[41] and with the observation made during the Tracer affinity determination experiment for EGFR L858R, in which the highest concentration points exhibited anomalous behavior in comparison to the sigmoidal trend of the lower concentration points, indicating that above 500 nM the thermophoretic mobility begins to be governed by events beyond the simple Tracer-protein interaction.

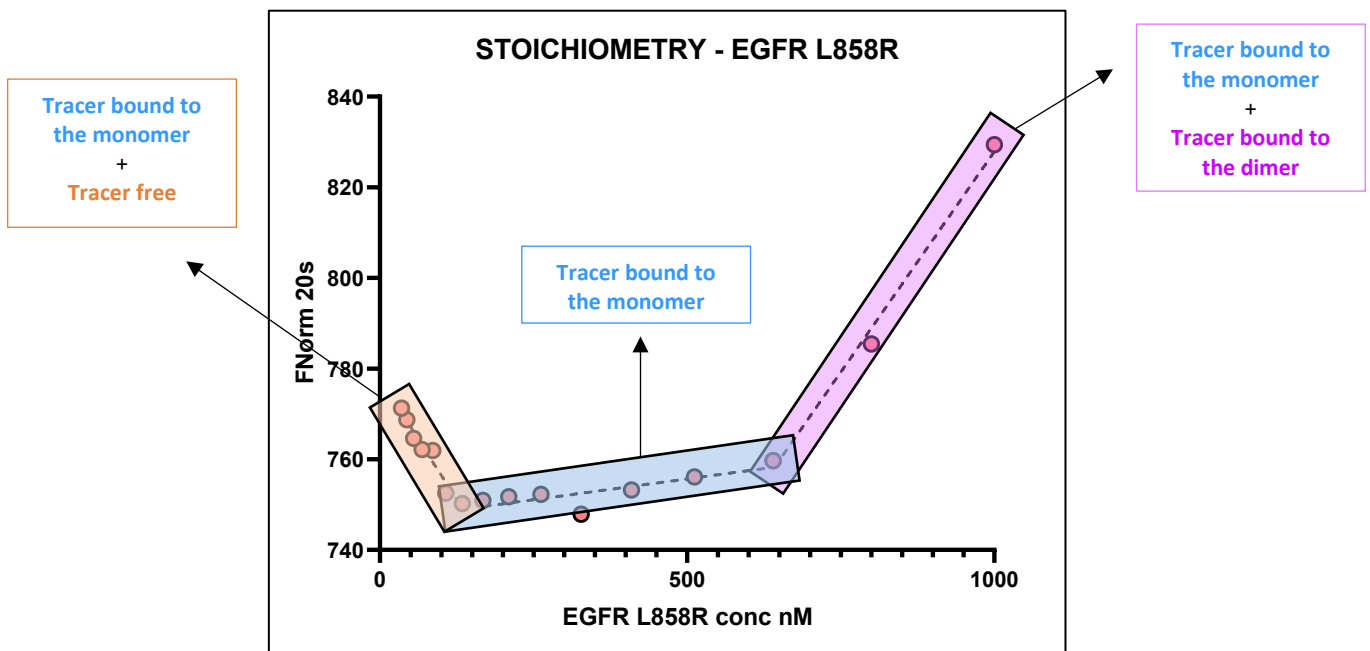


Figure 20 Interpretation of the stoichiometry assay with EGFR L858R: the first linear regression (orange) is related to the combination of Tracer mobility alone and bound to the monomer; the second linear regression (blue) is related to the mobility of the Tracer completely bound to the monomer; the third linear regression (pink) could be related to the coexistence of Tracer mobility both bound to EGFR monomer and dimer.

Regarding the active fraction of the protein, also in this case the nominal concentration of the Tracer is fixed at 50 nM, therefore the breaking point that appears at 135.18 nM should be the percentage of the protein in monomeric form that is able to bind the Tracer. The value is the **37 %** of the total amount of the protein.

$$\% \text{ active sites (EGFR L858R)} = \frac{50 \text{ nM}}{135.18 \text{ nM}} 100 = 37 \%$$

These results indicate that the two isoforms of EGFR, wild type and L858R, exhibit two different percentage of active sites and two different tendency to dimerization.

	% active site (able to bind the Tracer 199)
EGFR WT	12.8 %
EGFR L858R	37.0 %

As a result, the analysis of the direct binding data between the two isoforms of the EGFR and the Tracer 199 needs an adjustment in terms of protein concentration (x-axis).

EGFR WT (nM nominal conc)	12.8 % active sites (nM)	Log10 (M)
1880	240.64	-6.6
470	60.16	-7.2
117.5	15.04	-7.8
29.4	3.8	-8.4
7.3	0.9	-9.0
1.8	0.2	-9.6
0.5	0.06	-10.2
0.001*	0.0001*	-12

**fictional value assigned to the zero concentration to obtain a real Log10 value*

EGFR WT ACTIVE FRACTION ADJUSTMENT (12.8%)	T199 25 nM		T199 5 nM	
	LOGISTIC FITTING (four parameters)	QUADRATIC FITTING	LOGISTIC FITTING (four parameters)	QUADRATIC FITTING
pK_D	7.97	8.01	7.99	8.12
K_D (nM)	10.7	9.9	10.2	7.6
R²	0.99	0.99	0.96	0.96
HILL COEFF	0.85	/	1.34	/
RESPONSE AMPLITUDE	58.04	54.89	53.45	55.75
MST-on TIME	20	20	20	20

fitting performed by letting "float" the Tracer concentration as adjustable parameter.

By considering the real fraction of the protein competent for the Tracer binding the pK_D of EGFR WT increases by an order of magnitude. Even in this case both the logistic and the quadratic fitting yields quite the same information: at 25 nM the system is probably in tight binding condition but the fact that the [Tracer]/2 value is 12.5 nM, thus close to the real affinity of the Tracer, might mask the affinity dependence for the Tracer concentration.

EGFR L858R (nM nominal conc)	37 % active sites (nM)	Log10 (M)
2160	799.2	-6.1
540	199.8	-6.7
135	50.0	-7.3
33.8	12.5	-7.9
8.4	3.1	-8.5
2.1	0.8	-9.1
0.5	0.2	-9.7
0.001*	0.0004*	-12

**fictional value assigned to the zero concentration to obtain a real Log10 value*

EGFR L858R ACTIVE FRACTION ADJUSTMENT (37%)	T199 25 nM		T199 5 nM	
	LOGISTIC FITTING (four parameters)	QUADRATIC FITTING	LOGISTIC FITTING (four parameters)	QUADRATIC FITTING
pK _D	7.72	8.20	8.55	8.65
K _D (nM)	18.9	6.3	2.8	2.2
R ²	0.87	0.85	0.94	0.94
HILL COEFF	1.37	/	0.76	/
RESPONSE AMPLITUDE	33.15	32.67	21.51	19.09
MST-on TIME	20	20	20	20

fitting performed by letting "float" the Tracer concentration as adjustable parameter.

In the case of EGFR L858R the affinity gain is less evident because the active fraction of the protein is larger and thus already closer to its nominal concentration. Observing the results at the lower Tracer concentration, 5 nM, both the logistic and quadratic fitting give similar information, most likely for the same reason as the wild-type experiment at 25 nM: the real affinity would be most probably close the [Tracer]/2 value, so, despite the tight binding conditions, a reliable fitting with the logistic fitting is still possible. Regarding the [Tracer] = 25 nM experiments, the quadratic fitting highlights the tight binding conditions that the logistic fitting partially masked (with the exception of the high Hill coefficient).

In **Figure 21** and **22** it is possible to observe the pK_D values and their changes by considering the nominal protein concentration or its active fraction.

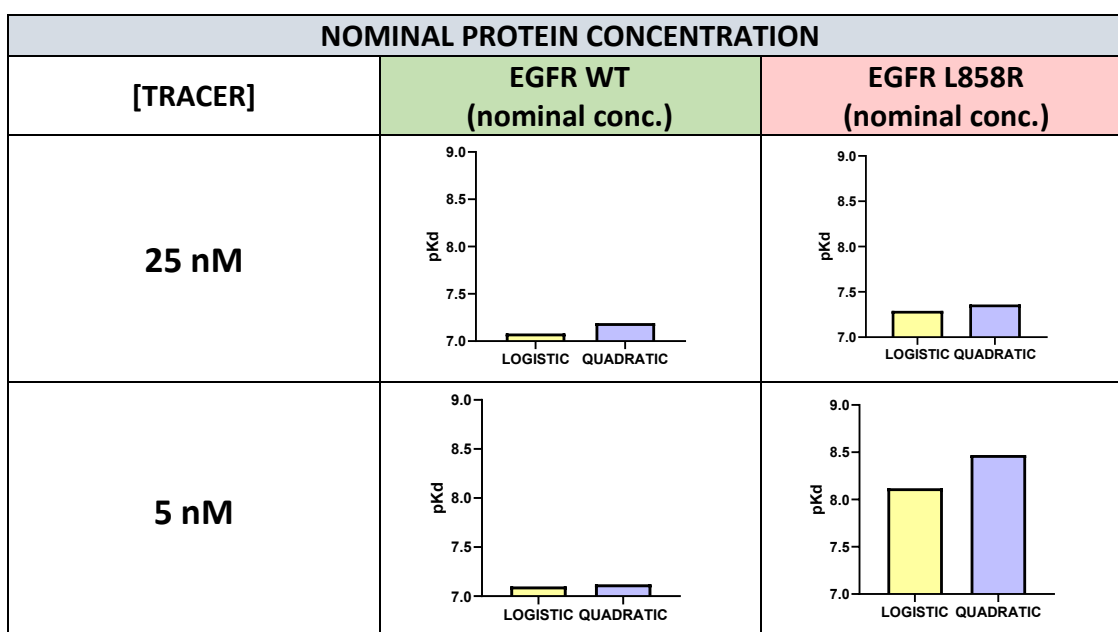


Figure 21 Comparison between the pK_D (obtained considering the nominal concentration of the protein) at 25 nM and 5 nM of the Tracer. In light yellow the value obtained by the logistic fitting and in light purple the quadratic.

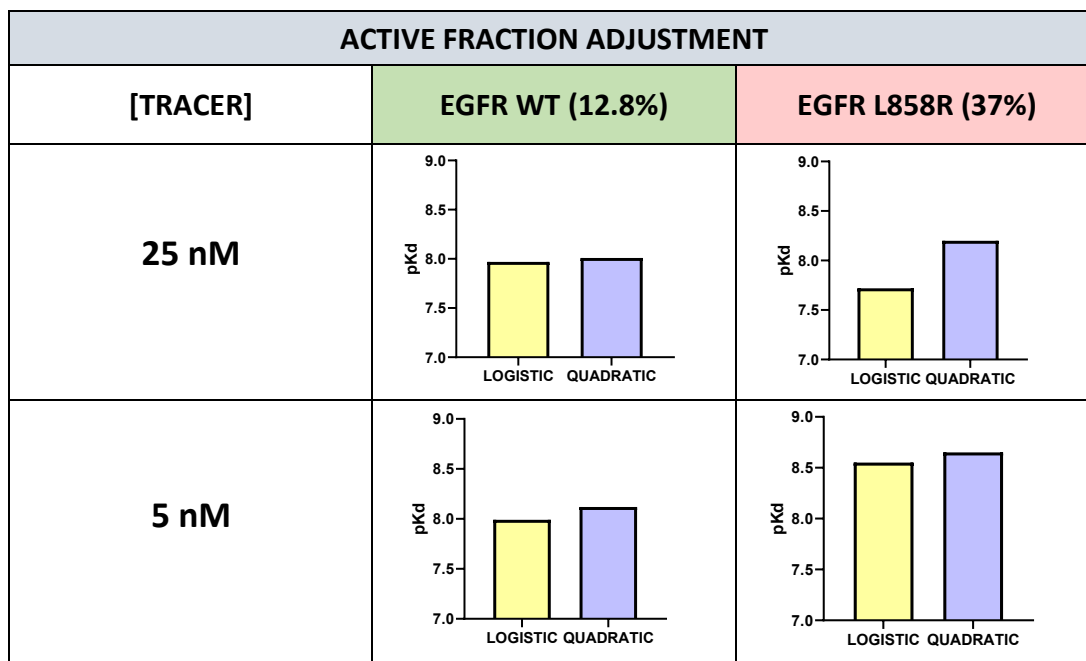


Figure 22 Comparison between the pK_D obtained (considering the adjusted protein concentration on the basis of the stoichiometry assay) at 25 nM and 5 nM of the Tracer. In light yellow the value obtained by the logistic fitting and in light purple the quadratic.

In summary, from this MST characterization emerged that EGFR wild type has less active sites that can bind Tracer 199 than EGFR L858R; even when this difference is taken into consideration in the data interpretation of the direct binding between the Tracer and the proteins, the EGFR L858R seems to have a higher affinity for the tracer than the EGFR WT, a condition that is more evident at lower Tracer concentrations.

However, it was observed from these data that, in some cases, quadratic fitting yielded meaningless and indeterminate parameters, so the data resulting from those fitting (and reported in the tables as blue italic font) was obtained by treating the Tracer concentration as a floating parameter.

The reason of this indetermination could be a non-sufficiently precise determination of the active fraction or the fact that the system has reached a level of complexity where a quadratic fitting is insufficient to reliably describe the interaction. A more complex fitting model, such as a cubic equation, may be required in these cases.

The following competition assays with potent inhibitors will introduce a further element of complexity and a possible double tight binding condition will occur leading to an even more difficult parameter determination. Therefore, for the following paragraph (4.1.2 COMPETITION ASSAYS), the Akaike's Information Criterion (AIC) has been applied to help decide whether to treat the protein concentration in the quadratic equation as a constant or as an adjustable parameter and the values

reported in the results tables will take into account this information. Further considerations on the interaction system interpretation will follow at the end of the aforementioned paragraph.

EGFR AND TRACER 199 TIME DEPENDENCE

Another aspect evaluated was the change in Tracer thermophoretic mobility over time.

The assay was performed by pre-incubating for three hours an appropriate volume of three solutions:

- Tracer 199 alone 5 nM
- Tracer 199 5 nM + EGFR WT 20 nM
- Tracer 199 5 nM + EGFR L858R 20 nM

During this time four capillaries for every condition were loaded and analyzed at every selected time point (10, 40, 60, 90, 120, 150 and 180 minutes). As usual, the thermophoretic mobility on the y-axis is referred to the Tracer mobility.

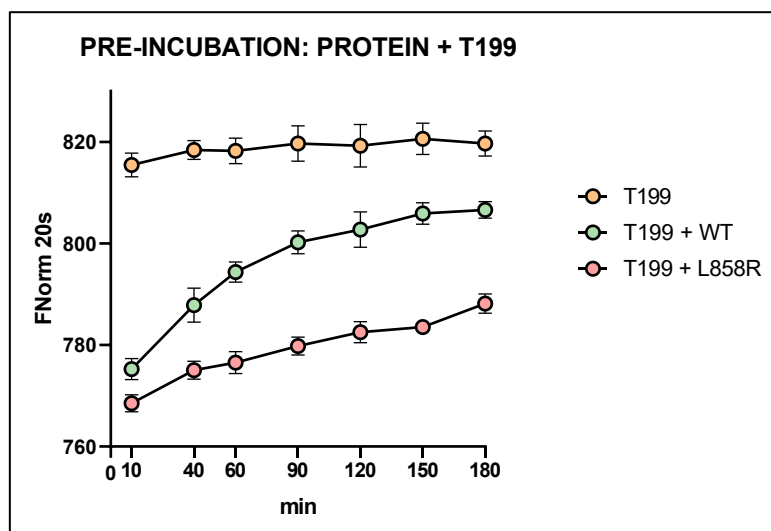


Figure 23 Time dependence of the complex mobility protein-Tracer. In orange is reported the thermophoretic mobility of Tracer 199 alone during time as control. In green is reported the mobility over time of the complex EGFR WT + Tracer 199 and in pink the mobility over time of the complex EGFR L858R + Tracer 199.

In **Figure 23** it is evident that, also in this case, EGFR WT and EGFR L858R show different behaviors. Since the Tracer mobility in the bound state gets closer to the Tracer alone mobility, it is possible to assume the wild type undergoes some conformational change that either could cause:

- A loss in Tracer binding.
- A change in the complex mobility that casually approaches the Tracer alone.

In both cases the thermophoretic mobility reaches a steady state after two hours of pre-incubation. EGFR L858R also undergoes a conformational change resulting in thermophoretic mobility that is similar to Tracer alone, but the process is much slower.

To determine if the conformational change was caused solely by the presence of the Tracer, the same experiment was repeated with the pre-incubation of the protein alone and the Tracer addition right before loading the capillaries at each time point.

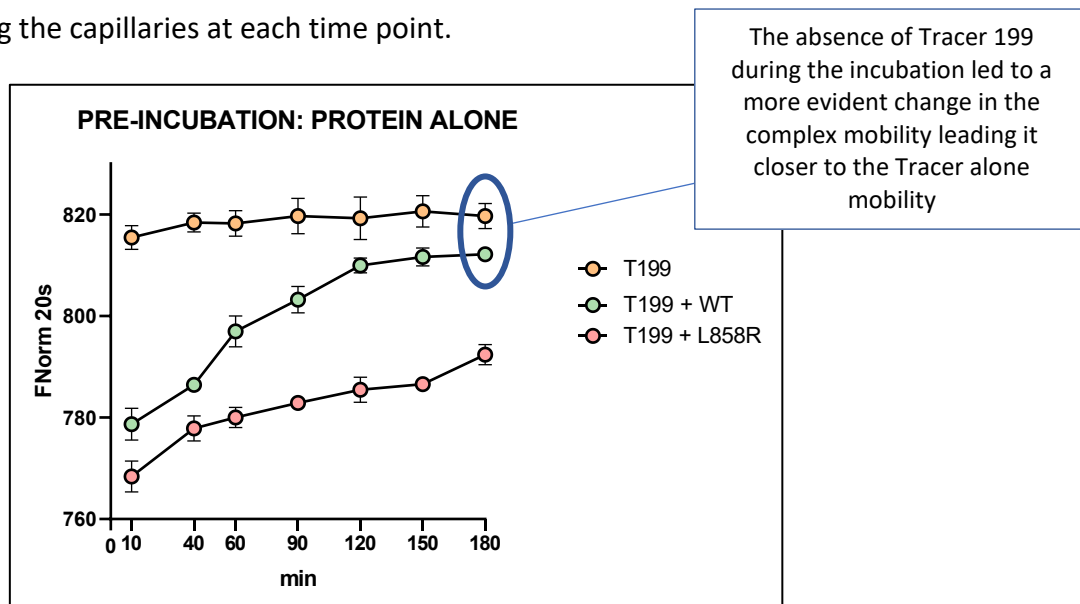


Figure 24 Time dependence of the complex mobility protein-Tracer prior incubation of the protein alone. In orange is reported the thermophoretic mobility of Tracer 199 alone during time as control. In green is reported the mobility over time of the complex EGFR WT + Tracer 199 and in pink the mobility over time of the complex EGFR L858R + Tracer 199.

In **Figure 24** it is evident that, even in the absence of Tracer 199 during the pre-incubation phase, EGFR WT undergoes anyway a conformational modification that brings Tracer-protein complex mobility even closer to mobility of Tracer alone. The EGFR L858R seems to undergo the same process, albeit at a slower and less pronounced rate.

Therefore, Tracer 199 presence in the system is not the direct reason of the conformational change. However, in both cases, time plays an important role in the conformational changes of the two EGFR isoforms and must be considered during competition assays with orthosteric inhibitors or other experiments aimed at describing the time dependence of a specific inhibitor.

Furthermore, it is important to emphasize that the Response Amplitude of a competition assay recorded at longer time points (> 120 minutes) will tend to decrease; indeed, the unbound points correspond to Tracer-protein mobility, whereas the high inhibitor concentration points correspond to Tracer alone mobility. This could be problematic in any assay that suffers from low Response Amplitude from the beginning.

4.1.2 COMPETITION ASSAYS

The Tracer 199 – EGFR interaction system is now described and it is possible to benefit of this information to approach the characterization of three EGFR inhibitors having different binding modes:

- a. Gefitinib: type I, reversible potent binder
- b. Lapatinib: type II, reversible slow binder
- c. Osimertinib, irreversible binder

As previously mentioned in paragraph 4.1, the common feature of these inhibitors is to be orthosteric and to compete with the ATP, hence with the Tracer 199, for the binding to the ATP binding pocket.

In a competition assay the protein and Tracer are fixed at a convenient concentration that enables to minimize fluorescence noise caused by free Tracer in solution. The orthosteric inhibitor is then titrated from a saturating concentration and competes with the Tracer for protein binding. The registered thermophoretic mobility will vary from the Tracer signal when fully associated to the protein and the signal related to the free Tracer in solution when the inhibitor concentration allows its complete displacement.

GEFITINIB - TIGHT BINDING CONDITIONS

Gefitinib is a reversible Type I inhibitor that is EGFR L858R selective^{[40][42][43]}; therefore, the aim of this section was to investigate the Gefitinib-EGFR system with both the wild type and the mutated form to better understand how MST can describe highly potent interactions and if a good experimental design could highlight a difference in Gefitinib L858R selectivity over the wild type.

A critical aspect to take into consideration during the design of a competition assay with a potent inhibitor is the corresponding affinities of Tracer and the inhibitor itself.

To reduce the noise produced by free Tracer in solution, the protein and Tracer concentrations may be fixed excessively high, resulting in a tight binding condition as soon the potent inhibitor is added to the system.

On the other side, it is possible that by decreasing too much the protein/Tracer concentrations the fluorescent difference between the bound and the unbound state will be hardly noticeable, leading to an uncertain situation.

A valuable strategy could be to perform a preliminary competition experiment by using high protein/Tracer concentration which certainly will result in a good signal-to-noise ratio. Once the binding of the inhibitor is confirmed it is possible to decrease the protein/Tracer concentration and to observe the relative pIC_{50} : if the system is in tight binding conditions the pIC_{50} will vary with the protein concentration. It is then possible to decrease the protein concentration until the stabilization of the pIC_{50} is reached or either when the noise becomes too high to obtain reliable information.

In both cases the quadratic fitting could help to better interpret the competition experiments and to highlight an affinity value near to the real one. The **Figure 25** reports a decision scheme that is possible to apply when studying a potent compound.

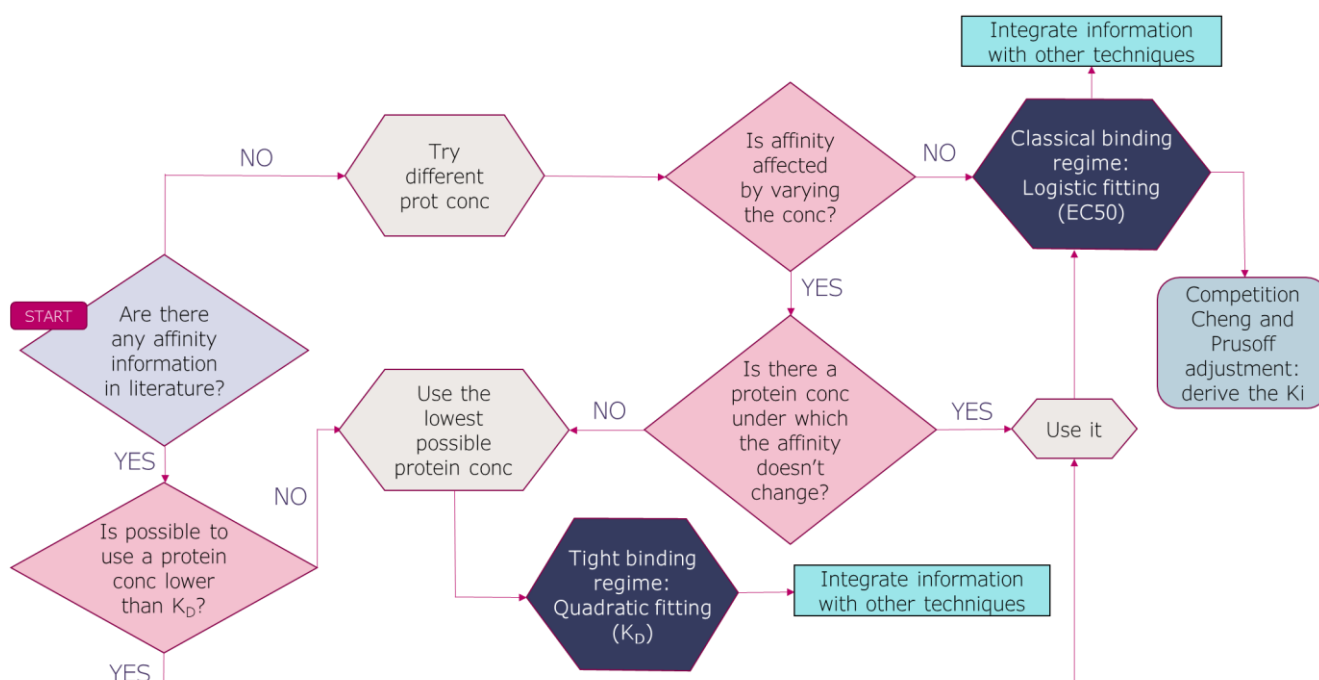


Figure 25 Decision scheme to help in approaching a potent compound to avoid tight binding conditions.

- EGFR WILD TYPE

For the characterization of the Gefitinib-EGFR interaction seven protein concentrations were tested, while the Tracer concentration was held constant at 5 nM. The experimental conditions and the indication of both nominal and adjusted protein concentrations based on the previous activity site determination are reported in the table below.

[EGFR]	140 nM; 70 nM; 30 nM; 20 nM; 15 nM;10 nM; 5 nM
[GEFITINIB]	300 nM – 0.07 nM + CONTROL POINTS
[TRACER 199]	5 nM
TITRATION	1:3, 8 POINTS IN DUPLICATE
DILUTION BUFFER	50 mM HEPES (pH 7.5), 150 mM NaCl, 1 mM TCEP, 0.005% Tween 20
TEMPERATURE	25°C

To determine the amount of Tracer 199 bound to the protein at each tested concentration, the interaction data between EGFR WT and the Tracer itself (reported in the previous paragraph) was normalized by considering the top of the curve (at the highest protein concentration) as the 100 % of bound Tracer and the bottom of the curve (at the lowest protein concentration) as the 0 % of bound Tracer. The logistic nonlinear regression was used to interpolate the logarithms of the seven protein concentrations to obtain the assumed percentage of Tracer bound. It is worth to mention that, regardless of the nominal protein concentration added to the system and reported in the left column, the *visible* amount competing with the Gefitinib is represented by the only Tracer concentration effectively bound to the protein and reported in the right column. Furthermore, as the protein concentration decreases, the amount of free Tracer increases, explaining the progressively reduction of Response Amplitude (**Figure 26**).

[EGFR] (nominal)	[EGFR WT] (12.8% active sites)	[TRACER 199]	% TRACER BOUND TO THE PROTEIN*	[TRACER] BOUND TO THE PROTEIN
140 nM	17.92 nM	5 nM	66.56 %	3.33 nM
70 nM	8.96 nM		47.16 %	2.36 nM
30 nM	3.84 nM		26.12 %	1.31 nM
20 nM	2.56 nM		19.54 %	0.98 nM
15 nM	1.92 nM		16.21 %	0.81 nM
10 nM	1.28 nM		13.00 %	0.65 nM
5 nM	0.64 nM		10.11 %	0.51 nM

*interpolation of the Log₁₀[protein] from the normalized EGFR WT-TRACER 199 binding curve

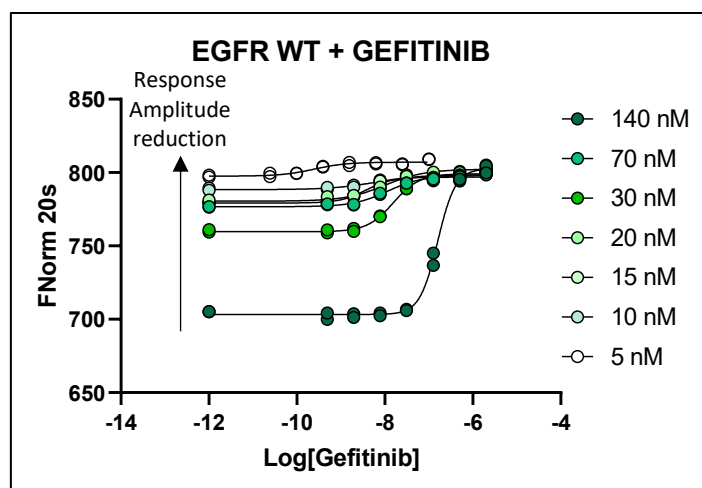


Figure 26 Competition curves with EGFR WT, Tracer 199 and Gefitinib. Every curve is obtained with a different fixed protein concentration, the Response Amplitude reduction by decreasing the protein concentration is a consequence of the higher amount of free Tracer in solution due to the reduction of protein sites.

EGFR WT (nominal conc.)	LOGISTIC FITTING (four parameters)				QUADRATIC FITTING		
	pIC ₅₀	IC ₅₀ (nM)	Hill slope	R ²	pIC ₅₀	IC ₅₀ (nM)	R ²
140 nM	7.63	23.64	2.13	1.00	7.53	29.4	0.98
70 nM	8.75	1.77	1.09	0.98	9.12	0.76	0.98
30 nM	8.63	2.36	1.46	1.00	9.05	0.90	1.00
20 nM	8.82	1.53	0.95	0.98	8.98	1.05	0.97
15 nM	9.25	0.56	1.45	0.96	9.74	0.18	0.96
10 nM	9.03	0.94	0.83	0.90	9.24	0.58	0.90
5 nM	9.61	0.25	1.17	0.92	10.54	0.02	0.92

fitting performed by letting "float" the Tracer concentration as adjustable parameter.

The interaction curve has a very good fit at 140 nM, a Response Amplitude of nearly 100 units, and an R² of 1. This protein concentration, however, yields potency information that is far from reality: it is known from the literature that Gefitinib has a consistently higher potency for EGFR wild type than pIC₅₀ = 7.63^[56], so these experimental conditions, despite their good fit, are likely masking the true value of its affinity. To better describe the interaction, it is necessary to further decrease the protein concentration.

When the protein concentration is decreased the Response Amplitude, the Hill slope, and R² decrease as well, while the potency value gradually increases confirming that the system is indeed moving through tight binding conditions.

With the exception of the first two concentrations 140 nM (where the system has most likely entered a *titration regime*) the quadratic fitting appears to reveal a higher potency at all

concentrations, helping in obtaining a more reliable affinity indication even under tight binding conditions.

- EGFR L858R

The same experimental set up was applied also at EGFR L858R.

[EGFR]	140 nM; 70 nM; 30 nM; 20 nM; 15 nM;10 nM; 5 nM
[GEFITINIB]	300 nM – 0.07 nM + CONTROL POINTS
[TRACER 199]	5 nM
TITRATION	1:3, 8 POINTS IN DUPLICATE
DILUTION BUFFER	50 mM HEPES (pH 7.5), 150 mM NaCl, 1 mM TCEP, 0.005% Tween 20
TEMPERATURE	25°C

[EGFR] (nominal)	[EGFR L858R] (nM) (37% active sites)	[TRACER 199]	% TRACER BOUND TO THE PROTEIN*	[TRACER] BOUND TO THE PROTEIN
140 nM	51.80 nM	5 nM	92.64 %	4.63 nM
70 nM	25.90 nM		88.80 %	4.44 nM
30 nM	11.10 nM		80.69 %	4.03 nM
20 nM	7.40 nM		75.03 %	3.75 nM
15 nM	5.55 nM		70.25 %	3.51 nM
10 nM	3.70 nM		62.52 %	3.13 nM
5 nM	<i>1.85 nM</i>		47.58 %	<i>2.38 nM</i>

*interpolation of the Log10[protein] from the normalized EGFR L858R-TRACER 199 binding curve

The interpolated concentration resulted higher than the protein active sites concentration: at these low concentrations small errors in the determination of the active site fraction or in the interpolation may lead to impacting errors in describing the interaction system and in obtaining the effective amount of active protein competent for binding. Therefore, in quadratic fitting this value will be a priori treated as adjustable parameter.

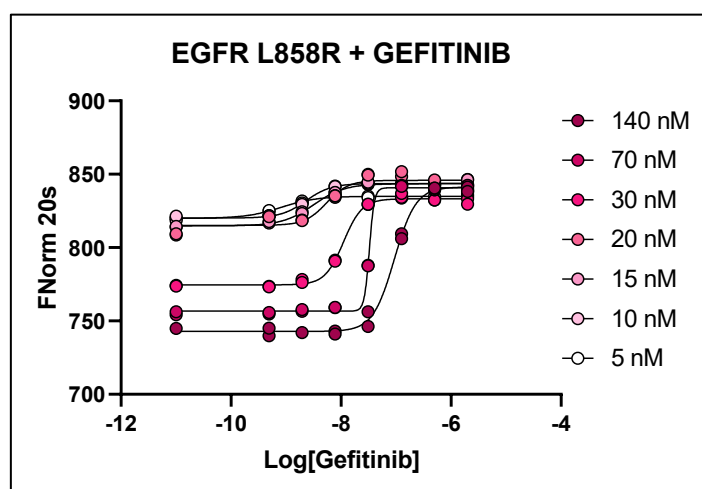


Figure 27 Competition curves with EGFR L858R, Tracer 199 and Gefitinib. Every curve is obtained with a different fixed protein concentration, the Response Amplitude reduction by decreasing the protein concentration is a consequence of the higher amount of free Tracer in solution due to the reduction of protein sites.

EGFR L858R (nominal conc.)	LOGISTIC FITTING (four parameters)				QUADRATIC FITTING		
	pIC ₅₀	IC ₅₀ (nM)	Hill slope	R ²	pIC ₅₀	IC ₅₀ (nM)	R ²
140 nM	7.03	92.63	2.25	1.00	7.16	68.63	0.98
70 nM	7.47	33.52	7.67	1.00	7.63	23.25	0.97
30 nM	7.95	11.19	2.57	1.00	9.38	0.42	1.00
20 nM	8.26	5.50	2.19	0.89	8.70	2.00	0.89
15 nM	8.50	3.18	1.52	0.99	8.88	1.32	0.99
10 nM	8.64	2.31	1.89	0.99	9.20	0.63	0.99
5 nM	9.08	0.83	1.35	0.97	9.40	0.40	0.97

**fitting performed by letting "float" the Tracer concentration as adjustable parameter.*

Tracer 199 has a higher affinity for EGFR L858R and a larger amount of active sites is present in the protein, so the percentage of Tracer bound at each protein concentration is higher. This aspect is beneficial for increase Response Amplitude that remains high even at low protein concentrations (**Figure 27**), but it is limiting for the fitting model ability to yield reliable potency information. Indeed, experimental tight binding conditions can influence the system across a wider range of protein concentrations. At every protein concentration the Hill slope remains significantly high, and the quadratic fitting reveals a significant potency difference when compared to the logistic fitting.

The quadratic fitting also in this case proves to be a useful tool to highlight tight binding experimental conditions.

A further triplicate for the three selected concentrations of 70 nM, 20 nM, and 5 nM was performed to consolidate the difference between the two fitting approaches and to possibly highlight Gefitinib selectivity towards L858R (**Figure 28**).

[EGFR]	70 nM; 20 nM; 5 nM
[GEFITINIB]	100 nM – 0.02 nM + CONTROL POINTS
[TRACER 199]	5 nM
TITRATION	1:3, 8 POINTS IN DUPLICATE
DILUTION BUFFER	50 mM HEPES (pH 7.5), 150 mM NaCl, 1 mM TCEP, 0.005% Tween 20
TEMPERATURE	25°C

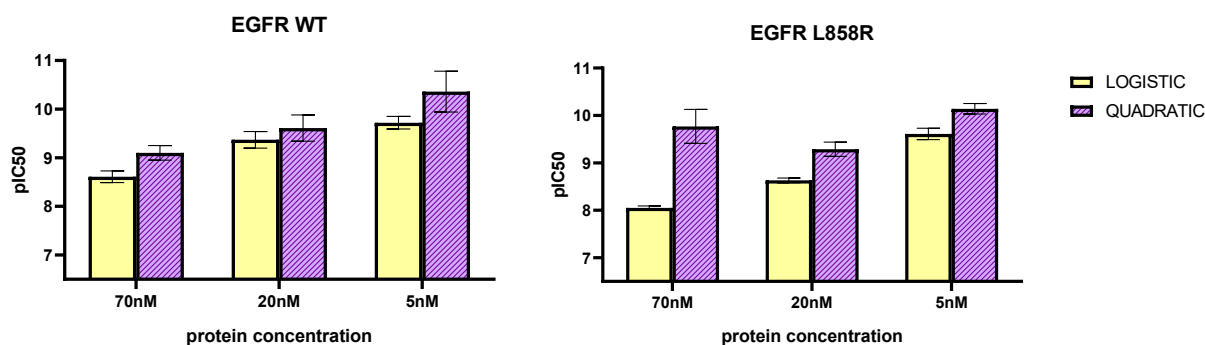


Figure 28 pIC₅₀ values obtained from logistic (yellow) and quadratic (purple) fitting in competition assay of EGFR WT and L858R with Gefitinib. Three protein concentrations have been tested (70 nM, 20 nM and 5 nM) and the potency value are the mean and standard deviation of independent triplicates.

EGFR WT (nominal conc.)	LOGISTIC FITTING (four parameters)				QUADRATIC FITTING		
	pIC ₅₀	IC ₅₀ (nM)	Hill slope	R ²	pIC ₅₀	IC ₅₀ (nM)	R ²
70 nM	8.61	2.46	1.43	0.99	9.04	0.90	0.99
20 nM	9.38	0.42	1.15	0.97	9.54	0.29	0.97
5 nM	9.71	0.20	0.77	0.92	9.71	0.20	0.92

fitting performed by letting "float" the Tracer concentration as adjustable parameter.

EGFR L858R (nominal conc.)	LOGISTIC FITTING (four parameters)				QUADRATIC FITTING		
	pIC ₅₀	IC ₅₀ (nM)	Hill slope	R ²	pIC ₅₀	IC ₅₀ (nM)	R ²
70 nM	8.05	8.96	2.63	0.99	9.61	0.25	0.99
20 nM	8.63	2.36	1.58	0.99	9.23	0.58	0.99
5 nM	9.59	0.26	1.29	0.94	9.91	0.12	0.94

fitting performed by letting "float" the Tracer concentration as adjustable parameter.

The data show that the experimental settings used for both EGFR WT and EGFR L858R resulted in tight binding. The 5 nM concentration might be identified as the concentration that best describes the inhibitor true efficacy, however a robust quantification of the interaction at low concentrations and in a double tight binding situation (protein-Tracer and protein-Gefitinib) is difficult to obtain.

As a result, it is not possible to establish whether the registered slight difference between WT and L858R leaning toward a higher affinity for the mutant form is a true value or a result of parameter indetermination.

Furthermore, the AIC analysis indicated that the model more likely to be correct is the one that considers Tracer concentration as an adjustable parameter, validating the hypothesis that the system has reached a level of complexity that is better described by models with more parameters (propending again for the application of a cubic model).

In summary, **MST enabled the identification of tight binding conditions**, owing to the low sample consumption and rapidity of analysis, which allowed the testing of a large number of protein concentrations; however, a more complex model would be required to quantify the interactions in these conditions.

As a result, even though the data appear to imply a higher potency for EGFR L858R, **the selected models does not allow to highlight with sufficient confidence actual Gefitinib selectivity toward EGFR mutant form.**

It is worth noting that the 5 nM condition for both EGFR WT and Tracer 199 in interaction with Gefitinib yielded a potency value consistent with earlier literature studies^{[52][56]} and, in particular, with the one reported by Castelli et al.^[53]. The interaction assay used in the latter cited work was the Invitrogen LanthaScreen® Eu Kinase Binding Assay, which is based on TR-FRET; the authors used the same EGFR construct used in this thesis experiments, and the obtained IC₅₀ value (0.47 ± 0.05 nM) was 10-fold lower than the protein concentration (5 nM). These findings were in agreement with the MST potency data here reported, as well as the observation of the low percentage of EGFR active sites, which can explain how a very low amount of ligand present in the solution (0.47 nM) could bind half of the total number of 5 nM nominal binding sites. These evidences support MicroScale Thermophoresis as a helpful orthogonal assay to other biophysical methods to investigate protein-ligand interactions.

Finally, in interaction systems that may have a lower Tracer affinity and a higher protein active site concentration, it is important to mention that the competition assay might not be the best approach to obtain quantitative information about a potent inhibitor. In such cases, the competition assay should only be used to provide a qualitative indication of binding, with the quantitative description relying on orthogonal assays like direct binding registration through the use of labeling. An example of this situation will be reported later for the kinase system of ROCK.

LAPATINIB - SLOW BINDING TYPE II INHIBITOR

Lapatinib has been chosen for the investigation, through MST, of time dependent Type II inhibition in EGFR wild type system.

Since Lapatinib is known to have a time-dependence mechanism for the interaction with EGFR^{[42][44]}, its interaction during time has been monitored and the selected time points for the analysis were 10, 40, 75, 120 and 180 minutes.

Moreover, a further 2.5-hour pre-incubation of the complex protein-Tracer alone was done before adding the inhibitor, based on previously registered protein-Tracer changes in thermophoretic mobility over time. The interaction was then examined for two hours after the inhibitor was added.

In summary, the two experiments were performed as follow:

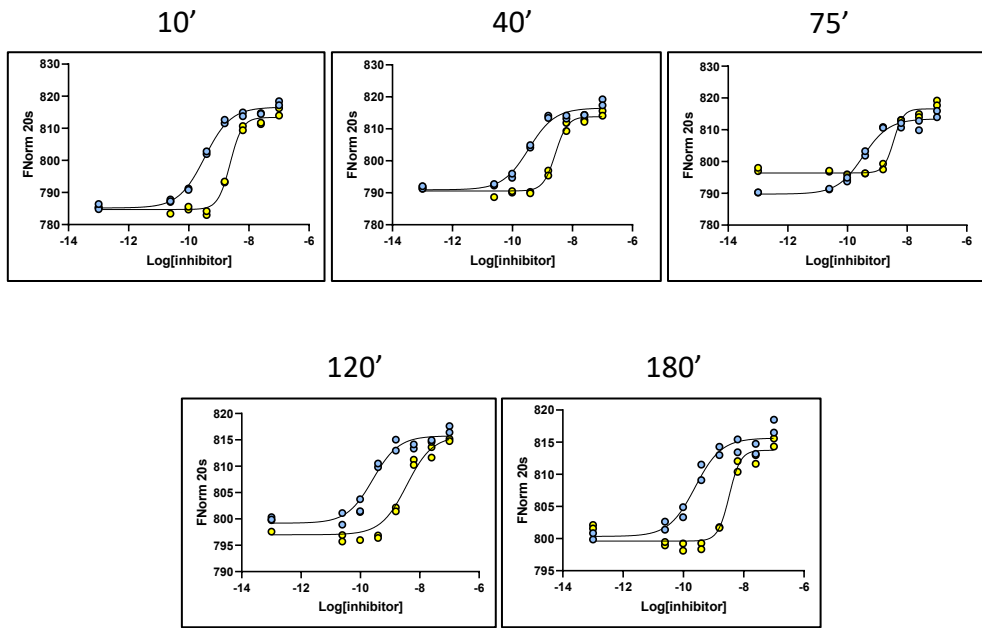
1. **No preincubation:** preparation of the titration (EGFR WT, Tracer199, inhibitor) and capillary loading of the same solution at the defined time points of 10, 40, 75, 120 and 180 minutes.
2. **Preincubation (2.5h):** preparation of the solution EGFR WT-Tracer 199 and preincubation for 2.5h. Then addition of the titrated inhibitor and capillary loading of the same solution at the defined time points of 10, 40, 75, and 120 minutes.

The goal of the two analyses was to observe the interaction change over time while the protein-Tracer equilibrium was changing, and then to compare the interaction time dependency after the protein-Tracer equilibrium was reached.

Gefitinib was also tested in the same conditions as reference.

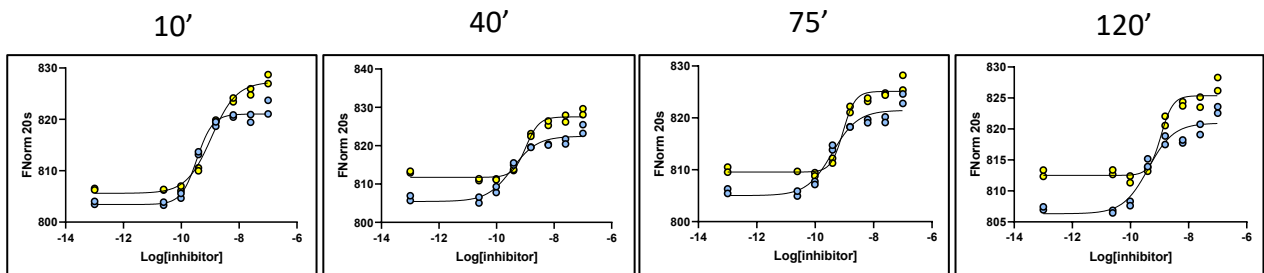
[EGFR WT]	20 nM
[INHIBITOR]	100 nM – 0.02 nM + CONTROL POINTS
[TRACER 199]	5 nM
TITRATION	1:3, 8 POINTS IN DUPLICATE
DILUTION BUFFER	50 mM HEPES (pH 7.5), 150 mM NaCl, 1 mM TCEP, 0.005% Tween 20
TEMPERATURE	25°C
INTERACTION TIME (no preincubation)	10', 40', 75', 120', 180'
INTERACTION TIME (after 2.5h preincubation)	10', 40', 75', 120'

NO PREINCUBATION



	GEFITINIB				LAPATINIB			
	pIC ₅₀	IC ₅₀ (nM)	Hill slope	R ²	pIC ₅₀	IC ₅₀ (nM)	Hill slope	R ²
10'	9.47	0.3	1.18	0.99	8.62	2.4	2.15	0.99
40'	9.46	0.4	1.36	0.98	8.57	2.7	2.15	0.99
75'	9.48	0.3	1.25	0.98	8.45	3.5	2.64	0.98
120'	9.60	0.3	1.52	0.97	8.54	2.9	1.80	0.96
180'	9.61	0.2	1.03	0.96	8.48	3.3	2.33	0.96

2.5H PREINCUBATION (PROTEIN-TRACER)



	GEFITINIB				LAPATINIB			
	pIC ₅₀	IC ₅₀ (nM)	Hill slope	R ²	pIC ₅₀	IC ₅₀ (nM)	Hill slope	R ²
10'	9.46	0.3	1.59	0.99	8.99	1.0	1.29	0.99
40'	9.47	0.3	1.13	0.97	8.98	1.0	1.90	0.98
75'	9.43	0.4	1.10	0.96	9.05	0.9	2.10	0.98
120'	9.40	0.4	1.08	0.95	8.95	1.1	2.13	0.97

By considering the "no preincubation" analysis, the pIC₅₀ value for Gefitinib (light blue) and Lapatinib (yellow) does not change significantly over time.

Interestingly, allowing the system protein-Tracer 199 to equilibrate for 2.5 hours prior to the addition of the inhibitors revealed a significant difference between the two compounds: whereas Gefitinib kept its pIC₅₀ value constant, Lapatinib showed a 0.5 logarithm increase in potency. This new pIC₅₀, however, is maintained in the time dependency analysis that follows.

By observing the intermediate concentration of 1.5 nM over time (red circle in **Figure 29** and **Figure 30**), this difference becomes more evident:

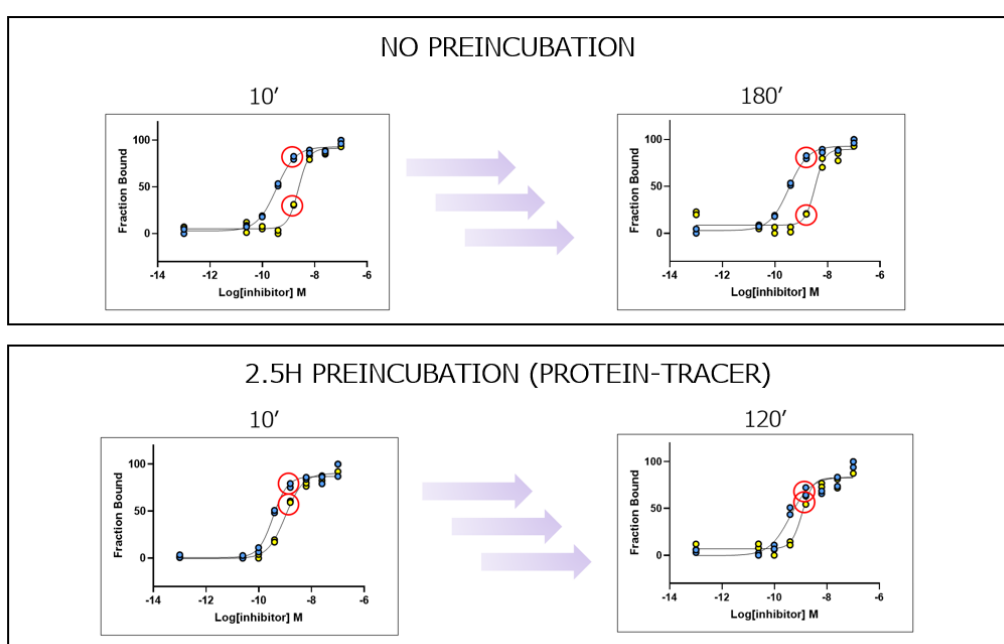


Figure 29 Comparison between competition curves obtained with Gefitinib (blue) and Lapatinib (yellow). Up the condition without preincubation while down the condition with 2.5h of preincubation between protein and Tracer. In the red circles is indicated the 1.5 nM concentration.

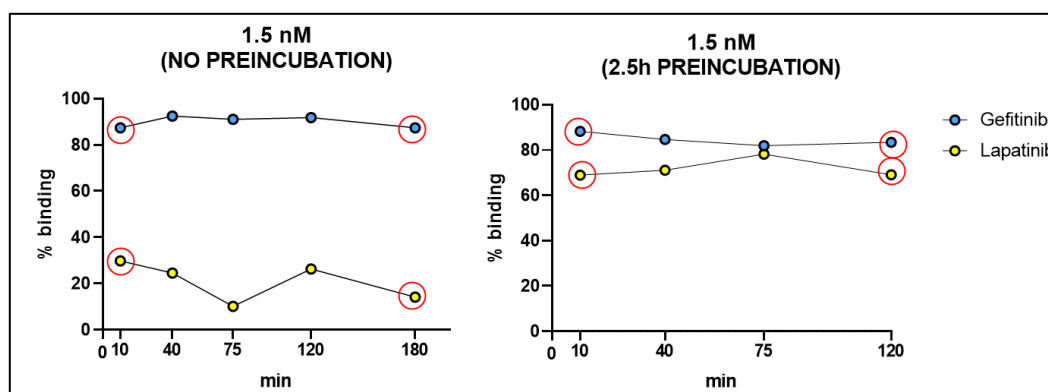


Figure 30 Focus on the 1.5 nM concentration and its contribution to the change in thermophoretic mobility of the Tracer over time.

As a result, the increased potency over time appears to be attributed to the slow conformational change of the protein alone over time, rather than the addition of the inhibitor itself, which appears to stabilize the system in whatever state it would be in when added.

This observation is consistent with the literature evidence indicating the slow mechanism of Lapatinib as a result of the time required for EGFR conformational change to the inactive state^{[34][36][41]}.

The second explored aspect was the difference in binding mode of Gefitinib and Lapatinib. Gefitinib is known to bind EGFR in its active state (Type I inhibitor), while Lapatinib is a Type II inhibitor, binding the inactive form of the protein^{[42][57]}.

Thus, the goal of the following experimental section was to understand if MicroScale Thermophoresis could differentiate the binding of Type I and Type II inhibitors.

To do so, stoichiometry experiments were performed to highlight differences of Gefitinib and Lapatinib in Tracer 199 displacement. Differently from the stoichiometry experiment used to identify the active fraction of the protein, in which EGFR was titrated over a fixed Tracer concentration, the titrating agent in this case is the inhibitor (Gefitinib or Lapatinib), and the protein-Tracer complex is fixed at a concentration that guarantees tight binding conditions. With this experimental setup the breaking points will highlight the inhibitor concentration capable of displace Tracer 199.

[EGFR WT]	140 nM
[TRACER 199]	5 nM
[INHIBITOR]	100 nM – 3.5 nM
TITRATION	4:1, 16 POINTS
DILUTION BUFFER	50 mM HEPES (pH 7.5), 150 mM NaCl, 1 mM TCEP, 0.005% Tween 20
TEMPERATURE	25°C

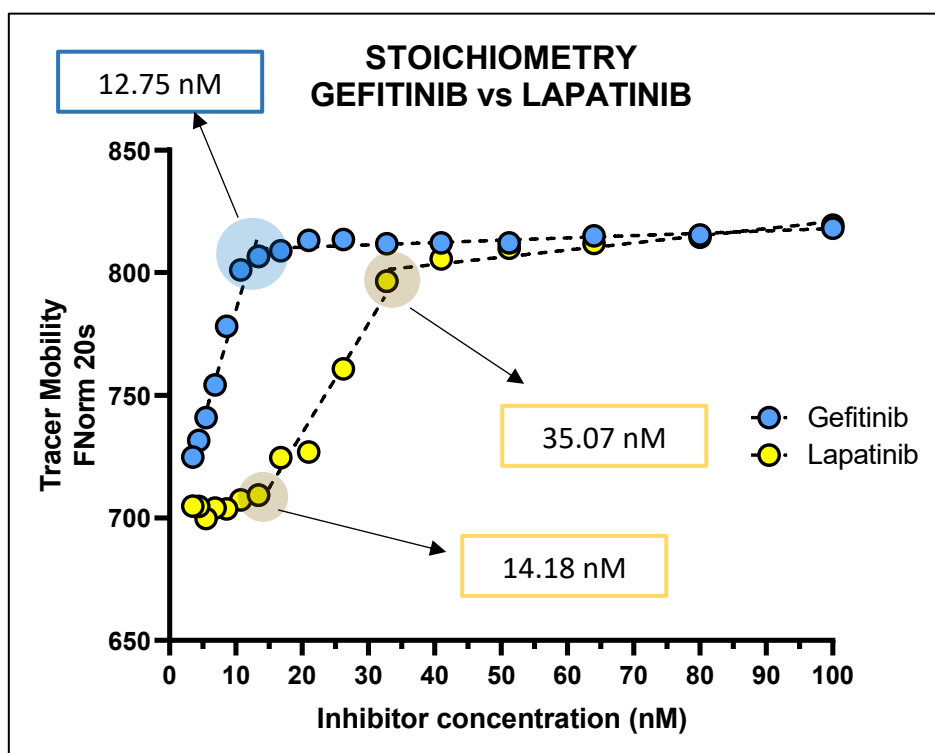


Figure 31 Stoichiometry assay in which Gefitinib (blue) or Lapatinib (yellow) are titrated over a fixed concentration EGFR WT and Tracer 199.

GEFITINIB	LINEAR REGR. #1	LINEAR REGR. #2	Breaking Point (nM)
Slope	9.12	0.095	12.75
Y-intercept	693.4	808.4	
R²	0.96	0.71	

LAPATINIB	LINEAR REGR. #1	LINEAR REGR. #2	LINEAR REGR. #3	Breaking Point #1 (nM)	Breaking Point #2 (nM)
Slope	0.57	4.47	0.29	14.18	35.07
Y-intercept	700.4	645.1	791.7		
R²	0.47	0.96	0.87		

Interestingly the data show a different behavior of Gefitinib and Lapatinib (**Figure 31**). By considering the high inhibitor concentrations, both drugs demonstrate the ability to displace Tracer 199, indeed the Tracer mobility does not change, settling its value around 800 units of normalized fluorescence. Then, by decreasing the inhibitor concentration, the two compounds start to differentiate: Gefitinib allows the binding of the first small amount of Tracer 199 at 12.75 nM, while Lapatinib at 35.07 nM. Lapatinib then reaches the concentration of 14.18 nM at which Tracer 199 is

not displaced anymore, leading to a second *plateau*. This can be explained by considering the presence of different protein states:

- By titrating Gefitinib, the breaking point at 12.75 nM corresponds to the inhibitor concentration necessary to bind all the sites that Gefitinib shares with Tracer 199. Under that concentration a sufficient amount of sites are available for the Tracer binding. This fraction amounted to **9 %**.

$$\% \text{ Gefitinib(like) sites} = \frac{12.75 \text{ nM}}{140 \text{ nM}} 100 = 9 \%$$

- In the Lapatinib experiment, the lowest concentrations of inhibitor up to 14.18 nM resulted non capable of Tracer displacing, then Lapatinib starts to bind the same sites of Tracer 199 displacing it. Thus, since the system is in tight binding conditions and Lapatinib must be sequestered and depleted even at low concentrations, under 14.18 nM the Lapatinib molecules must be bonded at a different site population than Tracer 199. As a result, at concentrations below 14.18 nM Tracer 199 is completely bound to its sites (*plateau* at 700 FNorm), whereas Lapatinib is bound to a *not visible* protein fraction that Tracer 199 does not have the ability to bind: the **10 %** of the total protein amount.

$$\% \text{ Lapatinib(like)sites} = \frac{14.18 \text{ nM}}{140 \text{ nM}} 100 = 10 \%$$

The first breaking point corresponds to the concentration of Lapatinib that saturates the first population (Lapatinib-like sites); above that, Lapatinib begins to bind the Tracer-shared sites (probably the active conformation), for which the inhibitor has a lesser tendency to bind, preferring to saturate the others first. Then, the second breaking point at 35 nM is the Lapatinib concentration that does not allow Tracer binding anymore: thus, it corresponds to the total amount of Lapatinib sites (the sum of Lapatinib-like and Tracer-like). This fraction is around **25 %** of the total amount.

$$\% \text{ Global Lapatinib sites} = \frac{35.07 \text{ nM}}{140 \text{ nM}} 100 = 25 \%$$

Finally, the residual amount, i.e. **75 %**, is referred to the protein fraction not capable of binding Tracer 199 and not highlighted by Lapatinib binding. In this fraction can be listed the protein amount denatured and all the protein molecule in a conformational state not able to bind Tracer 199 and thus *not visible*.

Therefore, some assumption can be made:

- Lapatinib binds two different protein states (it is possible to speculate the active and the inactive state) one of which is shared with Tracer 199 (otherwise displacement could not be possible); however Lapatinib prefers to bind the inactive state at low concentrations and starts to occupy active sites only after the saturation of the inactive form.
- Tracer 199 binds only one of the two states highlighted by Lapatinib (presumably the active state), otherwise the *plateau* state at low Lapatinib concentration would not be visible.
- Gefitinib binds first all the Tracer sites but it is not possible to know by these experiments if it occupies also other sites with a lower affinity once the Tracer sites are completely saturated.
- The higher protein fraction is however constituted by protein non-active in terms of Tracer 199 binding.

These considerations are summarized in **Figure 32**.

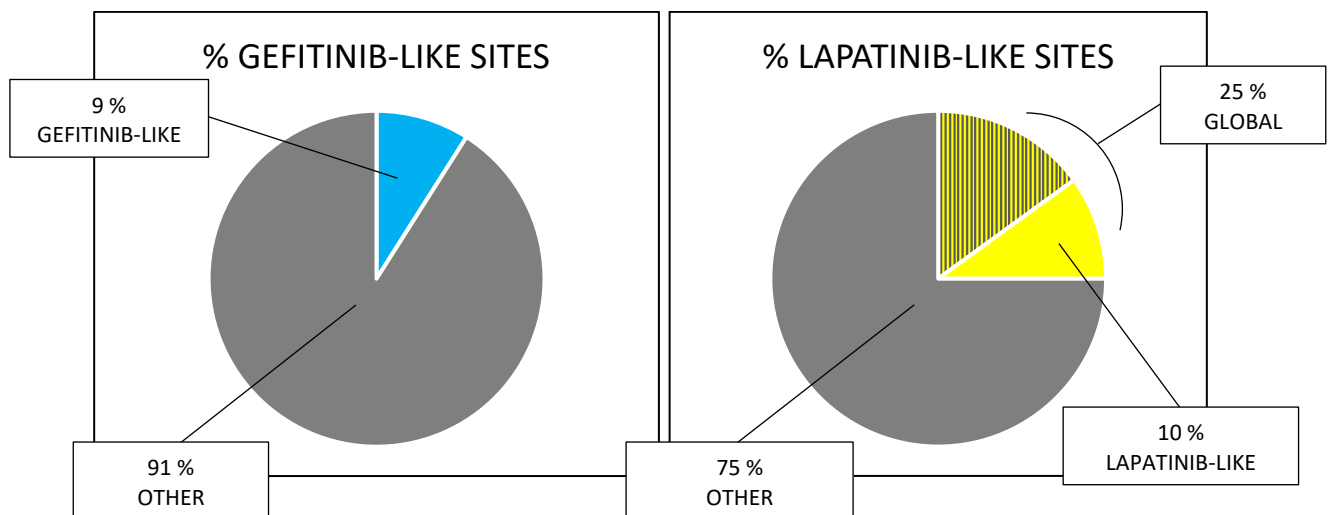


Figure 32 Representation of the different EGFR population highlighted from Gefitinib and Lapatinib stoichiometry assays. For Lapatinib graph (on the right) the shadowed section is referred to the fraction obtained for difference from the Global and the Lapatinib-like sites. It is reasonable to assume that this fraction overlaps with the fraction identified by Gefitinib stoichiometry assay (on the left).

In conclusions, **MST allowed the differentiation of Type I and Type II inhibitors**, by highlighting the presence of multiple conformational states and the inhibitors different propensity to bind them.

OSIMERTINIB - IRREVERSIBLE BINDING

As discussed in the paragraph 1.1.6 - MODES OF INHIBITOR INTERACTIONS - COVALENT BINDING, the irreversible mechanism is usually described from a kinetic point of view, with the k_{inact}/K_i constant, a potency indication that takes into consideration the inhibitor affinity (K_i) and the irreversible inactivation rate (k_{inact}). By performing a classical binding or competition assay, is still possible to obtain a sigmoidal curve and an apparent IC_{50} value that, in this case, is dependent on the incubation time. Indeed, a proper potency measurement relies on specific kinetic assays, but that does not differ much from a reversible inhibitor binding curve in terms of shape and fitting.

As it can be observed in **Figure 33** (in which the same sample preparations have been loaded and tested in MST at 10' and after three hours of incubation at room temperature), the difference in binding mechanisms of Gefitinib (reversible) and Osimertinib (irreversible) emerges only by observing their potency over time, not in any particular changes in their sigmoidal shape.

[EGFR]	20 nM
[INHIBITOR]	100 nM – 0.02 nM + CONTROL POINTS
[TRACER 199]	5 nM
TITRATION	1:3, 8 POINTS IN DUPLICATE
DILUTION BUFFER	50 mM HEPES (pH 7.5), 150 mM NaCl, 1 mM TCEP, 0.005% Tween 20
TEMPERATURE	25°C

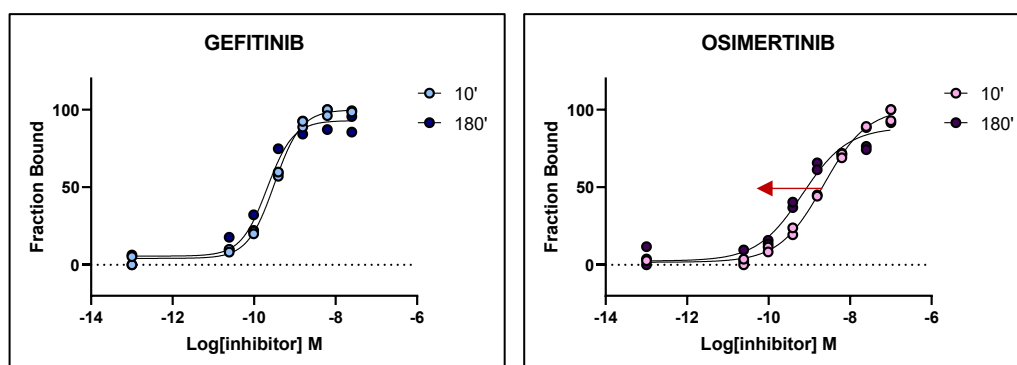


Figure 33 Competition curves with Gefitinib (left) and Osimertinib (right) monitored over time at 10' and 180'.

	GEFITINIB				OSIMERTINIB			
	pIC ₅₀	IC ₅₀ (nM)	Hill slope	R ²	pIC ₅₀	IC ₅₀ (nM)	Hill slope	R ²
10'	9.5	0.3	1.33	1	8.7	2.2	0.80	1
180'	9.7	0.2	1.33	0.98	9.2	0.7	0.78	0.97

Therefore, an important aspect to evaluate when dealing with unknown potentially covalent inhibitors, is to find a way to test the reversibility of the binding. This feature is usually investigated

with enzymatic assays which indicate the activity recovery of a target after the incubation with the inhibitor of interest and the subsequently rapid and massive dilution of the protein-inhibitor complex (*Jump-Dilution*)^[17].

Nevertheless, this type of approach is challenging to perform in a competition setting like the one that has been applied so far. The main issues involve the protein and inhibitor concentrations and the high potency of the inhibitor. Indeed, the typical protocol would require a pre-incubation of the protein at a concentration 100-fold higher than the concentration used in the following competition assay and the inhibitor at a concentration 10 times higher than its IC₅₀. By considering the EGFR WT system and the Gefitinib as the reference compound, the initial conditions should be:

	Initial conc.	Final conc.
[EGFR WT]	2 μ M 100x the final conc.	20 nM
[Gefitinib]	3 nM 10x its IC ₅₀ (0.3 nM)	0.03 nM
[Tracer 199]	/	5 nM

Good final concentrations but not ideal initial concentrations due to the massive protein/inhibitor ratio.

It is clear that in these experimental conditions (protein:inhibitor > 600-fold) the bound fraction of the protein can be neglected also in the initial state and with every type of inhibitor making the measurement incapable of distinguishing between reversible and irreversible interaction: Tracer 199 would be able to bind its small amount of protein even in the presence of Gefitinib.

This problem would be overcome with a less potent inhibitor for which the 10-fold IC₅₀ initial concentration might be near to the protein concentration.

On the other hand, by decreasing the protein concentration at nanomolar values to allow Gefitinib binding at a significant number of sites (e.g. 40 nM, at which the active sites will be 5 nM, based on the 12.8% active fraction), the final concentration after a 100-fold jump dilution would be too small (0.4 nM), and the addition of Tracer 199 as fluorescent marker at its consolidated concentration of 5 nM would completely cover the complex signal. Moreover, decreasing Tracer 199 concentration below 5 nM would result in a poor fluorescence signal.

	Initial conc.	Final conc.
[EGFR WT]	40 nM 100x the final conc.	0.4 nM
[Gefitinib]	3 nM 10x its IC ₅₀ (0.3 nM)	0.03 nM
[Tracer 199]	/	5 nM

Good initial concentrations but not ideal final concentrations due to the low [EGFR WT] related to the [Tracer 199].

For these reasons in the context of the present work an alternative method has been developed for the differentiation of reversible and irreversible inhibitors in the EGFR wild type system.

This method, summarized in **Figure 34**, involves three phases:

1. Pre-incubation at two different times, 60 and 150 minutes, of the protein and the inhibitor (reversible or irreversible) at a low concentration that still allows the saturation of all the protein active sites. The system is then preliminary tested in a Binding Check experiment by adding 5 nM of the Tracer 199 to confirm the complete saturation of the protein.
2. Purification of the complex through a size exclusion spin column (Zeba™ Spin Desalting Columns, 7K MWCO, 0.5 mL, Thermo), which should retain every molecule smaller than 7 kDa not covalently bound to the protein.
3. A second Binding Check experiment with the addition of the Tracer 199 5 nM after the purification, in order to identify which inhibitors have been reversibly removed from the system and now allow the binding of the Tracer to the protein.

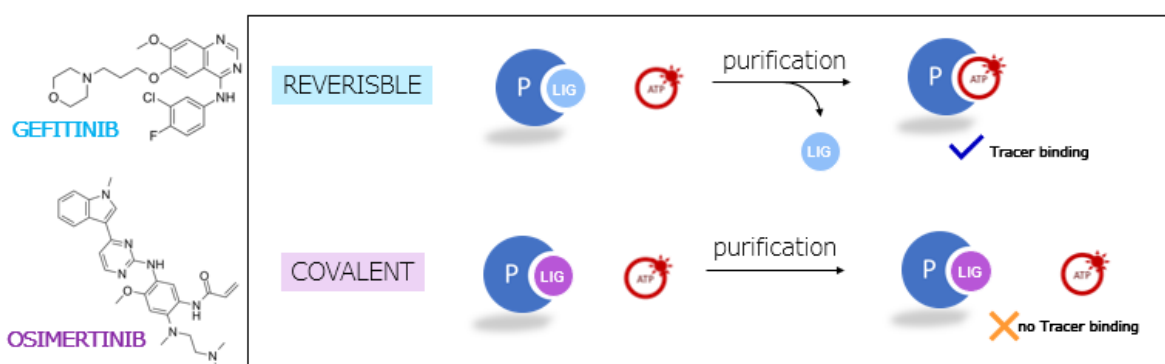


Figure 34 Scheme of the developed method for the differentiation of reversible and irreversible ligands.

For the setup of the experiment two inhibitor concentrations have been tested, 100 nM and 10 nM to confirm in a single concentration experiment that both were saturating concentrations.

[EGFR WT]	20 nM
[Gefitinib]	100 nM or 10 nM
10' pre-incubation of protein-inhibitor	
[Tracer 199]	5 nM

After the protein and inhibitor pre-incubation of 10 minutes, 5 nM of Tracer 199 were added. In the graph every dot corresponds to a single capillary scanned into the instrument and the y-axis is always referred to as the Tracer mobility that in every condition is added at a concentration of 5 nM. As it can be seen in **Figure 35**, when the Gefitinib is added to the system at both 100 nM (pink dots) and 10 nM (light blue dots) the response is the same, the Tracer cannot bind the protein; so

its mobility in the presence of the inhibitor is equal to the one registered for the free Tracer condition (orange dots). When only the protein is present in the system, the Tracer can bind to it, and the registered mobility is referred to as the protein-Tracer complex (dark blue dots).

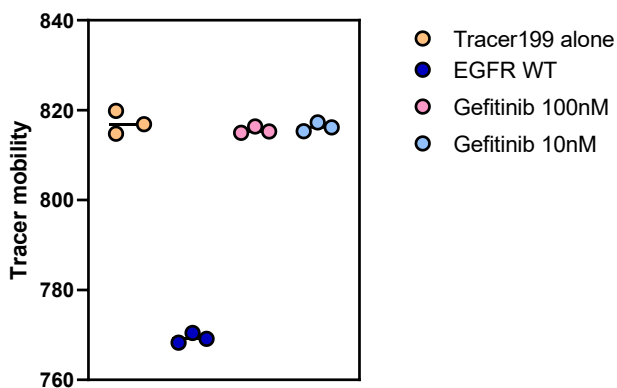


Figure 35 Binding Check of EGFR WT/Tracer 199 with two concentrations of Gefitinib (100 nM and 10 nM) to verify that the saturation with the 10 nM concentration was still occurring.

With this preliminary experiment it has been confirmed that the concentration of 10 nM is able to saturate 20 nM of the protein, therefore it has been chosen for the second part of the setup.

The following part of the method involves the determination of how many cycles of purification through the size exclusion column are required to complete the removal of a reversible reference inhibitor, Gefitinib.

Three spin cycles have been tested and after every cycle a Binding Check experiment has been performed by adding Tracer 199 to the system in order to identify the extent of inhibitor removal.

[EGFR WT]	20 nM
[Gefitinib]	10 nM
10' pre-incubation of protein-inhibitor	
1, 2 or 3 purification cycles	
[Tracer 199]	5 nM

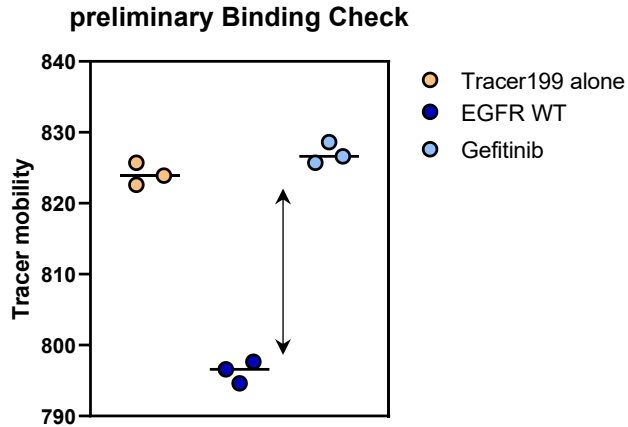


Figure 36 In the preliminary Binding Check is visible how the presence of Gefitinib in the solution of EGFR and Tracer 199 (light blue) does not allow the interaction of the tracer with the protein: Tracer 199 migrates at the same rate of the Tracer 199 alone (orange dots).

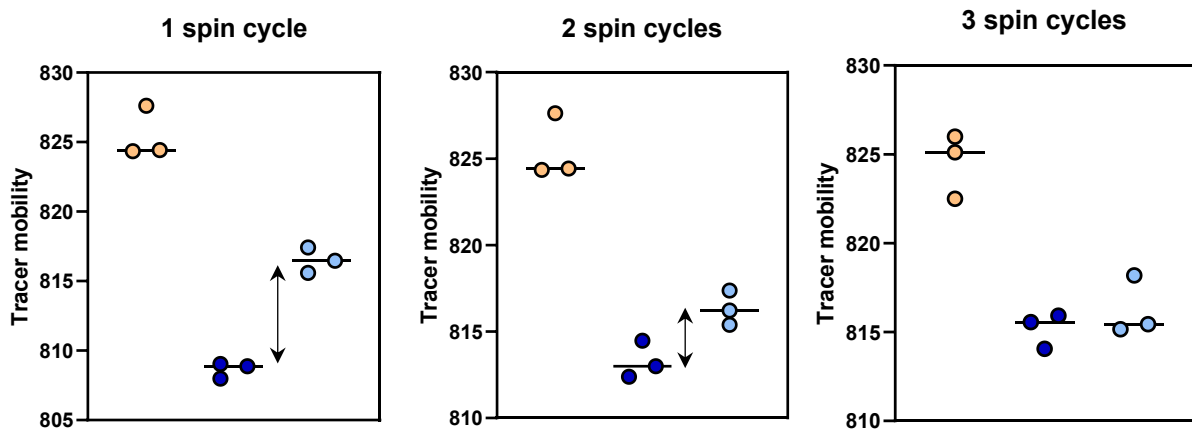


Figure 37 Binding Check after each spin cycle: the first highlights that not all Gefitinib has been removed, thus only a fraction of Tracer 199 can bind the protein. After three spin cycles all Gefitinib has been removed and Tracer 199 can completely bind EGFR, thus its mobility is equal to the complex Tracer-EGFR (dark blue dots).

After every spin cycle the Amplitude of mobility between the Tracer alone (orange dots) and the complex Tracer-EGFR (dark blue dots) decreases (**Figure 36** and **Figure 37**). This could be due either to the time that, as previously demonstrated, causes a reduction of the Response Amplitude, or to the mechanical passage through the spin column that in some way might modify the protein conformation and its ability to bind the Tracer 199. However, by comparing the Gefitinib dots (light blue) to the Tracer-EGFR dots (dark blue), it is possible to overcome this issue and to track the efficiency of the purification at each passage. A one-way ANOVA test ($P < 0.05$) has been performed to statistically verify the mean mobility difference between the different conditions. In particular the Tukey multiple comparisons test has been applied to every Binding Check result set.

Preliminary Binding Check	P Value	Significant?
Tracer199 alone vs. EGFR WT	<0.0001	Yes (****)
Tracer199 alone vs. Gefitinib	0.13	No
EGFR WT vs. Gefitinib	<0.0001	Yes (****)
1 spin cycle	P Value	Significant?
Tracer199 alone vs. EGFR WT	<0.0001	Yes (****)
Tracer199 alone vs. Gefitinib	0.0003	Yes (***)
EGFR WT vs. Gefitinib	0.0006	Yes (***)
2 spin cycles	P Value	Significant?
Tracer199 alone vs. EGFR WT	<0.0001	Yes (****)
Tracer199 alone vs. Gefitinib	0.0004	Yes (***)
EGFR WT vs. Gefitinib	0.08	No
3 spin cycles	P Value	Significant?
Tracer199 alone vs. EGFR WT	0.0007	Yes (***)
Tracer199 alone vs. Gefitinib	0.0014	Yes (**)
EGFR WT vs. Gefitinib	0.68	No

Therefore, from this assay, it emerges that at least two spin cycles are necessary to completely remove a potent but reversible inhibitor from the system and to allow the subsequent binding of Tracer 199 to the protein; however, with three spin cycles, the P value resulting from the comparison between EGFR WT and Gefitinib increases to 0.68, allowing a more confident statement of the complete removal of Gefitinib from the system.

The method is now validated, and it is possible to add a further variable, a known-irreversible inhibitor, to the system: Osimertinib. In this case, the three spin cycles should not interfere with the binding of the covalent interaction. However, an irreversible interaction usually occurs in two steps: the first is the formation of a reversible bond, followed by the formation of an irreversible bond. As a result, two interaction times were tested in order to investigate the time-dependence of irreversible bond formation. Moreover, in the same experiment set, Gefitinib has been tested as well, to monitor the success of each phase (**Figure 38** and **Figure 39**).

[EGFR WT]	20 nM
[Gefitinib] or [Osimertinib]	10 nM
60' or 150' pre-incubation of protein-inhibitor	
3 purification cycles	
[Tracer 199]	5 nM

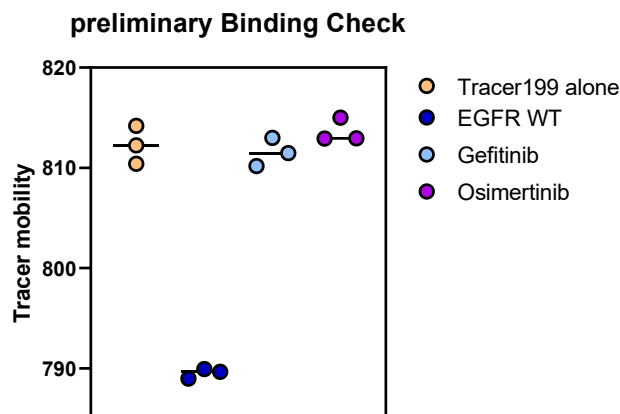


Figure 38 Preliminary Binding Check which confirmed the complete interaction of Gefitinib and Osimertinib with EGFR WT (Tracer mobility in presence of the inhibitors is equal to the Tracer alone mobility).

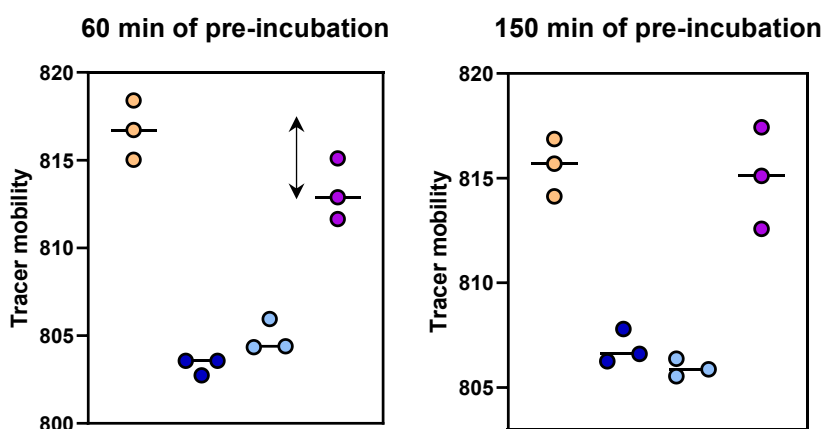


Figure 39 Binding Check after 3 cycles of purification; on the left the results after 60 minutes of preincubation between EGFR WT and inhibitors, on the right the results after 150 minutes of preincubation.

The one-way ANOVA statistical test was also used in this case, and it revealed that the system was properly functioning because Gefitinib was completely removed from the interaction system, allowing Tracer 199 to bind to the protein. Moreover, no difference between 60 and 150 minutes was registered in the binding mode of Gefitinib.

On the contrary, Osimertinib behaves in a different way. After one hour of incubation followed by three cycles of purification, only a fraction of the inhibitor detaches from the protein, and consequently only a fraction of Tracer 199 can bind to it. As a consequence, after the purification and the addition of the Tracer to the system, the Osimertinib dots (purple) are in between the free Tracer dots (orange) and the Tracer-EGFR complex dots (dark blue). When the longer interaction time of two and a half hours is taken into account, the difference between the free Tracer dots (orange) and the Osimertinib dots (purple) is not significant, indicating that the majority of the protein is now involved in the covalent interaction with the Osimertinib. By introducing more time points between time zero and 60 minutes, it would be possible to better describe the kinetics of the covalent bond formation.

Preliminary Binding Check	P Value	Significant?
Tracer199 alone vs. EGFR WT	<0.0001	Yes (****)
Tracer199 alone vs. Gefitinib	0.90	No
Tracer199 alone vs. Osimertinib	0.64	No
EGFR WT vs. Gefitinib	<0.0001	Yes (****)
EGFR WT vs. Osimertinib	<0.0001	Yes (****)
Gefitinib vs. Osimertinib	0.31	No
60 min of pre-incubation	P Value	Significant?
Tracer199 alone vs. EGFR WT	<0.0001	Yes (****)
Tracer199 alone vs. Gefitinib	<0.0001	Yes (****)
Tracer199 alone vs. Osimertinib	0.02	Yes (*)
EGFR WT vs. Gefitinib	0.17	No
EGFR WT vs. Osimertinib	<0.0001	Yes (****)
Gefitinib vs. Osimertinib	0.0002	Yes (***)
150 min of pre-incubation	P Value	Significant?
Tracer199 alone vs. EGFR WT	0.0004	Yes (***)
Tracer199 alone vs. Gefitinib	0.0002	Yes (***)
Tracer199 alone vs. Osimertinib	0.97	No
EGFR WT vs. Gefitinib	0.85	No
EGFR WT vs. Osimertinib	0.0006	Yes (***)
Gefitinib vs. Osimertinib	0.0003	Yes (***)

In summary, the developed method allowed for the **differentiation of reversible and irreversible** kinase inhibitors through a mechanical retention of the molecule not covalently bound to the protein, as well as the possible investigation of the **time-dependence** for the formation of the irreversible interaction.

4.2 ROCK (Rho-associated protein kinase)

The ROCK system was selected to differentiate two other kinase inhibitor binding modes by MicroScale Thermophoresis:

- **Orthosteric** interaction (inhibitors that bind to the same ATP site)
- **Allosteric** interaction (inhibitors that do not compete with the ATP for the binding to the ATP binding pocket).

The ROCK-1 isoform was employed in this experiment set.

Three inhibitors were chosen and characterized for this purpose:

- **Compound A** (reference, orthosteric)
- **Compound B** (allosteric)
- **Compound C** (allosteric)

In this case, the two orthogonal approaches of the competition assay and the binding assay were applied in combination to obtain complementary information about the system.

While both the competition and the direct binding assay should be able to give information about an orthosteric interaction (**Figure 40**), only the direct binding assay should register the interaction of the protein with an allosteric inhibitor (**Figure 41**). Thus, a discrepancy between the two approaches might be able to highlight a non-competitive binding mode occurring with allosteric compounds.

ORTHOSTERIC INTERACTION

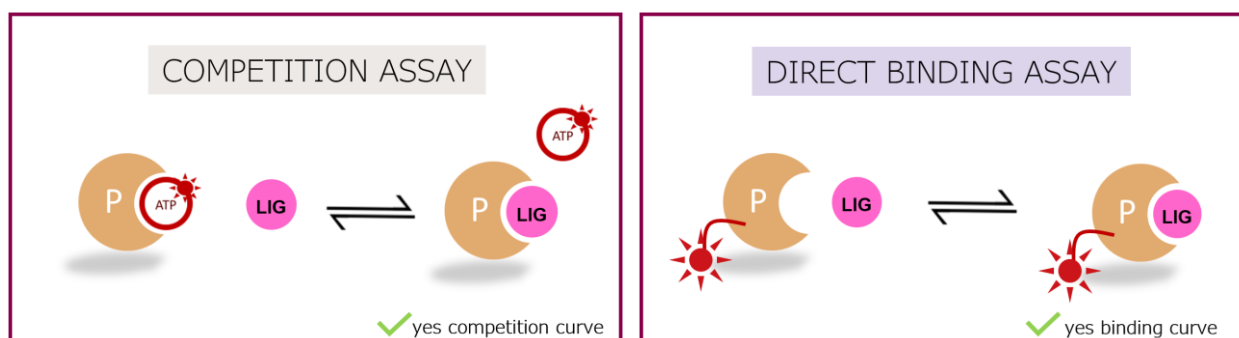


Figure 40 With orthosteric compounds both Competition and Direct Binding assay are able to detect the interaction.

ALLOSTERIC INTERACTION

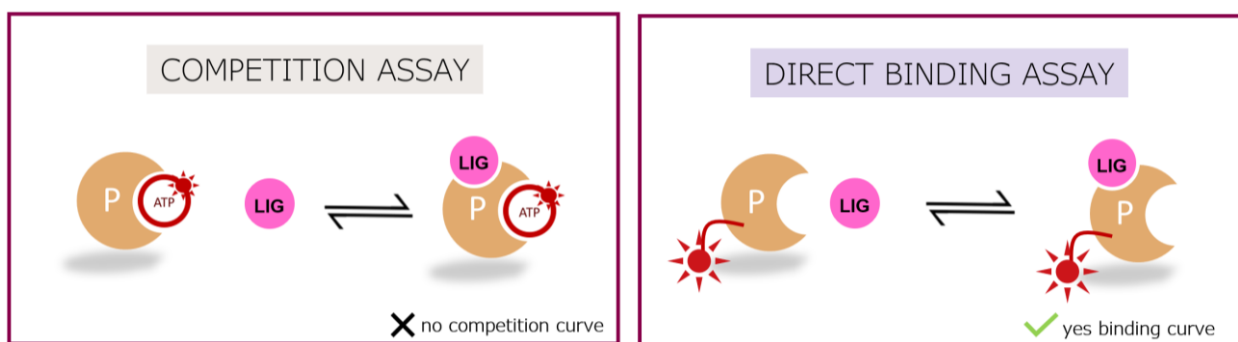


Figure 41 With allosteric compounds a discrepancy between Competition and Direct Binding assays could occur, due to the missing ATP fluorescent displacement during the Competition Assay.

4.2.1 COMPETITION ASSAYS

INTERACTION WITH KINASE TRACER 236

The interaction between ROCK-1 and its fluorescent ATP analog (Kinase Tracer 236, Thermo) has also been investigated in this case.

In analogy with the EGFR system, two Tracer concentrations have been tested, 25 nM and 5 nM, and the results are reported in **Figure 42**.

[ROCK-1]	15 μ M – 3.6 nM + CONTROL POINTS
[TRACER 236]	25 nM / 5 nM
TITRATION	1:3, 8 POINTS IN DUPLICATE
DILUTION BUFFER	50 mM HEPES (pH 7.5), 150 mM NaCl, 2 mM DTT, 0.01% Tween 20
TEMPERATURE	22°C

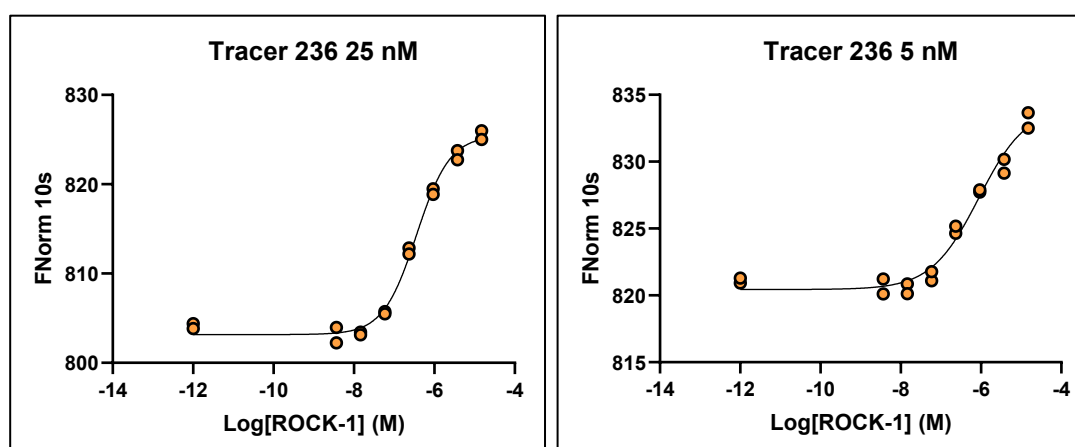


Figure 42 Binding assay between ROCK-1 and T236 at 25 nM (on the left) and 5 nM (on the right).

ROCK-1	T236 25 nM		T236 5 nM	
	LOGISTIC FITTING (four parameters)	QUADRATIC FITTING	LOGISTIC FITTING (four parameters)	QUADRATIC FITTING
pK _D	6.44	6.45	6.06	6.22
K _D (nM)	359.4	352.0	878.11	598.27
R ²	0.99	0.99	0.97	0.97
HILL COEFF	1.05	/	0.73	/
RESPONSE AMPLITUDE	22.31	22.52	13.68	11.85
MST-on TIME	10 s	10 s	10 s	10 s

In this case, the quadratic and the logistic fitting at 25 nM yield the same affinity values, well above the nominal Tracer concentration, suggesting that the system should not be in tight binding conditions.

By decreasing the Tracer concentration to 5 nM, the affinity value does not increase, confirming that the system is not in tight binding conditions and the logistic fitting is sufficient to describe the interaction.

OPTIMIZATION OF THE INTERACTION WITH COMPOUND A

Three protein doses were tested to better characterize the interaction between ROCK-1 and the orthosteric Compound A: 200 nM, 50 nM, and 20 nM (**Figure 43**). The experimental conditions are detailed in the table below. The Tracer concentration of 15 nM was chosen since 5 nM tried in the preliminary testing produced an insufficient fluorescence signal.

[ROCK-1]	200 nM, 50 nM, 20 nM
[INHIBITOR]	1 μM – 0.24 nM + CONTROL POINTS
[TRACER 236]	15 nM
TITRATION	1:3, 8 POINTS IN DUPLICATE
DILUTION BUFFER	50 mM HEPES (pH 7.5), 150 mM NaCl, 2 mM DTT, 0.01% Tween 20
TEMPERATURE	22°C

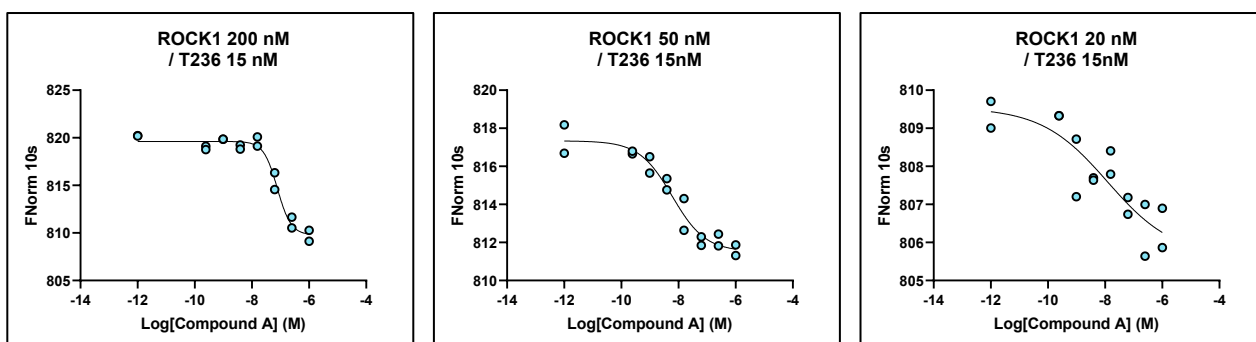


Figure 43 Competition assays with ROCK-1 tested at three concentrations (200 nM, 50 nM and 20 nM), Tracer 236 and Compound A.

ROCK-1 (nominal conc.)	LOGISTIC FITTING (four parameters)				QUADRATIC FITTING		
	pIC ₅₀	IC ₅₀ (nM)	Hill slope	R ²	pIC ₅₀	IC ₅₀ (nM)	R ²
200 nM	7.11	77.3	1.81	0.97	7.02	94.5	0.96
50 nM	8.22	6.0	0.75	0.95	8.64	2.3	0.93
20 nM	7.92	12.0	0.37	0.77	7.79	16.3	0.69

When the protein concentration is reduced from 200 nM to 20 nM, the noise increases due to the increased concentration of free Tracer 236 in solution. Even with the best R² value, the 200 nM condition has a Hill slope greater than one, indicating that the experimental conditions are not ideal for describing the system: the high protein concentration likely causes inhibitor depletion, which is reflected in the visible amount competing with the Tracer, however small it may be due to the tracer low affinity for the protein. As evidence, decreasing the protein concentration changes the pIC₅₀ value of Compound A.

In this case, 50 nM is probably the best compromise between a good fit and reliable information on potency, but due to the low affinity of the Tracer 236 for the protein, it is important to consider that every potent inhibitor might be underestimated in terms of pIC₅₀. Therefore, as previously mentioned, in these conditions, the competition assay could be solely applied to obtain qualitative information about interaction, relying on the direct binding assay to obtain quantitative information.

COMPETITION WITH ALLOSTERIC COMPOUNDS

Once the experimental conditions for the competition assay are chosen, the allosteric inhibitors (Compound B and Compound C) have been tested (**Figure 44**).

[ROCK-1]	50 nM
[INHIBITOR]	1 μ M – 0.24 nM + CONTROL POINTS
[TRACER 236]	15 nM
TITRATION	1:3, 8 POINTS IN DUPLICATE
DILUTION BUFFER	50 mM HEPES (pH 7.5), 150 mM NaCl, 2 mM DTT, 0.01% Tween 20
TEMPERATURE	22°C

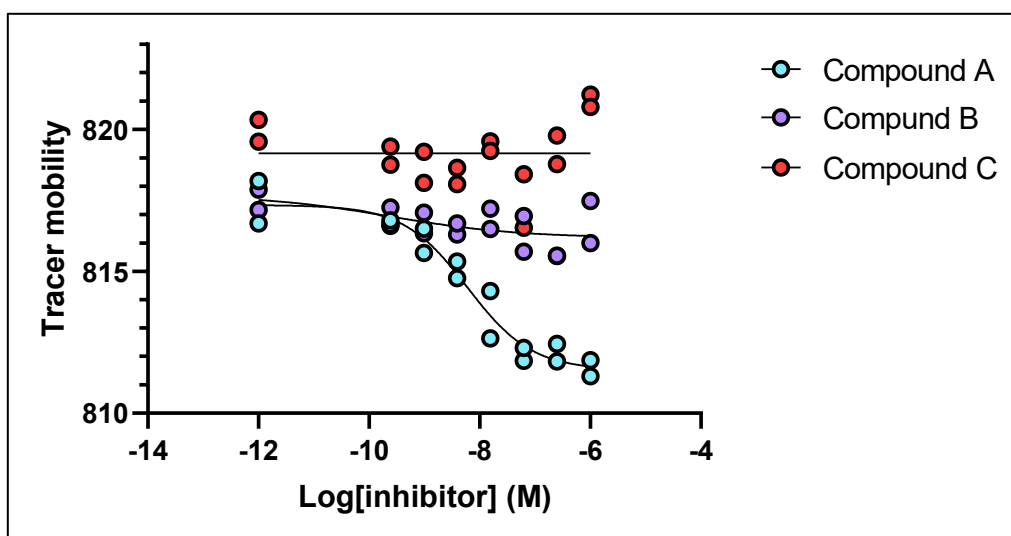


Figure 44 Competition assay with ROCK-1, Tracer 236 and Compounds A, B and C.

	pIC ₅₀	IC ₅₀ (nM)	Hill slope	Response Amplitude	R ²
COMPOUND A	7.11	77.3	1.81	5.8	0.97
COMPOUND B	~ 9.6	~ 0.2	1.50	1.5	0.34
COMPOUND C	-	-	-	-	-

As can be seen in **Figure 44**, the only compound giving a robust competition curve is the Compound A. By testing the compounds in a single concentration test (Binding Check, **Figure 45**) at 1 μ M, no significant difference is registered between the Tracer 236 mobility only bound to the protein (dark blue) and the Tracer 236 registered in the presence of the Compounds B and C (purple and red dots).

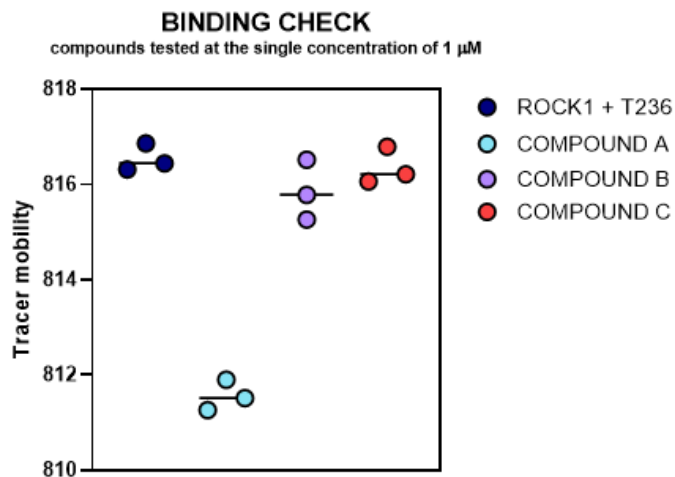


Figure 45 Binding Check with ROCK-1 in complex with Tracer 236 (dark blue), the same complex with the addition of orthosteric Compound A (light blue) and the allosteric Compounds B and C (purple and red).

Binding Check	P Value	Significant?
ROCK-1 vs. Compound A	<0.0001	Yes (****)
ROCK-1 vs. Compound B	0.28	No
ROCK-1 vs. Compound C	0.95	No
Compound A vs. Compound B	<0.0001	Yes (****)
Compound A vs. Compound C	<0.0001	Yes (****)
Compound B vs. Compound C	0.51	No

However, in the competition assay, the Compound B showed a slight sigmoidal trend, albeit with a very low R^2 and Response Amplitude, while the Compound C showed a tendency to increase Tracer mobility at higher concentrations.

To verify if the trends of the two allosteric compounds would be confirmed in a replicate and at higher concentrations, both compound B and C were additionally tested with an initial titrating concentration of 10 μ M.

[ROCK-1]	50 nM
[INHIBITOR]	10 μ M – 2.4 nM + CONTROL POINTS
[TRACER 236]	15 nM
TITRATION	1:3, 8 POINTS IN DUPLICATE
DILUTION BUFFER	50 mM HEPES (pH 7.5), 150 mM NaCl, 2 mM DTT, 0.01% Tween 20
TEMPERATURE	22°C

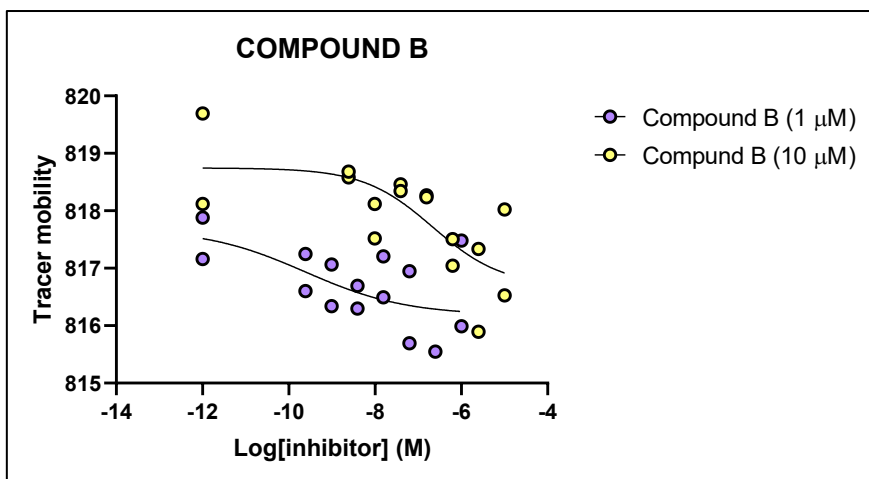


Figure 46 Comparison between two competition assays with Compound B, one starting from 1 μM (purple) and the second starting from 10 μM (yellow).

	pIC ₅₀	IC ₅₀ (nM)	Hill slope	Response Amplitude	R ²
COMPOUND B (1 μM)	~ 9.6	~ 0.2	1.50	1.5	0.34
COMPOUND B (10 μM)	~ 6.7	~ 218.0	0.53	2.1	0.53

The point trends for Compound B in both tested conditions are not robust enough to conclude that Tracer 236 displacement is occurring (**Figure 46**). However, on the basis of the slight trend of the points toward lower Tracer mobility values, it is not possible to completely exclude the possibility that increased Compound B concentrations could impact the Tracer 236-ROCK-1 interaction or have some non-quantifiable distal effect on the ATP binding site.

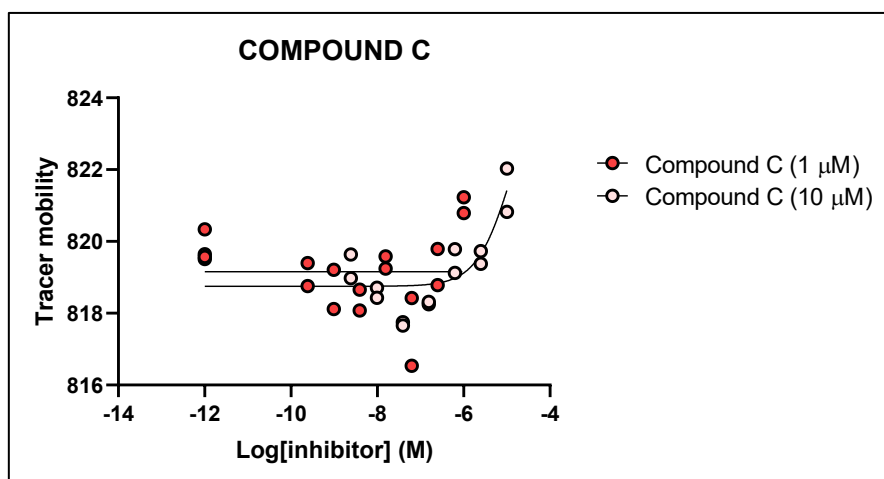


Figure 47 Comparison between two competition assays with Compound C, one starting from 1 μM (red) and the second starting from 10 μM (light pink).

	pIC ₅₀	IC ₅₀ (nM)	Hill slope	Response Amplitude	R ²
COMPOUND C (1 μM)	-	-	-	-	-
COMPOUND C (10 μM)	~ 4.9	~ 1263	1.08	6.10	0.65

Also for Compound C no robust fitting is occurring in the competition assay. At 10 μM an increased Tracer 236 mobility is registered (**Figure 47**). Since the Tracer is moving in the opposite direction of the free-Tracer mobility (registered at high concentrations of Compound A), it is not possible to assume that a displacement is taking place, therefore two other hypotheses can be made on this situation:

- The highest concentrations points of Compound C induce an aberrant movement of the protein-Tracer complex due to its closeness to the solubility limit and to the potential formation of aggregates.
- Compound C at higher concentrations is able to bind the protein in another site with respect to the Tracer 236 but also to induce a conformational change responsible for the different mobility of the ternary complex ROCK-1-Tracer 236-Compound C.

In summary, from the competition experimental set it is possible to conclude that Compound B and Compound C have a different binding mode than the orthosteric Compound A.

4.2.2 DIRECT BINDING ASSAYS

ROCK-1 COVALENT LABELING AND BINDING COMPETENCE TEST

To perform a direct binding assay the protein ROCK-1 needed to be fluorescently labeled. The labeling protocol chosen for this purpose is the Monolith Protein Labeling Kit RED-NHS 2nd Generation (NanoTemper) and, after the labeling reaction, a binding test with Compound A was performed to verify the binding competence of the protein.

Two labeling conditions were tested:

1. Labeling in the presence of a low potent orthosteric inhibitor (Compound X, pIC₅₀ < 7) to protect the ATP binding pocket.
2. Labeling in the absence of any ligand (with the only addition of DMSO at the same percentage of the condition of the active site protection).

The reason of this comparison is to verify the possible interference of the covalent label with the binding competence of the protein.

	LABELING #1 (w/ active site protection)	LABELING #2
[ROCK-1]	10 μ M	
Dilution and labeling buffer	Labeling Buffer NHS (NanoTemper) 130 mM NaHCO ₃ , 50 mM NaCl, pH 8.2-8.3	
Pre-incubation (active site protection)	Compound X (pIC ₅₀ < 7) 100 μ M	DMSO 1 %
Time of pre-incubation	20 min	
Dye	RED-NHS 2nd Generation (NanoTemper)	
[Dye]	30 μ M	
Incubation	30' in the dark at 25°C	
Purification system	PD SpinTrap G-25 (Cytiva)	
Purification buffer	50 mM HEPES (pH 7.4), 150 mM NaCl, 2 mM DTT	

After the labeling reaction the proteins concentration and the Degree of Labeling (DOL) was measured through the acquisition of a UV spectra (**Figure 48**).

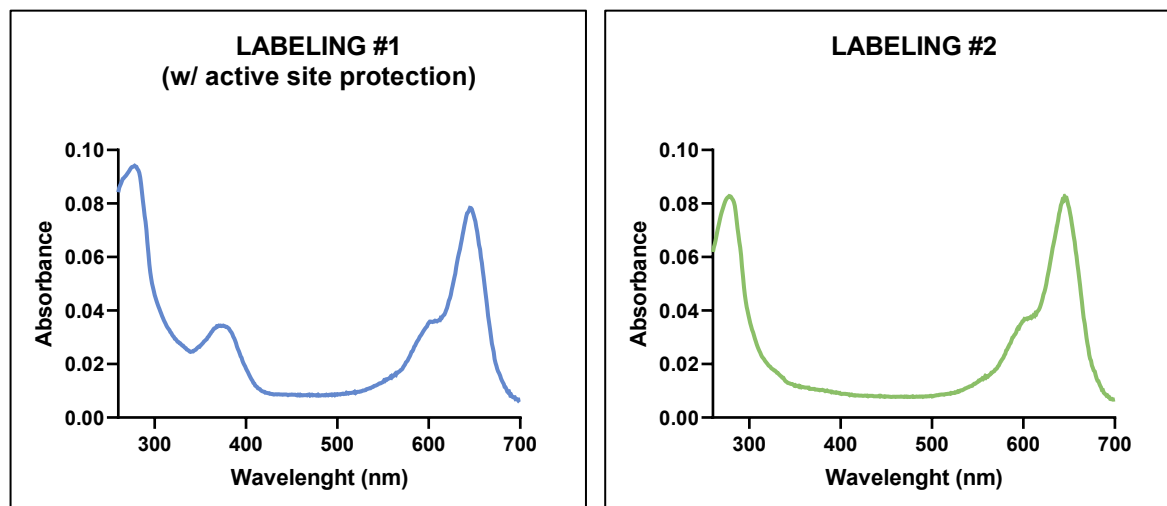


Figure 48 UV spectra of two labeled protein: on the left ROCK-1 labeled in the presence of Compound X to protect the active site, while on the right ROCK-1 labeled in the absence of active site protector.

	LABELING #1 (w/ active site protection)	LABELING #2
[ROCK-1 LB]	1.36 μ M	1.19 μ M
DOL	0.28	0.34

The two different labeling reactions led to similar results in terms of protein concentration and DOL. The main difference is the presence of an absorption peak at 375 nm, probably due to an incomplete

removal of Compound X from the system. The low affinity of Compound X is a necessary feature to facilitate its removal during the purification phase, but the use of a spin column for this phase probably reduced the efficiency of the process compared to a slower Gravity column (e.g. PD MiniTrap G-25, Cytiva). If necessary, it has been demonstrated that an additional purification step in a size exclusion spin column can be performed to better remove Compound X.

However, the residual presence of the compound seems not to interfere in the subsequent interaction assay with the reference Compound A, probably due to Compound X low potency and the further dilution of the binding assay. Indeed, the ROCK-1 LB #1 demonstrated a robust interaction profile with Compound A after the direct binding assay was performed to confirm the binding competence of the labeled proteins. On the contrary, the ROCK-1 LB #2 seemed not to be able to yield reliable binding information. This can be due to interference from the fluorescent label in the interaction between the protein and the reference Compound A (**Figure 49**).

[ROCK-1 LB]	20 nM
[INHIBITOR]	1 μ M – 0.24 nM + CONTROL POINTS
TITRATION	1:3, 8 POINTS IN DUPLICATE
DILUTION BUFFER	50 mM HEPES (pH 7.5), 150 mM NaCl, 2 mM DTT, 0.01% Tween 20
TEMPERATURE	22°C

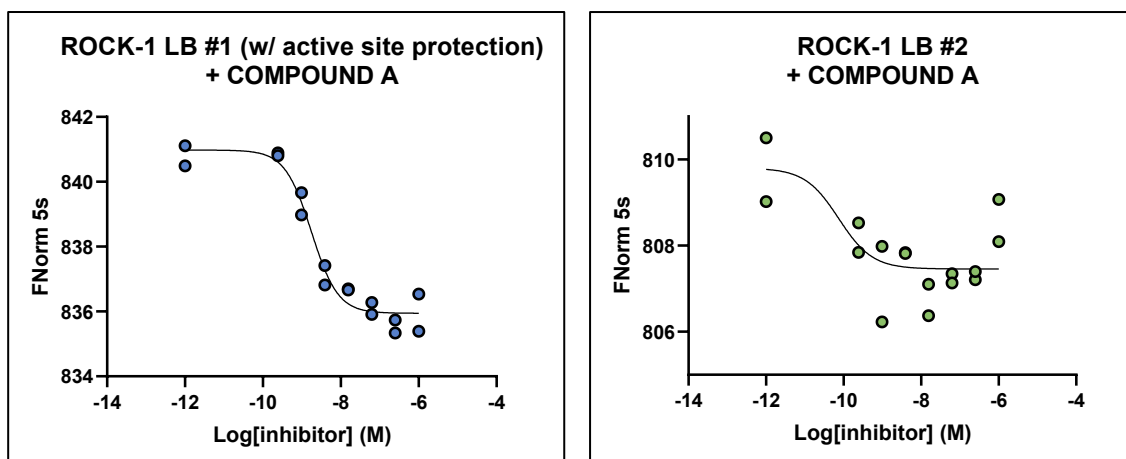


Figure 49 Direct binding assay with Compound A and ROCK-1 labeled in the presence of an active site protector (on the left) and in the absence of an active site protector (on the right).

	LABELING #1 (w/ active site protection)	LABELING #2
pIC ₅₀	8.75	~9.65
IC ₅₀ (nM)	1.8	0.2
R ²	0.96	0.54
HILL COEFF	1.28	9.61
RESPONSE AMPLITUDE	5.03	2.29
MST-on TIME	5 s	5 s

These data suggest that protection of the binding site with an orthosteric compound might be a valid choice in order to observe and quantitatively describe the interaction with orthosteric inhibitors and confirm the protein binding competence after labeling. The presence of a ligand during the labeling phase probably induces a reduction in protein mobility and a closure of its structure, avoiding the labeling of normally buried residues that are possibly involved in the formation of binding pockets.

To verify the robustness and reproducibility of the labeling procedure, an additional labeling under the same conditions as Labeling #1 has been performed, and the results are reported in **Figure 50**.

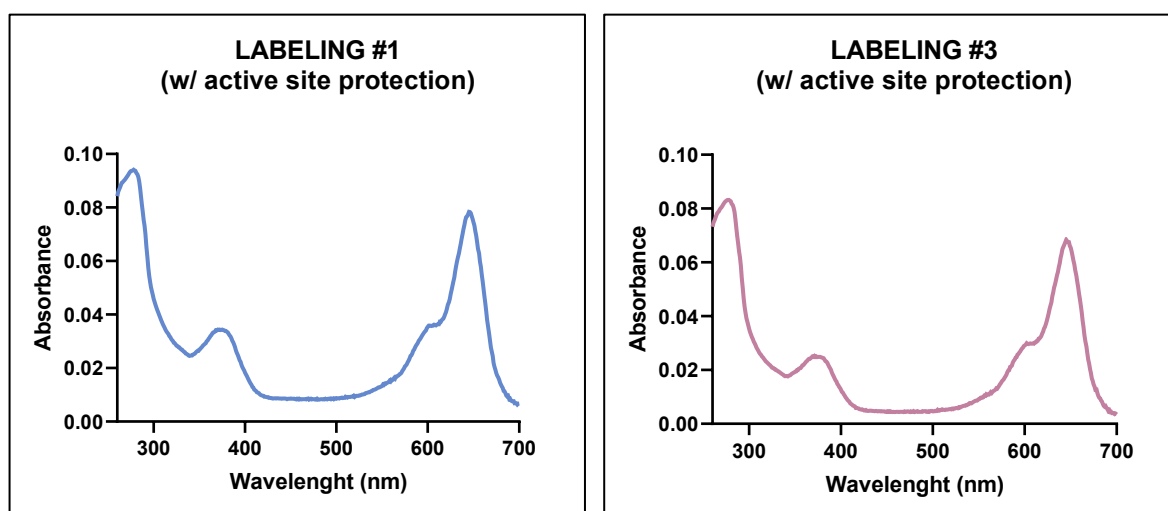


Figure 50 UV spectra of two labeled protein: on the left the already reported ROCK-1 labeled in the presence of Compound X to protect the active site, and on the right a replicate in the same experimental conditions.

	LABELING #1 (w/ active site protection)	LABELING #3 (w/ active site protection)
[ROCK-1 LB]	1.36 μ M	1.20 μ M
DOL	0.28	0.28

Based on the data, it is possible to conclude that the labeling reaction is reproducible and robust, as well as the DOL is not in the ideal range of 0.70-1. The low value obtained could be attributed to the poor reactivity of the protein lysines or to its limited exposure to the solvent. However, the value is maintained in the different reactions.

In the case of the Labeling #3, the interaction test with the Compound A was set starting from 100 nM to better center the titration range (**Figure 51**).

[ROCK-1 LB]	20 nM
[INHIBITOR]	- 1 μ M – 0.24 nM + CONTROL POINTS (LB #1) - 100 nM – 0.02 nM + CONTROL POINTS (LB #3)
TITRATION	1:3, 8 POINTS IN DUPLICATE
DILUTION BUFFER	50 mM HEPES (pH 7.5), 150 mM NaCl, 2 mM DTT, 0.01% Tween 20
TEMPERATURE	22°C

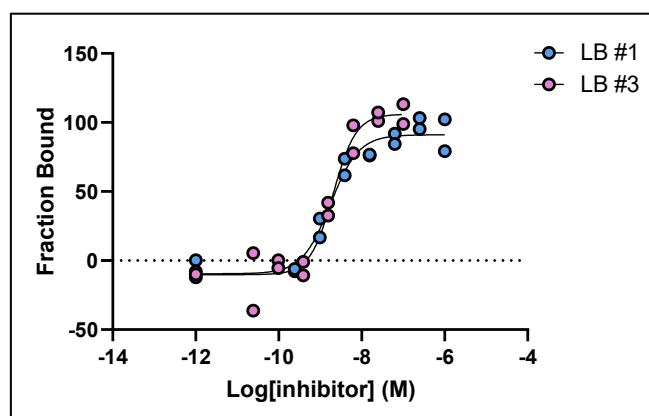


Figure 51 Binding assays with Compound A and the two batches of ROCK-1 labeled in the presence of an active site protector (ROCK-1 LB #1 and ROCK-1 LB #3).

	LABELING #1 (w/ active site protection)	LABELING #3 (w/ active site protection)
pIC₅₀	8.75	8.69
IC₅₀ (nM)	1.8	2.04
R²	0.96	0.96
HILL COEFF	1.28	1.57
RESPONSE AMPLITUDE	5.03	3.49
MST-on TIME	5 s	2.5 s

It is possible to conclude that the optimized labeling protocol led to obtain labeled proteins able to interact consistently with the reference compound.

For the following binding assays with the allosteric compounds the ROCK-1 LB #3 has been selected.

INTERACTION WITH ALLOSTERIC COMPOUNDS

The interaction with the allosteric compounds (B and C) has been performed following the experimental conditions reported in the table below.

[ROCK-1 LB #3]	20 nM
[INHIBITOR]	2.5 μ M – 0.24 nM + CONTROL POINTS*
TITRATION	1:3, 7 POINTS IN DUPLICATE
DILUTION BUFFER	50 mM HEPES (pH 7.5), 150 mM NaCl, 2 mM DTT, 0.01% Tween 20
TEMPERATURE	22°C

* the initial concentration was 10 μ M, but due to aberration traces, the highest concentration points have not been considered in the fitting analysis.

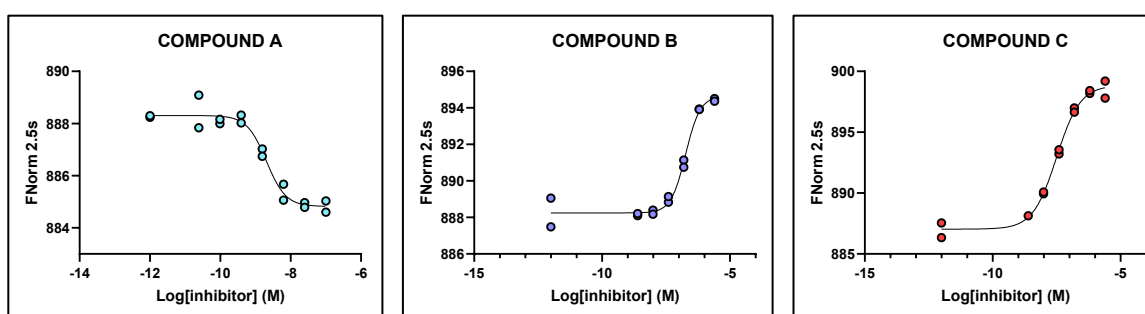


Figure 52 Direct binding assay with ROCK-1 LB #3 and Compounds A, B and C.

	pIC ₅₀	IC ₅₀ (nM)	Hill slope	Response Amplitude	R ²
COMPOUND A	8.69	2.04	1.57	3.49	0.96
COMPOUND B	6.74	183.3	1.52	6.40	0.98
COMPOUND C	7.50	31.5	0.94	11.81	0.99

The interaction between ROCK-1 and the allosteric compounds has been confirmed in a direct binding experiment (Figure 52).

Moreover, Compound B and C show an inverted fluorescence course of the labeled protein in comparison with the reference orthosteric Compound A, suggesting that a different binding mode and conformation is occurring (Figure 53).

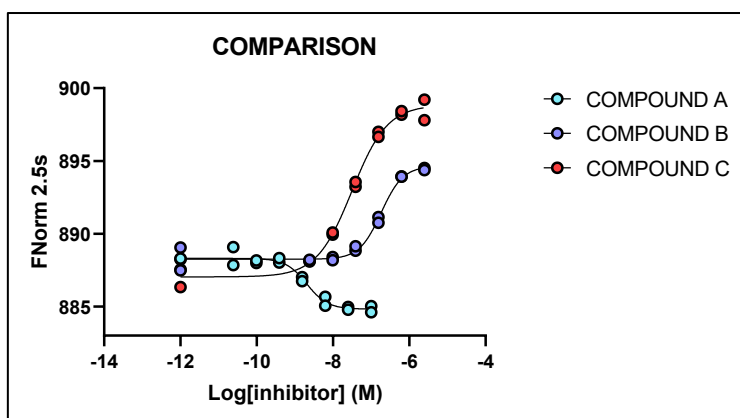


Figure 53 Comparison of the binding curve of ROCK-1 LB #3 and the Compounds A, B and C.

Finally, the allosteric compounds were tested with ROCK-1 LB #2 (labeled without the active site protector, Compound X) to investigate the effect of ATP-binding pocket protection during labeling on subsequent interactions with allosteric compounds (**Figure 54**).

[ROCK-1 LB #2]	20 nM
[INHIBITOR]	1 μ M – 0.24 nM + CONTROL POINTS
TITRATION	1:3, 8 POINTS IN DUPLICATE
DILUTION BUFFER	50 mM HEPES (pH 7.5), 150 mM NaCl, 2 mM DTT, 0.01% Tween 20
TEMPERATURE	22°C

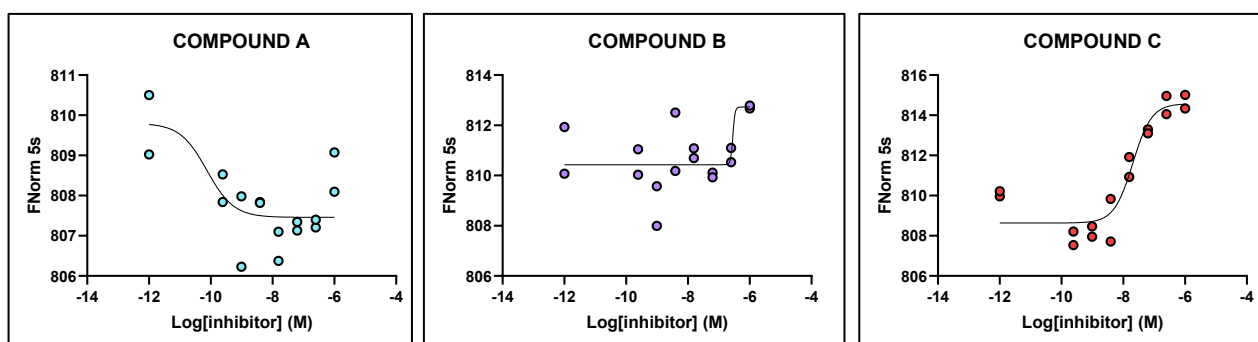


Figure 54 Direct binding assay with ROCK-1 LB #2 (labeled in the absence of an active site protector) and Compounds A, B and C.

	pIC ₅₀	IC ₅₀ (nM)	Hill slope	Response Amplitude	R ²
COMPOUND A	~9.65	0.2	9.61	2.29	0.54
COMPOUND B	-	-	-	-	-
COMPOUND C	7.69	20.0	1.43	5.94	0.92

Surprisingly, the interaction of Compound C resulted not affected by the absence of an active site protector during the labeling phase, unlike that of Compound A and Compound B. This leads to the conclusion that the dye position on the protein interferes with the binding of the two allosteric compounds in different ways, implying that compounds B and C may also have a different binding mode. Interestingly, the labeling reaction in the presence of an orthosteric protector in every case yields a more robust system, allowing each interaction (either orthosteric or allosteric) to be described with high reliability.

Therefore, it is possible to conclude that the combination of MST competition and binding assays for studies of different binding modes enabled, in the first instance, the **differentiation of orthosteric and allosteric inhibitors** and, secondarily, highlighted a possible different interaction mode or site due to the evidence of **different sensitivity to the dye position on the protein**.

5. CONCLUSIONS

The research activities reported in this work were oriented toward the comprehension and validation of MicroScale Thermophoresis as a biophysical tool for the characterization of various protein-ligand interaction systems.

For this purpose, two kinase proteins were considered and detailed:

- EGFR (Epidermal Growth Factor Receptor)
- ROCK (Rho-associated protein kinase)

In particular, to obtain orthogonal information, two different approaches have been employed: the competition assay, which requires a fluorescent ATP analog to compete with orthosteric inhibitors, and the binding assay, which uses a fluorescent label attached to the protein to observe the direct interaction between the target and the inhibitor.

Through this experimental design, different types of interactions were investigated with a focus on potent inhibitors, slow and allosteric binders, differentiation between Type I and Type II inhibitors and between reversible and irreversible compounds. The most accurate fitting model has been evaluated for every interaction system taken into consideration.

The project yielded to draw conclusions about different topics. In the first place MST allowed the differentiation of EGFR wild type and mutated L858R in terms of active fraction percentage and tendency to dimerization, an important aspect for the correct interpretation of subsequent analysis, such as competition assays.

Then, from the Gefitinib-EGFR interaction data resulted that MST could be a suitable approach for the characterization of potent interactions, leading to the depiction of potentially tight binding conditions thanks to the low sample consumption and its rapidity of analysis. Moreover, from these experiments emerged that reliable information need a detailed consideration of the initial conditions and the awareness that potency measurements can be affected by experimental choices. However, biological systems with a high level of complexity are possibly not quantitatively described with sufficient confidence from binding analyses alone: in those cases, a simple estimation of the potency range can be a useful starting point for further and orthogonal investigations.

Lapatinib interaction system enabled the investigation of a slow binder Type II inhibitor via MST. These findings highlighted the need of monitoring the time dependence of an occurring interaction

from the perspectives of both the inhibitor-protein complex and the protein alone conformational changes over time. Furthermore, stoichiometry analysis with Gefitinib (Type I) and Lapatinib (Type II) revealed different protein states as well as a different propensity of inhibitors to bind them.

The study of irreversible binding with Osimertinib enabled then the use of MST to develop an alternative approach to Jump Dilution for the differentiation of reversible and irreversible inhibitors, a potentially useful tool for the discovery of unknown covalent drugs.

Finally, ROCK system permitted to apply MST for the differentiation of orthosteric and allosteric binders, leading to valuable complementary information through the combination of competition and direct binding assays. Furthermore, an investigation of the best labeling conditions found discrepancies between the two tested allosteric compounds, revealing a possible distinct interaction mechanism due to their different sensitivity to the dye position on the protein.

In conclusion, MicroScale Thermophoresis emerged as a valuable tool for the characterization of several aspects of protein interactions, in addition to the simple determination of potency; thus, this project helped to better understand MST potentiality and applications through the establishment of benchmarks for several binding modes, and the acquired knowledge could potentially be applied to the future investigation of new chemical entity mechanisms, from the early to the late stages of Drug Discovery pipeline.

6. BIBLIOGRAPHY

- [1] X. Du *et al.*, “**Insights into protein–ligand interactions: Mechanisms, models, and methods**” *Int. J. Mol. Sci.*, vol. 17, no. 2, pp. 1–34, **2016**, doi: 10.3390/ijms17020144.
- [2] M. A. Williams, “**Protein-Ligand Interactions - Methods and Applications**”, *Methods in Molecular Biology*, vol. 1008, **2013**, doi: 10.1007/978-1-62703-398-5.
- [3] A. Copeland, “**Evaluation of enzyme inhibitors in Drug Discovery - A Guide for Medicinal Chemists and Pharmacologists**” *Angew. Chemie*, vol. 117, no. 40, **2005**, doi: 10.1002/ange.200585328.
- [4] C. Velours *et al.*, “**Macromolecular interactions in vitro, comparing classical and novel approaches**” *Eur. Biophys. J.*, vol. 50, no. 3–4, pp. 313–330, **2021**, doi: 10.1007/s00249-021-01517-5.
- [5] S. Markossian *et al.*, “**Assay Guidance Manual**,” *Eli Lilly & Company and the National Center for Advancing Translational Sciences, Bethesda (MD)*, **2020**.
- [6] T. D. Pollard, “**A guide to simple and informative binding assays**”, *Mol Biol Cell.*, vol. 21, no. 23, pp. 4061-4067, **2010**, doi:10.1091/mbc.E10-08-0683.
- [7] T. Kenakin, “**The mass action equation in pharmacology**,” *Br. J. Clin. Pharmacol.*, vol. 81, no. 1, pp. 41–51, **2016**, doi: 10.1111/bcp.12810.
- [8] R. A. Copeland, “**Enzymes: A Practical Introduction to Structure, Mechanism, and Data Analysis, 2nd Edition**”, *Wiley-VCH Verlag*, **2000**.
- [9] R. R. Neubig *et al.*, “**International Union of Pharmacology Committee on Receptor Nomenclature and Drug Classification. XXXVIII. Update on terms and symbols in quantitative pharmacology.**” *Pharmacological reviews* vol. 55,4: 597-606, **2003**, doi:10.1124/pr.55.4.4.
- [10] T. Kalliokoski, C. Kramer, A. Vulpetti, and P. Gedeck, “**Comparability of Mixed IC₅₀ Data - A Statistical Analysis**,” *PLoS One*, vol. 8, no. 4, p. 61007, **2013**, doi: 10.1371/journal.pone.0061007.
- [11] P. Newton, P. Harrison, and S. Clulow, “**A novel method for determination of the affinity of protein: Protein interactions in homogeneous assays**,” *J. Biomol. Screen.*, vol. 13, no. 7, pp. 674–682, **2008**, doi: 10.1177/1087057108321086.
- [12] E. C. Hulme and M. A. Trevethick, “**Ligand binding assays at equilibrium: validation and interpretation.**” *British journal of pharmacology* vol. 161,6, pp. 1219-37, **2010**, doi: 10.1111/j.1476-5381.2009.00604.x.
- [13] E. Maréchal, S. Roy, and L. Lafanechère, *Chemogenomics and Chemical Genetics – “A User’s Introduction for Biologists, Chemists and Informaticians”*. *Springer Heidelberg Dordrecht London New York*, **2011**, doi: 10.1007/978-3-642-19615-7
- [14] P. J. Tonge, “**Quantifying the Interactions between Biomolecules: Guidelines for Assay Design and Data Analysis**,” *ACS Infect. Dis.*, vol. 5, no. 6, pp. 796–808, **2019**, doi: 10.1021/acsinfecdis.9b00012.
- [15] H. Motulsky and A. Christopoulos, “**Fitting Models to Biological Data using Linear and Nonlinear Regression - A practical guide to curve fitting.**” *GraphPad Software Inc.*, **2003**.
- [16] I. Jarmoskaite, I. Alsadhan, P. P. Vaidyanathan, and D. Herschlag, “**How to measure and evaluate binding affinities**,” *Elife*, vol. 9, pp. 1–34, **2020**, doi: 10.7554/ELIFE.57264.
- [17] R. A. Copeland, “**Evaluation of enzyme inhibitors in Drug Discovery - A Guide for Medicinal Chemists and Pharmacologists**” *Wiley*, **2013**, doi: 10.1002/9781118540398.
- [18] P. Kuzmic, *et al.* “**High-throughput screening of enzyme inhibitors: simultaneous determination of tight-binding inhibition constants and enzyme concentration.**” *Analytical biochemistry* vol. 286,1, pp.

45-50, **2000**, doi:10.1006/abio.2000.4685P.

- [19] D. J. Murphy, “**Determination of accurate KI values for tight-binding enzyme inhibitors: An in silico study of experimental error and assay design**,” *Anal. Biochem.*, vol. 327, no. 1, pp. 61–67, **2004**, doi: 10.1016/j.ab.2003.12.018.
- [20] A. Tuley and W. Fast, “**The Taxonomy of Covalent Inhibitors**,” *Biochemistry*, vol. 57, no. 24. American Chemical Society, pp. 3326–3337, Jun. 19, **2018**, doi: 10.1021/acs.biochem.8b00315.
- [21] L. Boike, N. J. Henning, and D. K. Nomura, “**Advances in covalent drug discovery**,” *Nat. Rev. Drug Discov.*, vol. 21, no. December, **2022**, doi: 10.1038/s41573-022-00542-z.
- [22] P. Kuzmič, “**A two-point IC₅₀ method for evaluating the biochemical potency of irreversible enzyme inhibitors**,” *BioKin*, **2020**, doi: 10.1101/2020.06.25.171207.
- [23] J. M. Strelow, “**A Perspective on the Kinetics of Covalent and Irreversible Inhibition**,” *Journal of Biomolecular Screening*, vol. 22, no. 1, pp. 3–20, Jan. 01, **2017**, doi: 10.1177/1087057116671509.
- [24] A. Thorarensen *et al.*, “**The advantages of describing covalent inhibitor in vitro potencies by IC₅₀ at a fixed time point. IC₅₀ determination of covalent inhibitors provides meaningful data to medicinal chemistry for SAR optimization**,” *Bioorganic Med. Chem.*, vol. 29, p. 115865, **2021**, doi: 10.1016/j.bmc.2020.115865.
- [25] M. Jerabek-Willemsen, C. J. Wienken, D. Braun, P. Baaske, and S. Duhr, “**Molecular interaction studies using microscale thermophoresis**,” *Assay and Drug Development Technologies*, vol. 9, no. 4. pp. 342–353, Aug. 01, **2011**, doi: 10.1089/adt.2011.0380.
- [26] Y. Mao, L. Yu, R. Yang, L. B. Qu, and P. D. B. Harrington, “**A novel method for the study of molecular interaction by using microscale thermophoresis**,” *Talanta*, vol. 132, pp. 894–901, Jan. 2015, doi: 10.1016/j.talanta.2014.09.038.
- [27] SA. Seidel, *et al.* “**Microscale thermophoresis quantifies biomolecular interactions under previously challenging conditions**.” *Methods (San Diego, Calif.)* vol. 59,3, pp. 301-15, **2013**, doi: 10.1016/j.ymeth.2012.12.005.
- [28] T. H. Scheuermann, S. B. Padrick, K. H. Gardner, and C. A. Brautigam, “**On the acquisition and analysis of microscale thermophoresis data**,” *Anal. Biochem.*, vol. 496, pp. 79–93, Mar. **2016**, doi: 10.1016/j.ab.2015.12.013.
- [29] S. Duhr and D. Braun, “**Why molecules move along a temperature gradient**,” *PNAS*, vol. 103, 19678–19682, **2006**.
- [30] NanoTemper Technologies GmbH, “NanoPedia - Monolith NT.115.”
- [31] B. López-Méndez, S. Uebel, L. P. Lundgren, and A. Sedivy, “**Microscale Thermophoresis and additional effects measured in NanoTemper Monolith instruments**,” *Eur. Biophys. J.*, vol. 50, no. 3–4, pp. 653–660, **2021**, doi: 10.1007/s00249-021-01529-1.
- [32] J. M. Rainard, G. C. Pandarakalam, and S. P. McElroy, “**Using Microscale Thermophoresis to Characterize Hits from High-Throughput Screening: A European Lead Factory Perspective**,” *SLAS Discovery*, vol. 23, no. 3. pp. 225–241, Mar. 01, **2018**, doi: 10.1177/2472555217744728.
- [33] G. Manning, *et al.* “**The protein kinase complement of the human genome**.” *Science (New York, N.Y.)* vol. 298,5600, pp. 1912-34, **2002**, doi:10.1126/science.1075762G.
- [34] M. Congreve, C. W. Murray, and T. L. Blundell, “**Structural biology and drug discovery**,” *Drug Discov. Today*, vol. 10, no. 13, pp. 895–907, **2005**, doi: 10.1016/S1359-6446(05)03484-7.
- [35] Z. Zhao and P. E. Bourne, “**Progress with covalent small-molecule kinase inhibitors**,” *Drug Discov. Today*, vol. 23, no. 3, pp. 727–735, **2018**, doi: 10.1016/j.drudis.2018.01.035.

- [36] I. Galdadas, *et al.*, “**Structural basis of the effect of activating mutations on the EGF receptor,**” *Elife*, vol. 10, pp. 1–24, **2021**, doi: 10.7554/eLife.65824.
- [37] M. A. Morando *et al.*, “**Conformational Selection and Induced Fit Mechanisms in the Binding of an Anticancer Drug to the c-Src Kinase,**” *Sci. Rep.*, vol. 6, no. March, pp. 1–9, **2016**, doi: 10.1038/srep24439.
- [38] S. Sigismund, D. Avanzato, and L. Lanzetti, “**Emerging functions of the EGFR in cancer,**” *Mol. Oncol.*, vol. 12, no. 1, pp. 3–20, **2018**, doi: 10.1002/1878-0261.12155.
- [39] Z. Zhao, *et al.* “**Structural Insights into Characterizing Binding Sites in Epidermal Growth Factor Receptor Kinase Mutants.**” *Journal of chemical information and modeling* vol. 59,1, pp. 453-462, **2019**, doi: 10.1021/acs.jcim.8b00458.
- [40] L. Sutto and F. L. Gervasio, “**Effects of oncogenic mutations on the conformational free-energy landscape of EGFR kinase,**” *PNAS*, vol. 110, pp. 10616–10621, **2013**, doi: 10.1073/pnas.1221953110.
- [41] Y. Shan *et al.*, “**Oncogenic mutations counteract intrinsic disorder in the EGFR kinase and promote receptor dimerization,**” *Cell*, vol. 149, no. 4, pp. 860–870, May **2012**, doi: 10.1016/j.cell.2012.02.063.
- [42] C. Becker *et al.*, “**Monitoring Conformational Changes in the Receptor Tyrosine Kinase EGFR,**” *ChemBioChem*, vol. 17, no. 11, pp. 990–994, **2016**, doi: 10.1002/cbic.201600115.
- [43] K. S. Gajiwala *et al.*, “**Insights into the aberrant activity of mutant EGFR kinase domain and drug recognition,**” *Structure*, vol. 21, no. 2, pp. 209–219, Feb. **2013**, doi: 10.1016/j.str.2012.11.014.
- [44] E. R. Wood *et al.*, “**A Unique Structure for Epidermal Growth Factor Receptor Bound to GW572016 (Lapatinib): Relationships among Protein Conformation, Inhibitor Off-Rate, and Receptor Activity in Tumor Cells,**” *Cancer research* vol. 64,18, pp. 6652-9, **2004**, doi: 10.1158/0008-5472.CAN-04-1168.
- [45] T. S. Beyett *et al.*, “**Molecular basis for cooperative binding and synergy of ATP-site and allosteric EGFR inhibitors,**” *Nat. Commun.*, vol. 13, no. 1, **2022**, doi: 10.1038/s41467-022-30258-y.
- [46] Y. Yosaatmadja *et al.*, “**Binding mode of the breakthrough inhibitor AZD9291 to epidermal growth factor receptor revealed,**” *J. Struct. Biol.*, vol. 192, no. 3, pp. 539–544, **2015**, doi: 10.1016/j.jsb.2015.10.018.
- [47] Y. Feng, P. V. Lograsso, O. Defert, and R. Li, “**Rho Kinase (ROCK) Inhibitors and Their Therapeutic Potential,**” *J. Med. Chem.*, vol. 59, no. 6, pp. 2269–2300, **2016**, doi: 10.1021/acs.jmedchem.5b00683.
- [48] C. Hahmann, T. Schroeter, T. “**Rho-kinase inhibitors as therapeutics: from pan inhibition to isoform selectivity**” *Cell. Mol. Life Sci.* 67, 171–177, **2010**, doi: 10.1007/s00018-009-0189-x.
- [49] Wang, Qing *et al.* “**Advantages of Rho-associated kinases and their inhibitor fasudil for the treatment of neurodegenerative diseases.**” *Neural regeneration research* vol. 17,12, 2623-2631, **2022**, doi: 10.4103/1673-5374.335827.
- [50] L. Julian and M. F. Olson, “**Rho-associated coiled-coil containing kinases (ROCK), structure, regulation, and functions,**” *Small GTPases*, vol. 5, no. 2, **2014**, doi: 10.4161/sntp.29846.
- [51] J. K. Frank Schäfer *et al.* “**Purification of GST-Tagged Proteins.**” *Methods in enzymology* vol. 559, 127-39, **2015**, doi: 10.1016/bs.mie.2014.11.005.
- [52] F. Ferlenghi *et al.*, “**A sulfonyl fluoride derivative inhibits EGFR L858R/T790M/C797S by covalent modification of the catalytic lysine,**” *Eur. J. Med. Chem.*, vol. 225, **2021**, doi: 10.1016/j.ejmech.2021.113786.
- [53] R. Castelli *et al.*, “**Balancing reactivity and antitumor activity: heteroarylthioacetamide derivatives as potent and time-dependent inhibitors of EGFR,**” *Eur. J. Med. Chem.*, vol. 162, pp. 507–524, **2019**, doi: 10.1016/j.ejmech.2018.11.029.

- [54] M. Jerabek-Willemsen *et al.*, “**MicroScale Thermophoresis: Interaction analysis and beyond,**” *J. Mol. Struct.*, vol. 1077, pp. 101–113, Dec. **2014**, doi: 10.1016/j.molstruc.2014.03.009.
- [55] R. Magnez and C. Bailly, “**Microscale Thermophoresis as a Tool to Study Protein Interactions and Their Implication in Human Diseases,**” *International journal of molecular sciences* vol. 23,14 7672. 12 Jul. **2022**, doi: 10.3390/ijms23147672.
- [56] X. Zhai *et al.* “**Insight into the Therapeutic Selectivity of the Irreversible EGFR Tyrosine Kinase Inhibitor Osimertinib through Enzyme Kinetic Studies.**” *Biochemistry* vol. 59,14, pp. 1428-1441, **2020**, doi: 10.1021/acs.biochem.0c00104.
- [57] J. L. Macdonald-Obermann and L. J. Pike, “**Allosteric regulation of epidermal growth factor (EGF) receptor ligand binding by tyrosine kinase inhibitors.**” *The Journal of biological chemistry* vol. 293,35, pp. 13401-13414, **2018**, doi: 10.1074/jbc.RA118.004139.